Aalto-yliopisto
Insinööritieteiden
korkeakoulu

Laura Torres Salvador

Shear resistance of the interfaces of backfill components in nuclear waste deposition tunnels affected by changes in temperature, water content and salinity

Master's Thesis submitted on 27th of May 2013

Supervisor: Professor LEENA KORKIALA TANTTU

Advisor: GOWTHAMAN SINNATHAMBY

Aalto-yliopisto
Insinööritieteiden
korkeakoulu

Aalto-yliopisto, PL 11000, 00076 AALTO
www.aalto.fi

Abstract of master's thesis

Author Laura Torres Salvador

Title of thesis Shear resistance of the interfaces of backfill components in nuclear waste deposition tunnels affected by changes in temperatura, water content and salinity.

Department Civil and Environmental Engineering

Professorship Soil Mechanics and Foundation Engineering **Code of professorship** Rak-50

Thesis supervisor Leena Korkiala-Tanttu

Thesis advisor(s) / Thesis examiner(s) Gowthaman Sinnathamby Gow)

Date 27.05.2013 **Number of pages** 82 **Language** English

Abstract

The aim of this project was to study how the interface shear strength of the tunnel backfill materials would be affected by the changes in temperature, ground water salinity and water content. During the saturation of the deposition tunnels, the precompressed bentonite buffer would swell and generate high swelling pressures in the range of 7 to 15 MPa. Such high swelling pressures can cause upheaval and compression of the tunnel backfill that would eventually decrease the buffer density. Due to various reasons, the saturated buffer density must be kept within a narrow range of 1950 to 2050 kg/m^3 at all times. Shear strengths of different tunnel backfill material interfaces become vital in this regard as they provide resistance to the swelling of the buffer.

Proposed tunnel backfill materials such as Friedland clay blocks, bentonite pellets and granulated bentonite were used to form block/block, block/pellets and block/granulated bentonite interfaces and subsequently tested for interface shear strength. Tests were carried out using a large and a small direct shear boxes and Mohr Coulomb's shear strength parameters were determined. Material properties such as bulk density, dry density and water content were also determined. It was found that interface shear strength decreases with the temperature and water content. Nevertheless, when water (salty or distilled) is added to the block surface in small quantities, it leads to increased shear strength. The interface shear strength parameters obtained from this study will be used in the detailed modelling of the buffer-backfill interaction of KBS-3V.

Keywords KBS-3, bentonite, interface shear strength, temperature, water content, salinity.

Preface

I would like to thank Professor Leena Korkiala-Tanttu for teaching, guidance, time and giving me the opportunity to work in this project and also to Postdoctoral Researcher Gowthaman Sinnathamby whose patient guidance and useful critiques have been very helpful. I would also like to thank Laboratory Manager Matti Lojander for his advice and assistance. I also wish to extend my thanks to the personnel of the Department of Soil Mechanics and Foundation Engineering at Aalto University who have always made me feel very comfortable in the department. I am extremely grateful to Juan Gallardo Forés for his invaluable help and friendship.

Finally, I wish to thank my family and friends for their support and encouragement throughout my study. Without their help, none of this could have been possible.

Espoo 27.5.2013

Laura Torres Salvador

Laura Torres Salvador

Contents

List of symbols

S_R	[%]	Degree of saturation
c	[kN/m^2]	Cohesion
e_0		Initial void ratio
w	[%]	Water content
Δx	[mm]	Horizontal displacement
Δy	[mm]	Vertical displacement
ρ	[kg/m^3]	Bulk density
ρ_d	[kg/m^3]	Dry density
ρ_s	[kg/m^3]	Grain density
ρ_w	[kg/m^3]	Water density
τ	[kN/m^2]	Shear stress
σ	[kN/m^2]	Normal stress
φ	[°]	Friction angle

1. Introduction

Increased human needs for energy force a global increase in demand for nuclear energy. However, nuclear energy production results in highly radioactive waste that must be disposed carefully in order to protect the environment in a long-term. Different ways of disposing the nuclear waste have been discussed in the past and it has been decided to dispose these residues in an underground repository in which the radioactive substance is isolated from the environment by means of engineered multi-barrier systems.

Extensive researches are being underway in Finland to study the feasibility of the construction of an underground nuclear waste repository in crystalline rock in Olkiluoto island at a depth of approximately 420 meters. The Swedish KBS-3V concept (KBS is the abbreviation for a term which means Swedish nuclear safety) has been proposed for this repository. The KBS-3V concept utilizes a well-engineered multi-barrier system which would ensure the proper functionality of the barrier system even if a single barrier fails (Keto et al., 2008). Low permeable materials such as precompressed bentonite blocks, granulated bentonite and bentonite pellets have been proposed for backfilling the deposition tunnels in the KBS-3V repository, and hence tested in the present study.

One of the key aspects to ensure the proper functionality of the protective buffer-barrier system is that the saturated density of the buffer should be maintained within a narrow range of 1950 kg/m^3 and 2050 kg/m^3 at all times during the lifetime of the repository (Hansen et al., 2010). These density criteria become crucial particularly at the early stage of the saturation of the repository when the saturated buffer tends to swell and penetrate into the dry tunnel backfilling. Swelling of the buffer would eventually decrease its density and therefore it must be controlled in such a way that the density is kept within the above range. Interface shear strength of tunnel backfill materials plays a major role in controlling the swelling of the buffer and hence there was a need to study that in detail. Several recent numerical modellings of the buffer-backfill interaction suggested that a detailed experimental programme should be carried out in order to model the swelling of the buffer with realistic interface shear strength values (Börgesson & Hernelind, 2008; Korkiala-Tanttu, 2009; Leoni, 2012).

An experimental programme, 'Block Shear' was carried out at Aalto University to study the interface behaviour and to determine the shear strength parameters of different tunnel backfill materials. A total of 112 tests were carried out in the Soil Mechanics and Foundation Engineering laboratory at Aalto University by changing various parameters such as temperature, interface water content and salinity of the water. 'Block shear' is a subproject of a coordination project 'BOA' (Assessment of bentonite characteristics), which is one of the major projects in KYT2014 (Finnish Research Programme on Nuclear Waste Management) research programme, 2011-2014.

Objectives

In order to provide reliable interface shear strength parameters of tunnel backfill materials to model the buffer-backfill interaction, the following objectives have been set:

1. the effect of temperature on the interface shear strength of tunnel backfill materials
2. the effect of ground water salinity on the interface shear strength of tunnel backfill materials, and
3. the effect of the water content on the interface shear strength of tunnel backfill materials

Outline of the thesis

Chapter 2 explains the background of the proposed Finnish KBS-3V type repository and the deposition tunnel backfilling. Selection of the location and different components of the buffer-backfilling are also discussed in detail.

Chapter 3 reviews the general physical and chemical properties of the proposed tunnel backfill materials. It also discusses the performance of these materials under different circumstances such as changing temperatures, varying water contents and ground water salinity which are needed for a better understanding and to predict the behaviour of the buffer-backfill assembly in the KBS-3V.

Chapter 4 lists the basic geotechnical properties such as grain size, water content, dry density, bulk density, swelling index and pressure etc., of the proposed backfill materials**.**

Chapter 5 details the testing programme and the different direct shear apparatus used.

Chapter 6 presents all the test results from the laboratory experiments.

Chapter 7 corresponds to the analysis of the test results that are reported in Chapter 6.

Chapter 8 summarises the finding of this study and make suggestions for future research works.

2. Background

2.1. Nuclear Waste Management in Finland

Nuclear waste management in Finland is regulated by the Nuclear Energy Act (990/1987) and the Nuclear Energy Decree (161/1988). According to the Nuclear Energy Act which was rectified in 1994 and it states "*all the nuclear waste in Finland must be treated, stored and disposed in Finland, and no nuclear waste from other countries shall be imported to Finland. Therefore, each producer of nuclear waste is responsible for the safe handing, management and disposal of its waste*" (Posiva, 2010).

The Ministry of Trade and Industry established the decision 9/815/2003 in which it states that "*Teollisuuden Voima Oy (TVO) and Fortum Power and Heat Oy, as parties under nuclear waste management obligation shall, either separately, together, or through Posiva Oy, prepare to present all reports and plans required to obtain a construction license for a disposal facility by the end of 2012*". Posiva Oy is the company owned by the nuclear energy-producing power companies and its task is to manage the spent nuclear fuel in Finland. Finland has become the first country to apply for the construction license of a deep rock nuclear waste repository and if the license is successful it is expected to commence operation by 2020.

2.2. Final safe disposal - Olkiluoto Island, Finland

Between 1997 and 1999, Posiva Oy performed environmental impact assessments (EIA) for the final disposal of spent nuclear fuel at several locations in Finland. Different alternatives were considered for the final disposal; Olkiluoto in Eurajoki, Romuvaara in Kuhmo, Hästholmen in Loviisa and Kivetty in Äänekoski (Figure 2-1).

According to the EIAs performed, all the tested sites would have been suitable for the final disposal, however, due to the existing nuclear power plants in Loviisa and Olkiluoto, priority was given to these two locations. Of these two, Olkiluoto island in Eurajoki had a larger area reserved for the repository and also it had most of the spent nuclear fuel already on this island. Therefore, Olkiluoto was chosen for the final disposal of spent nuclear fuel.

Figure 2-1. Location of alternative disposal sites (Posiva, 1999)

Olkiluoto is located on the shore of the Gulf of Bothnia. The centre of the municipality is over 10 km to the north of the centre of Rauma. The final disposal site is in the vicinity of the power plant and this area is owned by Teollisuuden Voima Oy (TVO), Fortum and the Forest and Park Service. In the east, the area is bounded by agricultural and forestry lands and the closest residential buildings are situated in the eastern part more than a kilometre away (Figure 2-2) (Posiva, 1999).

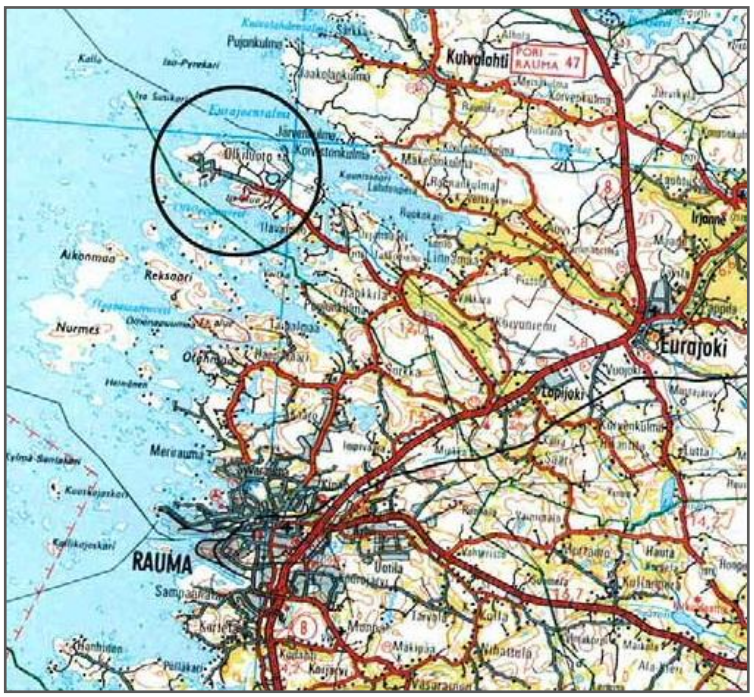

Figure 2-2. Location of Olkiluoto Island (Posiva, 1999)

Furthermore, the nuclear waste generated by Loviisa nuclear power plant would easily be transported by ship, rail and road to this location (Posiva, 1999).

2.3. KBS-3V and the multi-barrier concept

KBS is an abbreviation of a Swedish term "KärnBränsleSäkerhet" which means nuclear safety. The KBS-3 concept satisfies the requirements of safety, radiation protection and environmental protection. This method provides a long-term isolation and storage of spent nuclear fuel by adopting a system of multi-barriers, both engineered and natural, and by ensuring sufficient depth of disposal. With the disposal at a depth of approximately 420 meters below the existing ground level, the effects of the changes above ground can be avoided or minimized. In a multi-barrier, even a failure or deficiency of a single barrier would not affect the performance of the overall barrier and hence the purpose of the whole barrier is not lost (Keto et al., 2008).

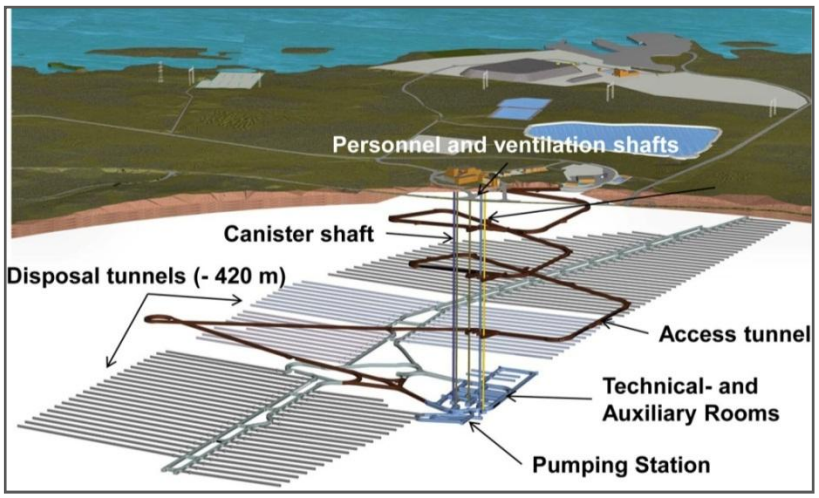

Figure 2-3. Final disposal facility (www.posiva.fi)

The proposed disposal facility at Olkiluoto consists of repository, central tunnels connecting deposition tunnels, other underground facilities, auxiliary facilities, vertical shafts, an access tunnel and aboveground auxiliary facilities (Figure 2-3). At the aboveground encapsulation plant the spent nuclear fuel is encapsulated in copper-iron canisters and transferred to the underground facilities through the canister shaft and transported to the deposition tunnels, where the following steps are carried out (Posiva, 2010):

- The canisters are deposited at approximately 420 meters depth into the deposition holes which are drilled in crystalline bedrock.
- The canisters are surrounded by a buffer preventing water uptake and protecting the canister against the external impacts such as bedrock movements and also from the microbial corrosion.
- The deposition tunnels are backfilled with precompressed bentonite blocks after removing HVAC systems (heating, ventilation and air conditioning systems).
- Once the tunnel is completely backfilled, the entrance will be sealed with a massive concrete plug.

The erection of the deposition tunnels will be performed gradually over the operational period of the repository, during which 10 to 20 tunnels will be excavated at a time and the distance between these tunnels should be more than 25 meters. The deposition holes will be bored into the floors of these deposition tunnels (Posiva, 2010).

In the KBS-3 multi-barrier concept, the surrounding bedrock act as a natural barrier while the engineered barrier composed of a canister, bentonite-based buffer, the tunnel backfill and other elements used for the sealing of the repository.

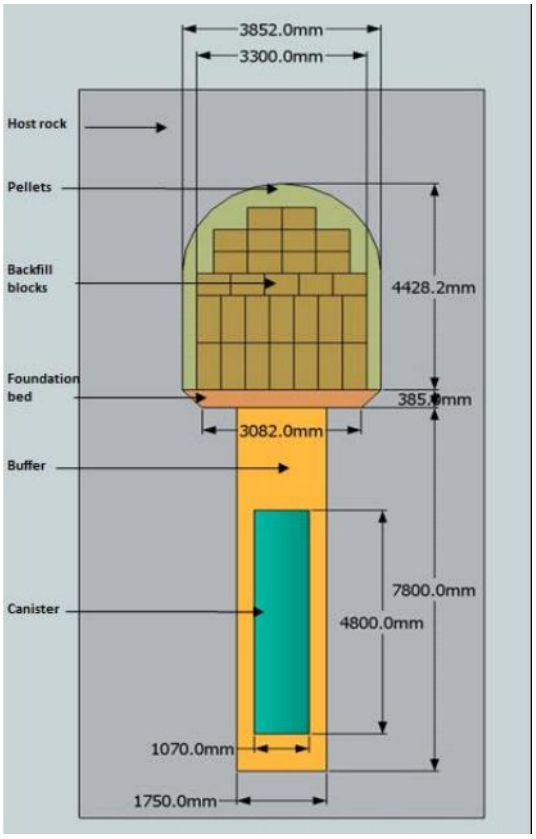

Figure 2-4. Schematic section of a KBS-3V (Leoni, 2012)

There are two canister orientations proposed in KBS-3 concept, namely, KBS-3V and KBS-3H. In KBS-3V, the copper canisters are placed in vertically drilled deposition holes while in KBS-3H they are placed in horizontally drilled deposition holes. The present study mainly focuses on the KBS-3V multi-barrier concept which is adopted by Posiva Oy in Finland. Figure 2-4 shows the cross section of the deposition tunnel - deposition hole geometry with different tunnel backfill components and canister-buffer arrangement.

Disposal canister

The disposal canister consists of a copper outer shell and a cast iron insert, inside which the spent nuclear fuel is placed (Figure 2-5). The outer shell of the canister is 50 mm thick and it protects the inner part from the corrosion. It has been proved that copper can last hundreds of thousands of years without corroding if the environmental conditions are favourable (Féron et al., 2008). Additionally, in a very deep location in the bedrock, where groundwater flows very slowly and with almost no oxygen, the corroding effect can be negligible (Posiva, 2010).

The most important function of the canister is to store the spent nuclear fuel inside for a long time without jeopardizing the exterior. This safety function rests on the mechanical strength of the cast iron insert and the corrosion resistance of the copper surrounding it.

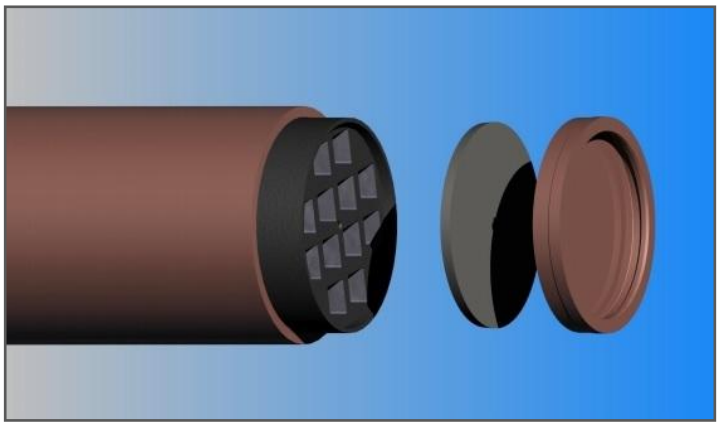

Figure 2-5. The copper canister – cast iron insert (Raiko, 2005)

Bentonite buffer

The canister is isolated from the surrounding bedrock by the buffer. The buffer has to be designed and constructed in such a way to improve the mechanical, geochemical and hydrogeological conditions which are beneficial for the canister. It also has to protect canister against external processes that could jeopardize the stability of the canister. In case of a failure, the buffer should avoid the contamination flux to the surrounding bedrock. In order to ensure these requirements, the buffer must fulfil the following conditions conditions (Posiva, 2010):

1. Low hydraulic conductivity to prevent any major advection.
2. Sufficient swelling pressure to ensure tightness and self-sealing ability and also to avoid microbiological activity near the canister and the sinking of the canister.
3. Small pore structure in order to prevent migration of radionuclides with colloids, in the event of a possible canister leak.

The hydraulic conductivity and the swelling pressure of the buffer are closely related to its density. Therefore, in order to meet the requirements the density should be kept in a certain range of 1950 to 2050 kg/m^3 (Juvankoski & Marcos, 2010).

Bentonite has been proposed as the buffer material in the Finnish KBS-3V repository and it meets the safety requirements to a greater extent. Bentonite is a type of clay that expands when coming into contact with water which leads to a very low water hydraulic conductivity (Murray, 1999; Phillips et al., 2011).

Deposition tunnel backfill

After the installation of canisters and the buffer, deposition tunnels are backfilled and sealed as soon as practicable. Precompressed Friedland clay blocks fill up the majority of the deposition tunnel's space while bentonite pellets fill up the space between the clay blocks and the host rock. Granulated bentonite has been chosen for the floor backfill (foundation bed) in order to provide an even foundation to lay the block-backfill on top of it as shown in Figure 2-6, but the floor material is yet to be finalised (Posiva, 2010).

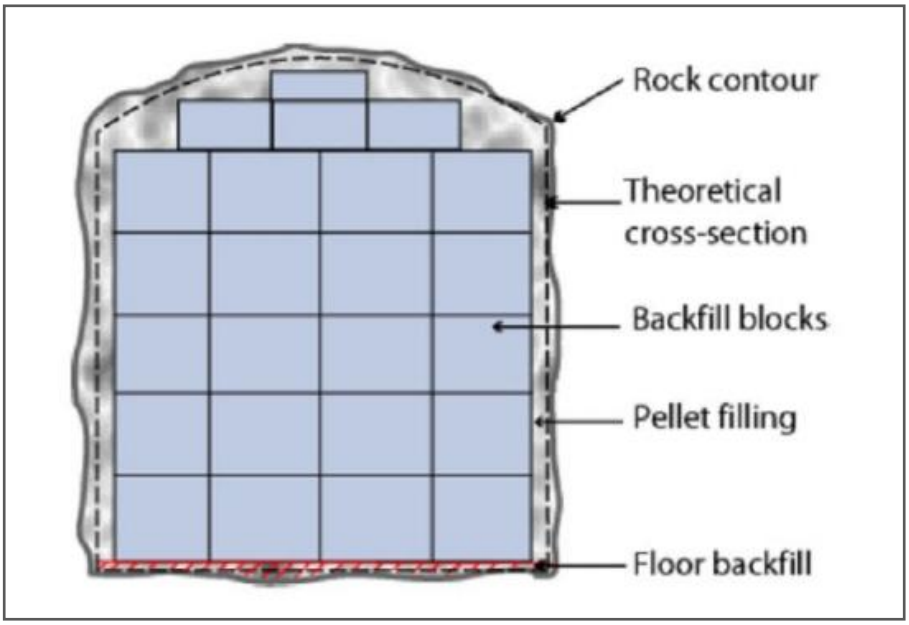

Figure 2-6. Components of tunnel backfilling (Posiva, 2010)

The principal function of the backfill is to ensure the safety of the whole system by keeping the individual barriers in a safety condition. Therefore, the backfill should meet the following requirements (Hansen et al., 2010):

1. Restrict advective transport.
2. Avoid the penetration of the buffer into the backfill.
3. Not affect the safety functions of any barrier.
4. To preserve its functions during the lifetime of the repository.

It is essential to fill up and seal the final disposal facility in such a way that the initial conditions are restored as much as practicable. The backfill prevents the tunnels and shafts from turning into flow routes for groundwater and thus maintains the mechanical stability of the tunnels and the stability of the repository as a whole. Vertical movements of canisters are possible, if the buffer expands into the backfill. The expansion of the buffer also decreases the saturated density of the buffer substantially. The loss of density should be prevented in order to avoid any microbial activities around the canister which would corrode the canister. Therefore the backfill should be designed in such a way that the movement of the buffer is avoided by providing enough resistance against the swelling pressure of the buffer.

As a tunnel backfill material, pellets should fulfil several aspects as outlined by Dixon (2011):

1. Minimize the density loss of the clay blocks by filling up the space between clay blocks and the host rock.
2. Provide short-term mechanical and hydraulic protection to the clay backfill blocks. Pellets can also assure more uniform wetting of the blocks during the saturation progress.

Friedland clay blocks as tunnel backfill material is expected to satisfy the following requirements (Keto, 2004):

1. Low compressibility in order to restrain the upward expansion of the buffer.
2. Resistance against erosion.
3. Low hydraulic conductivity and swelling pressure in order to prevent the advection of groundwater between adjacent blocks.
4. Long-time stability/Long-term performance.
5. No harmful effect on the other barriers. The clay may contain substances such as potassium that can adversely affect the backfill materials and the buffer by increasing the risk of illitization of the buffer or the presence pyrite can increase the corrosion of the copper canister.

Granulated bentonite as floor material is expected to fulfil the following requirements (Hansen et al. 2009):

1. Self-sealing capacity
2. Low hydraulic conductivity (below 1×10^{-10})
3. Good resistance against erosion to minimize the risk of formation of flow paths from backfill to the deposition hole.
4. High bearing capacity to support the weight of the blocks.

Host rock

The main rock type in Olkiluoto bedrock is migmatitic gneiss and several tests have been carried out to ensure that the bedrock it is suitable to shelter the waste disposal. The bedrock should protect the canisters against external impacts, should create mechanically and chemically stable conditions to the repository and limits the amount of groundwater leakage (Posiva, 2010). Nevertheless, some structures in the rock might be water conductive. In this case the situation of the tunnel should be analysed

before the deposition of the canisters and if it is necessary the tunnel will be abandoned.

The bedrock also stops direct radiation emanating from the canisters. If spent fuel would come into contact with groundwater, the substances dissolved would mainly remain in the bentonite and the bedrock.

3. Literature review

3.1. Introduction

Long-term performance of the KBS-3V multi-barrier system depends on several factors such as elevated temperature generated by the spent nuclear fuel, water uptake and subsequent swelling of the bentonite buffer and the backfill during saturation, stress redistribution as a result of the swelling of the buffer and the backfill, rock movements caused by excavation activities during the operational stage of the repository and etc. The above factors can vary significantly from one deposition hole to another (Pastina & Hellä, 2006).

Saturation of the bentonite buffer and the development of swelling pressure are important to dissipate the heat generated by the spent nuclear fuel. However, saturation of the buffer would lead to swelling and subsequent loss of buffer density. Loss of buffer density can adversely affect the copper canister in the following ways: (a) when the density decreases, the buffer becomes more permeable to ground water, which increases the accessibility of the canister surface to sulphides in the groundwater and subsequent corrosion of the copper canister, (b) when the density of the buffer decreases below certain limit it would allow microbial activities, which would induce corrosion of the canister (Pastina & Hellä, 2006).

Therefore, the swelling of the buffer should be controlled in such a way to protect the canister in a long-term. Since the host rock is practically incompressible, the buffer would tend to swell upwards into the deposition tunnel. Therefore, the resistance against the swelling of the buffer should be provided by the tunnel backfill right above the deposition hole. This highlights the importance to study the behaviour of the buffer-backfill interaction in order to control the swelling of the buffer within the limits.

Numerical modelling of the buffer-backfill interaction performed by Korkiala-Tanttu (2009), Börgesson & Hernelind (2009) and Leoni (2012) have emphasized the need for realistic interface shear strength data of tunnel backfill materials and demanded a detailed experimental programme.

A fully saturated buffer and a completely or partially dry tunnel backfill would exist during the early stages of saturation of the deposition tunnels. However, as the saturation progresses the interfaces between tunnel backfill materials would disappear,

leaving the tunnel backfill as a continuous mass. This means that the interface shear behaviour of tunnel backfill materials is crucial during the early stages of saturation (i.e., interfaces exist only when the tunnel backfill is dry) and the internal shear of tunnel backfill materials becomes vital during the later stages of saturation (i.e., interfaces disappear as the saturation progresses and become continuous mass).

The following sections of this chapter describe several aspects of the backfill materials such as origin, chemical composition and physicochemical behaviour. These properties would help to understand the behaviour of these backfill materials under different circumstances such as changing temperatures, varying water content and salinity. Similar studies on the interface shear strength of tunnel backfill materials are also reviewed at the later part of this chapter.

3.2. Swelling clay material as a backfill material

Swelling clay materials, like bentonite, have been chosen for backfilling the deposition tunnels due to their favourable properties. Bentonite is a compound of montmorillonite and other smectites. Its composition makes bentonite to be an expansive clay which is chemically and mechanically stable and adapts itself to plastic deformations (Rautioaho & Korkiala-Tanttu, 2009). Bentonite has a very low water permeability, however, it is permeable to gases (gas permeability, k_g, of up to 2.5 x 10^{-20} m^2) (Horseman et al., 1999). Another feature is that bentonite swells when it comes into contact with water. If a counter pressure is applied and then expanded, bentonite becomes very dense and subsequently exhibits a very low water hydraulic conductivity (in the order of 10^{-12} m/s) and a high swelling pressure, which can reach up to 10 MPa (Ahonen et al. 2008).

Origin

Bentonites are formed due to the alteration of volcanic ash or tuff. After volcanic eruptions, the ashes are deposited as tuff layers. At low temperatures and presence of excess alkali, the tuff reacts with water leading to the formation of the smectites (Rautioaho & Korkiala-Tanttu , 2009).

Bentonite consists of montmorillonite principally (see Figure 3-2). Montmorillonite is a common type of smectite whose structural formula is $(OH)_4Si_8Al_4O_{20}X\ nH_2O$ and has a

theoretical chemical composition of 66.7% of SiO_2, 28.3% of Al_2O_3 and 5.0% of H_2O (Carrasco et al., 2002).

Chemical description

Afore mentioned, the predominant mineral in bentonite is montmorillonite. This type of smectite is a phyllosilicate which has a laminate structure where each layer is formed by an octahedral central sheet that is sandwiched between two sheets of tetrahedrally coordinated cations, generally known as 2:1 structure (Figure 3-1). This 2:1 layer structure is difficult to be disturbed (Rautioaho & Korkiala-Tanttu, 2009). However, during the hydration of bentonite, water molecules can get into the interlayer space and consequently make the bentonite swell (Karnland et al., 2006).The octahedral sheet has aluminium (Al^{3+}) as the cation and the two tetrahedral sheets have silicon (Si^{4+}) as the central cation. Some of them are substituted by cations of lesser charge, causing that the layers are not electrically neutral and therefore it is needed the existence of cations in the interlayer space. The most common are alkali cations (Na^+ and K^+) or alkaline (Mg^{2+} and Ca^{2+}).

Swelling properties of bentonite are largely affected by the type of the compensating cation. For example, the sodium bentonite (Na-bentonite) expands to a greater volume of up to twenty times of its original volume in the presence of water at ambient temperature and atmospheric pressure. On the other hand, the calcium bentonite (Ca-bentonite) expands only five times of its original volume (Carrasco et al., 2002).

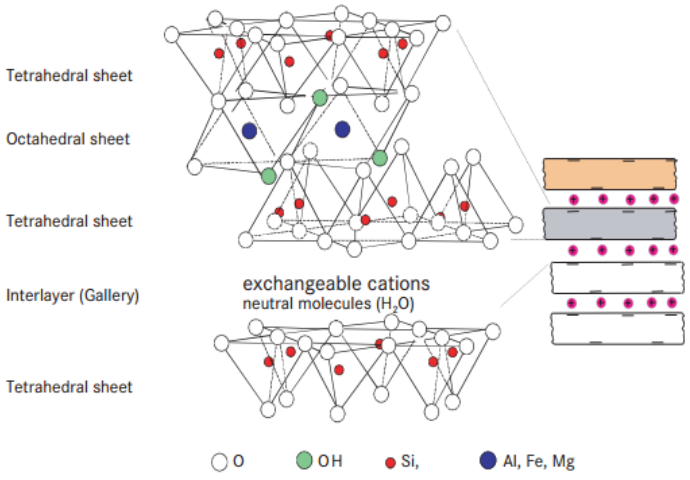

Figure 3-1. Basic units of smectite structure (Grim & Güven, 1978)

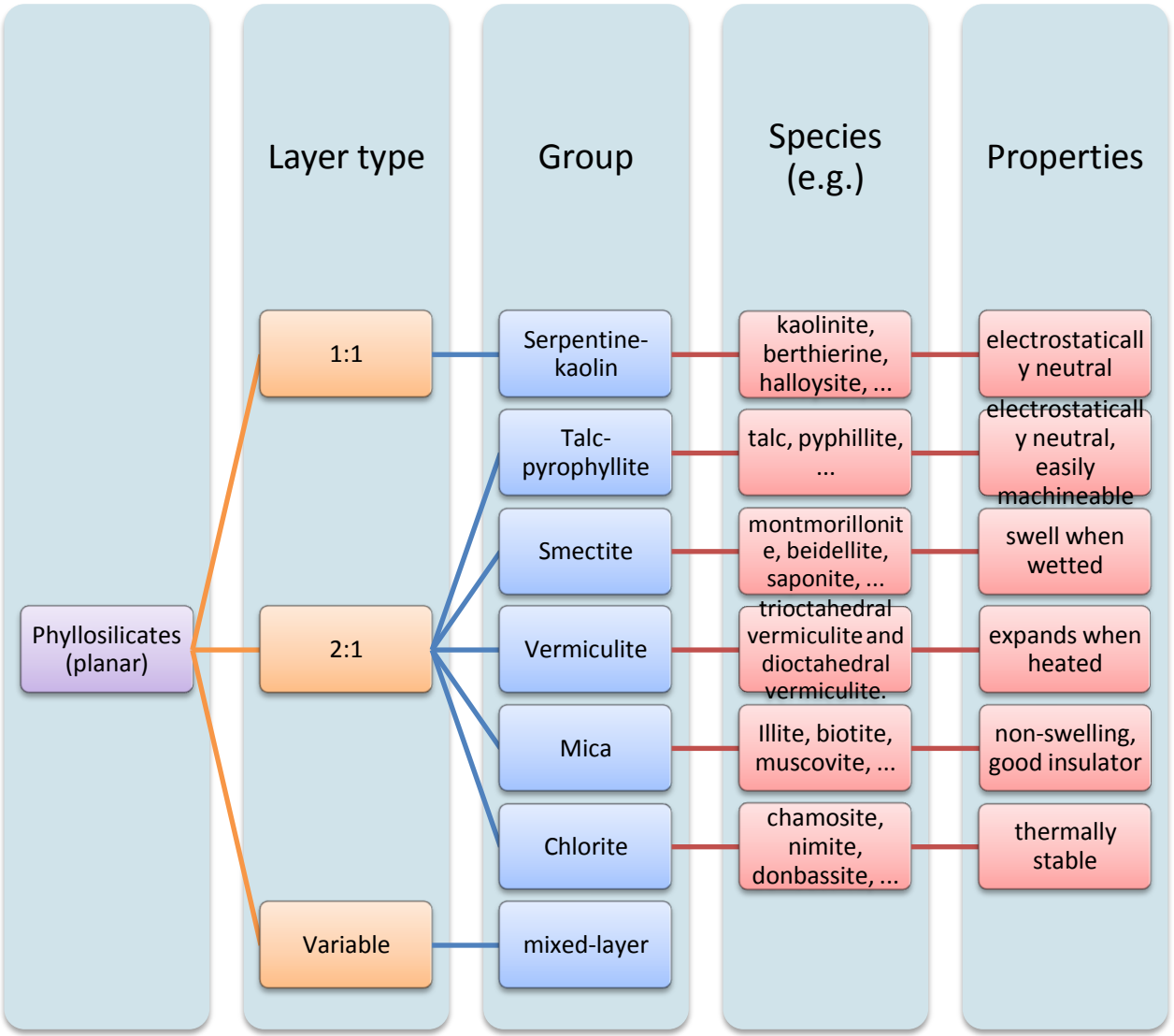

Figure 3-2. Classification of phyllosilicates (clay minerals)

Types of bentonite proposed

Characteristics of bentonite can vary depending on its origin and the cations that have been exchanged. The dominating cation is often used to describe the type of the bentonite. In order to know which type of bentonite is most appropriate for backfilling KBS-3V tunnels, several bentonites have been considered in the past (Table 3-1) (Rautioaho & Korkiala-Tanttu , 2009).

Table 3-1. Summary of bentonites evaluated (Rautioaho & Korkiala-Tanttu, 2009)

NAME	TYPE OF SWELLING CLAY	ORIGIN	MONTMORILLONITE CONTENT (%)	OTHER COMPONENTS
MX – 80 bentonite	Sodium bentonite	Wyoming, USA	65-85	quartz, feldspars, cristoballite, calcite and pyrite
FEBEX bentonite	Montmorillonite-illite mixed layer	Cortijo de Archidona, SPAIN	> 90	quartz, plagioclase, K-feldspar, calcite and opal-CT
Milos bentonite	Calcium bentonite	Isle of Milos, GREECE	75-80 (high grade)	calcite, quartz, plagioclase and pyrite
Friedland clay	Mixed-layer mica/montmorillonite	North-eastern Germany	45	quartz, mica, chlorite, feldspar, carbonate and kaolinite

- **MX-80 bentonite**

MX-80 bentonite originates from Wyoming, USA. This type of bentonite was formed by hydrothermal alteration of volcanic ash during the Cretaceous period. It is a Na-bentonite which consists mainly of montmorillonite (65-85%), quartz (4-12%) and feldspars (5-8%). It can also contain small amounts of cristobalite, calcite, pyrite and possibly traces of gypsum, illite and amphibole. The natural water content is in the range of 8 to 11% (Rautioaho & Korkiala-Tanttu, 2009).

- **Milos bentonite**

The Milos clay deposits on the isle of Milos, Greece were formed as a result of hydrothermal alteration of volcanic rocks during the Tertiary period. The Milos bentonite is non-activated Ca-bentonite and it has two different types, namely, high-grade and low-grade. The montmorillonite content of high-grade Milos Ca-bentonite is in the range of 75 to 80%. It also contains calcite (5-15%), quartz (<5%), plagioclase and pyrite. The low-grade Milos bentonite contains small amounts of smectite-group minerals. This type of bentonite can be found in large quantities and cheaper than high-grade bentonite (Rautioaho & Korkiala-Tanttu, 2009).

- **Friedland clay**

Friedland clay is a smectite-rich clay from north-eastern Germany. This is tertiary origin clay and was formed by a complex process including sedimentation, weathering, erosion and hydrothermal alteration. Its swelling component consists of mixed-layer mica/montmorillonite (45%) apart from other minerals, such as quartz (24%), mica (13%), chlorite (11%), feldspar (5%), carbonate (2%) and kaolinite. The predominant exchangeable cation is Na^+ but other cations can also be exchangeable, such as Ca^{2+}, Mg^{2+} and K^+ (Rautioaho & Korkiala-Tanttu, 2009).

Friedland clay is chemical stable. This means that when the Friedland clay comes into contact with salty water, the changes in its properties are not as dramatic as those in bentonite (Keto, 2004). However, on the downside, Friedlany clay has very grain size, which makes the in-situ compaction not technically feasible Due to this reason, precompressed Friedland clay blocks are formed for tunnel backfilling purposes (Pusch, 1998).

3.3. Factors affecting the behaviour of backfill materials

Among several other factors affecting the behaviour of bentonite based clays, it has been identified that the temperature, water content and the salinity of the ground water plays a major role. It has been reported in the literature that the swelling pressure of the bentonite buffer in a deposition hole is largely affected by the ground water salinity and the change in density of the bentonite (Rautioaho & Korkiala-Tanttu, 2009). This section reviews the factors affecting the performance of bentonite in the context of a KBS-3V type repository barrier.

3.3.1. Temperature

A series of research studies have been carried out over the past few years to understand the effect of elevated temperatures on the engineering properties and the performance of backfill materials. After the installation of the canister, the temperature in the deposition tunnels is expected to vary in the range of +33°C to +55°C for the first hundreds of years, and it is expected to decrease afterwards (Pastina & Hellä, 2006; Hansen et al., 2010). According to Karnland & Birgesson (2006), the expected evolution of the temperature in a KBS-3V deposition hole is shown in Figure 3-3. The temperature in the backfill is expected to be lower than that in the deposition hole.

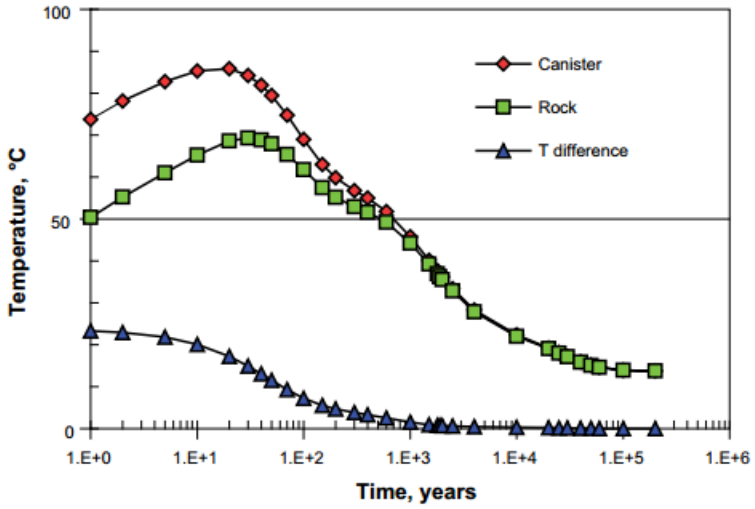

Figure 3-3. Temperature evolution in a KBS-3 deposition hole (Karnland & Birgesson, 2006)

Contradicting findings have been reported in the literature regarding the effect of temperature on the interface shear strength of backfill materials. According to Graham et al. (2001), temperature changes can cause positive and negative effects on the shear strength of a particular material since the end result depends on several other factors such as over consolidation ratios (OCRs), drainage conditions, and direction of temperature change (increase or decrease). Heating and (or) cooling may produce changes in the structure and thickness of the material and also the viscosity of the water. These changes can produce significant differences in the compressibility and strength of the material. Graham et al. (2001) concluded that the heating under drained conditions while keeping the effective pressure constant, leads to increased

strength. On the other hand, heating without providing drainage to the sample caused just the opposite effect due the pore water pressure increment.

Marques et al. (2004) studied the influence of the temperature on the behaviour of an over consolidated clay (OCR between 1.8 and 2.4) from St-Roch-de-l'Achigan, Quebec, Canada. Basic characterization tests, oedometer compression tests with permeability measurements, constant rate of strain (CRS) oedometer tests and triaxial isotropic compression tests were performed under constant temperatures varying between +10ºC and +50ºC. It was found that in triaxial tests the vertical yield stress and the entire limit state curve were temperature dependent, lowering the peak strength envelope when temperature increases (Figure 3-4).

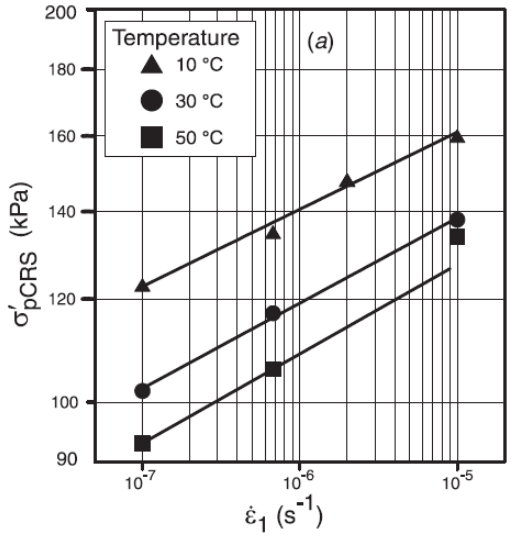

Figure 3-4. Influence of temperature on the vertical yield stress (Marques et al., 2004)

The Swedish company, SKB, which is responsible for the nuclear and radioactive waste management in Sweden, carried out a study called Temperature Buffer Test (TBT) in order to analyse the behaviour of buffers at elevated temperatures during the water saturation of deposition holes (Åkesson, 2012). Two steel heaters were placed in a KBS-3V type deposition hole to simulate the copper canister and were surrounded by compacted bentonite buffer (MX-80). The aim of this study was to measure the temperature, total pressure, pore pressure and relative humidity of the buffer as a result of the heat generated by the steel heaters over a period of 7 years. After the testing period, the buffer was removed and tested for hydro-mechanical and chemical-mineralogical properties were determined in order to compare with its original

properties. The results showed a reduction in swelling pressure, especially for the innermost part of the buffer and an increased hydraulic conductivity, which consequently means a reduction in the shear strength.

3.3.2. Water content

The effect of temperature on soils is closely related to their water retention capacity. Under a thermal gradient, the initially unsaturated compacted bentonite develops both liquid water and vapour flows, which in turn contribute to heat redistribution by advection (Åkesson et al., 2009). Nevertheless, Börgesson et al. (2001) analysed the hydraulic conductivity of water saturated buffer material in an oedometer at different temperatures and found that the influence of the temperature was almost entirely on the change in viscosity of the water.

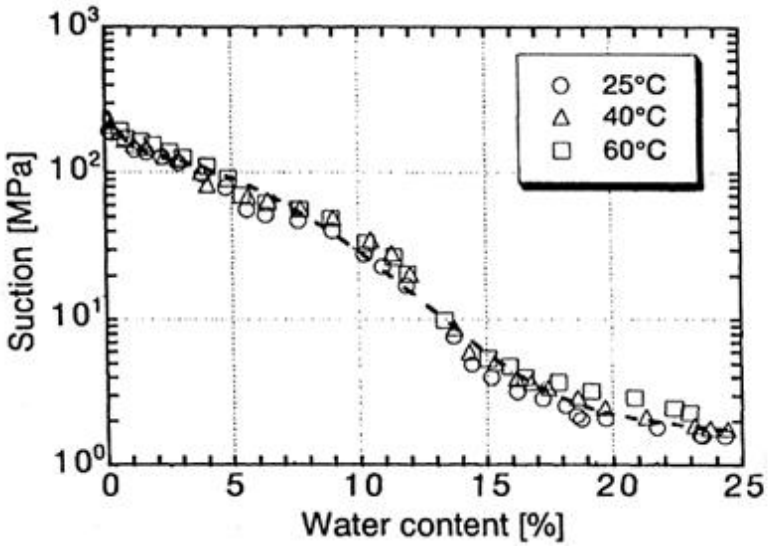

Figure 3-5. Water retention curve of OT-9607; Na-bentonite from Japan (Börgesson et al., 2001)

The design of KBS-3V engineered barriers includes compacted Friedland clay blocks, which are initially unsaturated and hence they would be affected by suction. Börgesson et al. (2001) measured the suction (negative water pressure) of the water unsaturated bentonite as a function of the water content and the temperature. The findings are shown in Figure 3-4 with the suction plotted as a function of the water content. It can be noted from Figure 3-5 that the influence of temperature is small.

Sivakumar et al. (2013) state that, in general, for an unsaturated compacted clay an increase of suction leads to a decrease of shear strength and reduction of stiffness. Consequently, an increase of water content will lead to a decrease of shear strength. In addition, Tonnizam et al. (2011) state that the water content has a high impact on the shear strength of older alluvium (semi cemented sediment), reducing the friction angle and cohesion as the amount of water increases. This is because the water lets the particles to slide between them easily and eventually decreasing the frictional resistance. In addition, the bond between the particles is reduced since the water tends to increase the distance between them, so the attractive forces decrease and consequently, the cohesion. The attractive forces of Van der Waals are inversely related to the square root of the distance between the particles. In other words, the higher the distance, the lower the attractive forces (Fowkes, 1964).

3.3.3. Salinity

The salinity of the groundwater is another factor that influences the shear strength of the backfill materials. The initial salinity at present at repository depth (~420 m below ground level) is in the order of 1% TDS (10 g/l). TDS is the abbreviation for "Total Dissolved Solids", which is a measure of the inorganic and organic substance contents present in a liquid, and hence it is generally used to explain the salt content in freshwater. The salinity of the groundwater at Olkiluoto site increases with depth and it is experted to increase in long-term. During the lifetime of the repository, a maximum local TDS concentration in the order of 7% (70 g/l) is expected at the repository level (Dixon et al., 2011).

Warkentin & Yong (1960) stated that the shear strength parameters are related to interparticle forces. The force of repulsion between the particles decreases with increasing salt concentrations. Therefore, the shear strength is expected to increase with the increasing salinity of the water due the increased interparticle attractive forces. Furthermore, at high salt contents, the montmorillonite can form a flocculated structure resulting in higher shear strengths.

3.4. Previous studies on interface shear strength

Interface shear strength of Finnish KBS-3V type tunnel backfill materials has been previously studied by means of laboratory experiments (Kuula-Väisänen et al., 2007; Gallardo, 2012) and by using Finite element modelling tools (Korkiala-Tanttu, 2009; Börgesson & Hernelind, 2009; Leoni, 2012).

Finite element modelling s is used to predict the performance and the behaviour of the tunnel backfilling components and the buffer at different stages of saturation. When the saturated buffer swells, it penetrates into the tunnel backfill by creating several shear planes within the backfill (Figure 3-6). Shear planes that exist along the backfill material interfaces plays a major role in limiting the swelling of buffer. By using different interface shear strength parameters in a finite element model, the swelling of the buffer can be calculated. It is therefore possible to predict the swelling of the buffer in a long-term. It also provides long-term safety evaluations involving the evolution of backfill and buffer (Korkiala-Tanttu, 2009).

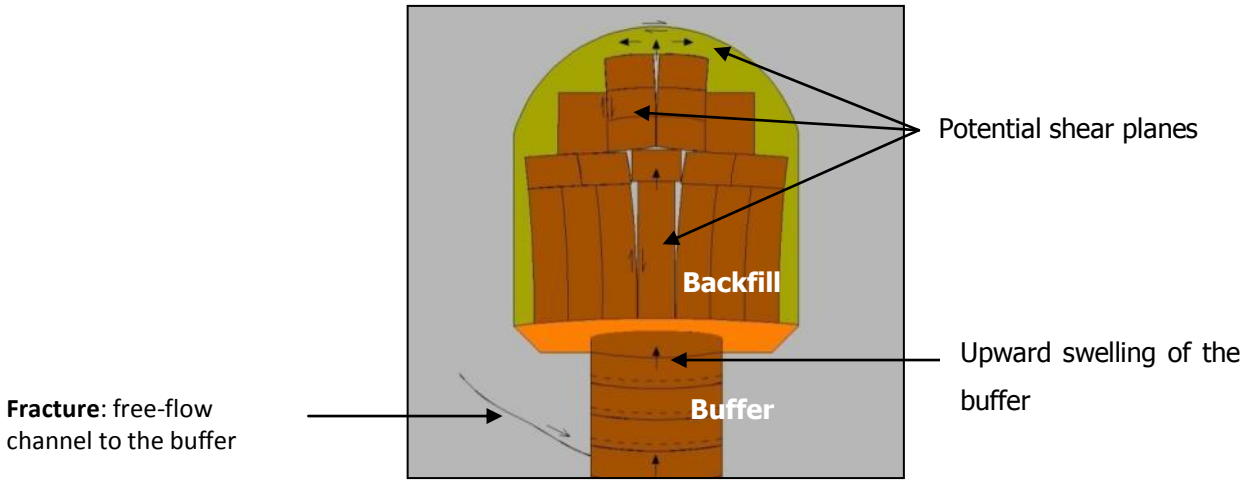

Figure 3-6. Potential shear planes in the tunnel backfill

In order to determine the maximum heave of the saturated buffer, Leoni (2012) carried out a numerical modelling study in which a fully saturated buffer and a completely dry tunnel backfill were considered as worst-case scenario. When the backfill is dry (i.e., when no opposing swelling pressure created by the tunnel backfill against the swelling buffer), it is possible for the saturated buffer to swell and penetrate into the tunnel backfill (Figure 3-6). If the upheaval of the tunnel backfill

exceeds certain limit, it would lead to a substantial decrease in the buffer density. According to the current KBS-3V proposal, the saturated density of the buffer right above the canister should not decrease below 1950 kg/m^3 at all times in order to protect the copper canisters from corrosion, by preventing microbial activities. An upper bound for the saturated buffer density of 2050 kg/m^3 has also been proposed. This is to prevent the host rock from possible damages that can be caused as a result of high swelling pressures in the range of 10 MPa (Juvankoski & Marcos, 2010). As the swelling directly influences the saturated buffer density, it must be controlled in such a way so as to ensure the saturated density is kept within the narrow limit mentioned above.

Mohr-Coulomb's parameters have been used by Leoni (2012) to determine the interface strength for the done calculations. Some of those parameters were assumed with a linear elastic constitutive law while others were taken from laboratory test results reported by Korkiala-Tanttu et al. (2007) and Johannesson et al. (2010). Table 3-2 show the soil strength parameters.

Table 3-2. Interface strength parameters (Leoni, 2012)

INTERFACES	c (kPa)	φ (°)
Block/block	0.0	24.0
Buffer/rock	0.0	8.69
Pellet/rock	0.0	10.0
Pellet/buffer	0.0	5.0
Foundation/rock	0.0	10.0
Foundation/block	0.0	5.0
Foundation/buffer	0.0	5.0
Foundation/pellet	10.0	27.0
Canister/buffer	0.0	5.0

Considering the above density limit, a maximum heave of 141 mm for the backfill has been reported by Leoni (2012) based on theoretical calculations. 2D model calculations with PLAXIS 2D were performed considering the interface shear strength parameters in Table 3-2. The used geometry was the one that is planned to be erected in Olkiluoto waste disposal and an axisymmetric case was used and the backfill was modelled as discrete blocks system (Figure 3-7). Taking into account these assumptions, a maximum calculated heave of less than 100 mm was obtained.

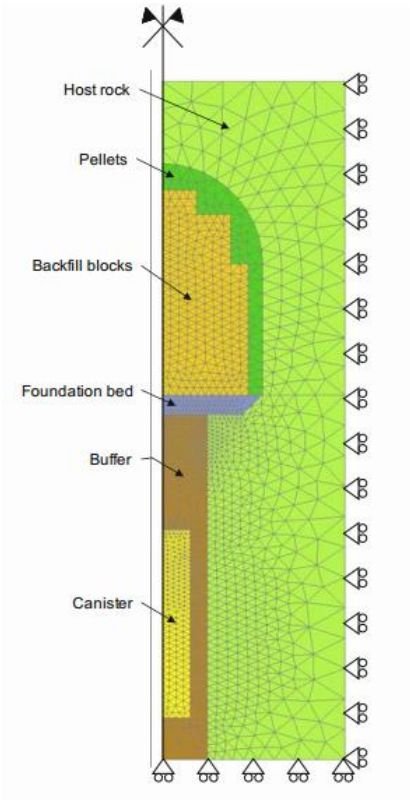

Figure 3-7. Axisymmetric model in PLAXIS 2D (Leoni, 2012)

Börgesson & Hernelind (2009) have also carried out several studies on the behaviour of the KBS-3V repository system. These studies have included in the third phase of the BACLO project (BAckfilling and CLOsure of the deep repository), which was a project to develop the backfilling concept. They used ABAQUS, which is a 3D finite element model, to perform a model to predict the mechanical interaction between the buffer and backfill in following conditions:

a) saturated buffer and dry backfill
b) saturated buffer and saturated backfill

In both cases, a quarter of a deposition hole and tunnel section was modelled having three symmetry planes yielding a model of a long tunnel with the deposition holes separated 6 m (Figure 3-8). The interface shear strength between the surfaces was included in this model and Mohr Coulomb's parameters were estimated as follows: a varying friction angle (ϕ) of 17.4º, 8.7º, 4.35º and 0º and without cohesion. The results showed that the friction angle had a great influence in the upheaval movement. The non-real scenario of no friction led to a vertical movement of 150 mm. This vertical movement corresponds to a buffer density less than 19.5 kN/m^3 and they

concluded that for satisfying this density criterion the friction angle should be higher than 8º.

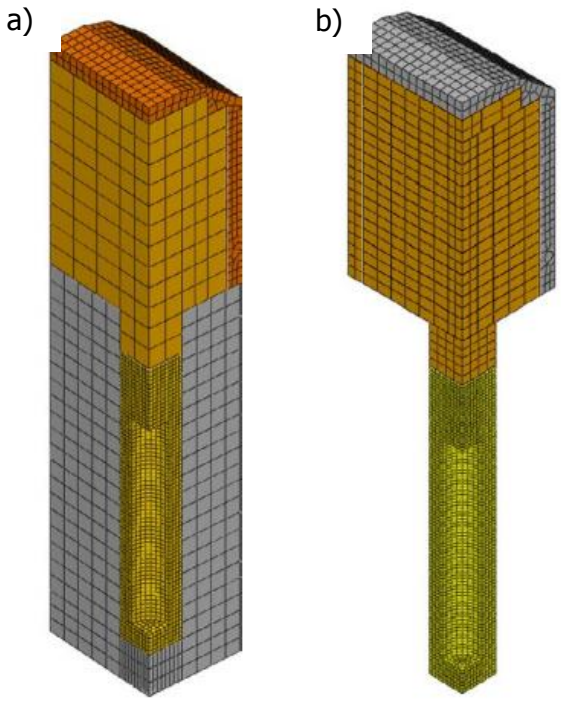

Figure 3-8. Finite element model with ABAQUS (a) with wet backfill and (b) with dry backfill (Börgesson & Hernelind, 2009)

Interface shear strength of identical tunnel backfill materials has been previously studied by Gallardo (2012) at Aalto University as part of KYT project. In this study, several interfaces were studied in natural state of the material with same direct shear apparatus. Samples with the dimension of 300 mm x 300 mm were tested in this study. Table 3 – 3 shows the initial properties of the tested materials from Gallardo (2012).

Table 3 – 3. Summary of initial properties of tested materials (Gallardo, 2012)

MATERIAL	ρ (kg/m^3)	ρ_d (kg/m^3)	w (%)	e_o	S_R (%)
Friedland clay block	2000	1880	6.24	0.484	37
Pellet	1140 – 1320	970 – 1130	17.40	1.57 – 1.87	26 – 33
Granulated bentonite	1290 – 1320	1080 – 1090	19.3 – 20.8	1.52 – 1.55	35 - 38
Foundation bed material[1]	1370 – 1380	1190 – 1230	12.7 – 15.5	1.20 – 1.27	29 - 33

[1] Foundation bed material is a mixture of AC-200 bentonite and crushed rock (50/50) that is no longer tested

The tested interfaces were block/block, block/pellet, block/granulated bentonite and block/foundation bed material. The resulted cohesion and friction angle from each test can be seen in Table 3 – 4. Figure 3 – 9 shows the corresponding Mohr-Coulomb failure lines which relate the applied normal stress (σ) and the resulted shear stress (τ) from each test.

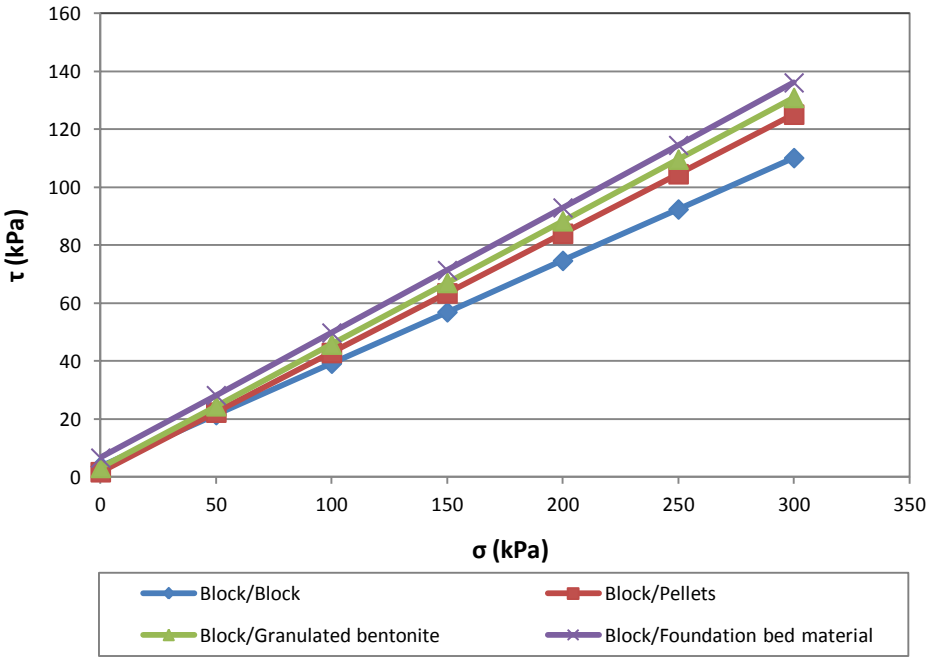

Figure 3 – 9. Mohr-Coulomb failure lines (Gallardo, 2012)

Table 3 – 4. Obtained strength parameters in direct shear box (Gallardo, 2012)

TEST	c (kPa)	φ (°)
Block / Block	3.70	19.50
Block / Pellets	1.69	22.36
Block / Granulated bentonite	3.17	23.06
Block / Foundation bed material	6.56	23.35

A similar study was done by Kuula-Väisänen et al. (2007) at Tampere University of Technology, Finland. Direct shear tests were performed to determine the shear strength parameters of the block/block interface in natural state and with the presence of both fresh and salt water (3.5% NaCl) in the interface. Cylindrical specimens with a diameter of 50 mm and a height of 50 mm were used in this study. Different axial stresses ranging between 100 and 800 kPa were applied to the specimen. The shearing rate was about 1.6 mm/min. The amount of water was 2g and 4g depending

on the test, which correspond to 250 g/m^2 and 500 g/ m^2, respectively. The results are summarized in Figure 3-10 and Table 3-5.

Table 3 – 5. Summary of friction test results (Kuula-Väaisanen et al., 2007)

TEST	c (kPa)	φ (°)
Dry test	0.7	24.4
Tap water 2g	16	18.4
Saltwater 2g	66.3	12.3
Saltwater 4g	13	18.5

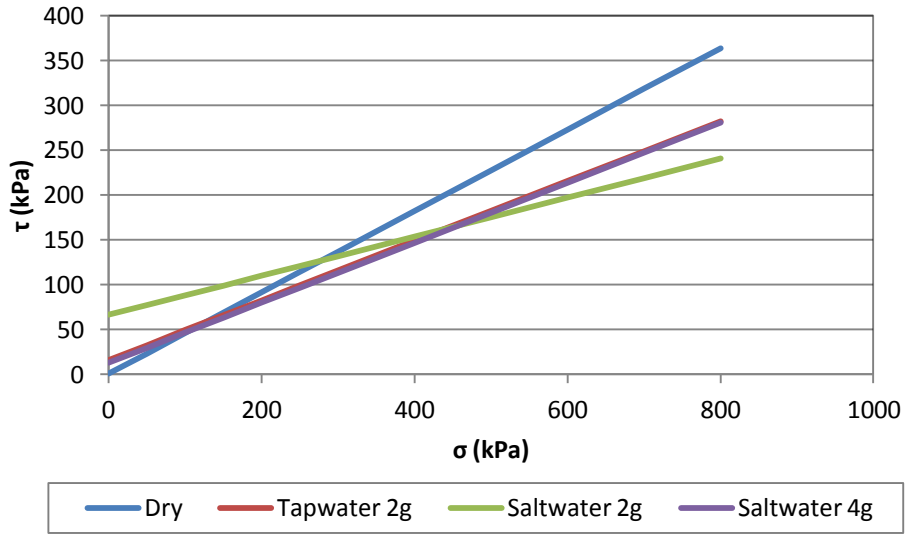

Figure 3 – 10. Obtained results for Mohr-Coulomb failure lines (Kuula-Väisänen et al., 2007)

To summarise, taking into account the assumptions made by Leoni (2012) and Börgesson & Hernelind (2009), the shear strength parameters used were conservative and could overestimate the vertical displacement of the buffer. In other words, if the experimental results from Kuula-Väisänen et al. (2007) and Gallardo (2012) were used in the modelling of the buffer-backfill interaction, it would predict more accurate vertical displacement and heave of the buffer and the backfill, respectively.

4. Materials

4.1. General

Clay based materials with swelling potential have been proposed for the tunnel backfilling in the Finnish KBS-3V type repository and hence used in the present study. The tested clay materials were Friedland-clay blocks, Cebogel QSE pellets and granulated bentonite. These materials were supplied by Ekokem Oy in Riihimäki, Finland. Cebogel QSE Pellets and granulated bentonite were received in plastic bags inside air-tight buckets. Precompressed Friedland clay blocks were received on a pallet which was immediately covered with plastic sheets in order to prevent any moisture loss from the blocks and to maintain the natural water content.

4.2. Cebogel QSE pellets

Cebogel QSE pellets consist of high quality sodium activated Milos Ca-bentonite, pressed to form cylinder shaped pellets with an average diameter of 6.5 mm and a varying length of 5 to 20 mm. It has montmorillonite content of 80 % and the initial water content is 13%. According to the manufacturer's specifications, pellets have a dry density of 2.10 kg/m^3 and a bulk density of 1.10 kg/m^3 (Keto et al., 2009).

Figure 4-1. Cebogel QSE Pellets (Scale is in cm)

Keto et al. (2009) reported liquid limit (LL) of 576% and swelling index of 11.9 ml/g to 14 ml/g. The liquid limit was found to be 343% in the present study, which is much lower than the value reported by Keto et al. (2009).

Sandén et al. (2008) also investigated the swelling pressure and the hydraulic conductivity of Cebogel QSE pellets. They reported swelling pressure of about 45 kPa and hydraulic conductivity 4.3 x 10^{-11} m/s.

4.3. Friedland clay blocks

Uniaxially compressed Friedland clay blocks were made from Friedland clay. The block had a dimension of 300 x 147 x 75 mm as shown in Figure 4-2. The initial water content was approximately 6%. The average bulk density for Friedland clay blocks was 2150 kg/m^3 and the dry density 1820 kg/m^3 (Hansen et al., 2010).

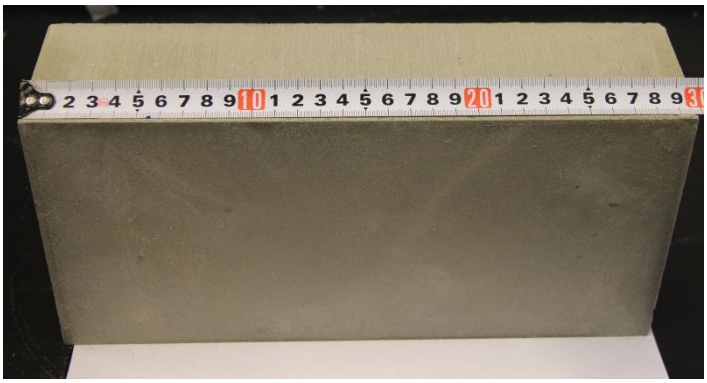

Figure 4-2. Friedland-clay block (Scale is in cm)

4.4. Granulated bentonite

Granulates of smectite-rich clay are in the form of crushed raw clay. The difference between granulated bentonite and bentonite pellets is that the pellets are manufactured from raw bentonite by compaction, while the granules consist of raw bentonite "lumps" (see Figures 4-1 & 4-2)). Due to this reason, individual pellets have higher density than individual granulates of bentonite. While manufacturing the granulated bentonite, the size of the crushed material can be chosen to achieve a continuous particle size distribution. This material has been proposed as foundation bed between the buffer and the blocks, at the base of the tunnel. However, granulated bentonite can cause problems while installation and compaction due to its workability at high water contents. Therefore, water contact should be avoided until the material is

placed in its desired location (Dixon, 2011). It should also be noted that particle size and high water content makes it difficult to spray it around the block backfill and hence pellets are preferred in this case.

The average initial water content of the granulated bentonite that was used in this study was around 20.5 %.

Figure 4-3. Granulated bentonite (Scale is in cm)

5. Testing program

5.1. Equipment

Two types of direct shear apparatus were used in order to carry out the testing programme; namely, large (300mm x 300 mm x 174 mm) and small (60 mm x 60 mm x 44 mm) shear box. Both consist of an apparatus structure, a shear box, a load plate and a load hanger. Furthermore, three transducers and a data logger are used to log the test data automatically to a computer.

The standard used to carry out the direct shear box tests was the European standard CEN ISO/TS 17892-10:2004.

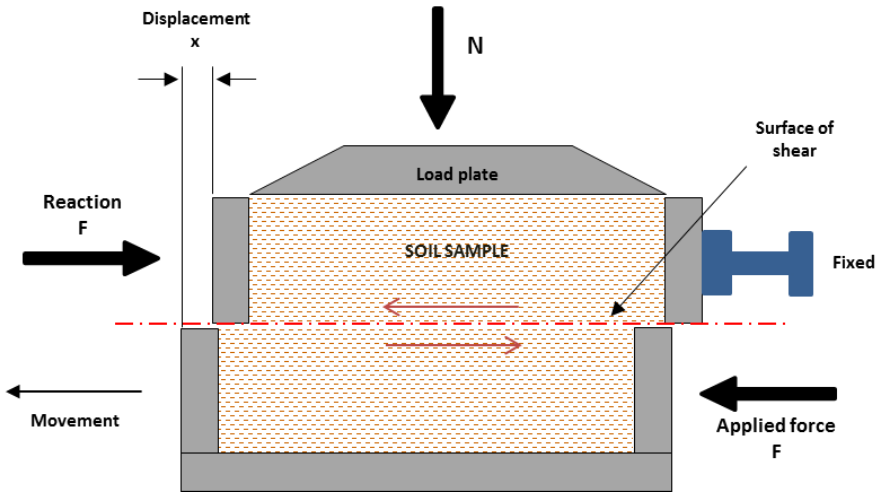

Figure 5-1. Direct shear box apparatus (Gallardo, 2012)

5.1.1. Apparatus structure

The large shear box apparatus consists of an electric motor, a load beam, a loading system and a hydraulic pressure system as shown in Figure 5-2. The function of the electric motor is to apply the required force to drive the lower half of the shear box while shearing. The user has an option to alter the rate of shearing by adjusting the speed of the motor. In this testing programme a shearing rate of 0.5 mm/s was used. The horizontal movement is transmitted by a piston connected to this motor. The role of the load beam is to support the load which was needed to apply the normal load to the sample.

Moreover, the hydraulic pressure system helps to align the placement of the load beam in the correct position, so that the load can be transmitted and the normal stress can be applied to the sample.

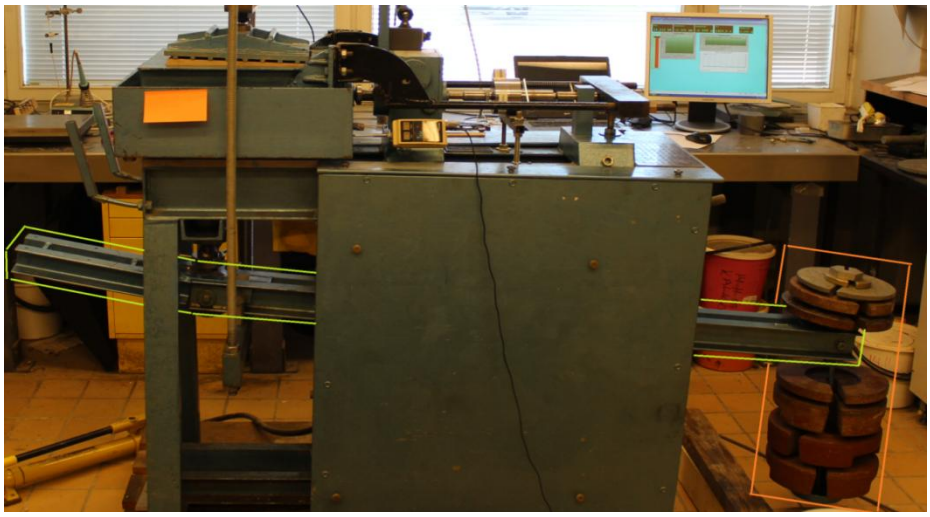

Figure 5-2. Load beam and loading system. Large shear box (Gallardo, 2012)

The small direct shear box has a more simple testing system. It only consists of an electric motor which transformed the energy into a rotational movement of a wheel. The task of this wheel is to apply the shear force. The load hanger is in charge for transmitting the normal stress which is explained later in section 5.1.4.

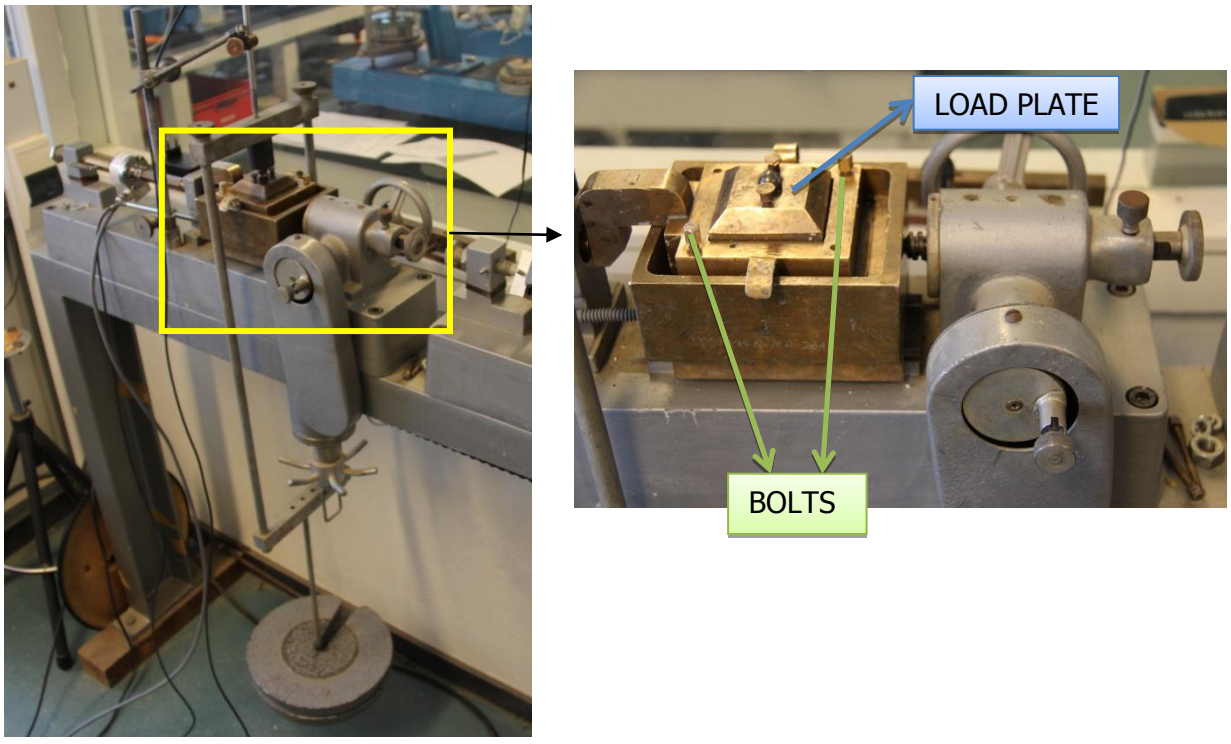

Figure 5-3. Small direct shear box set-up

5.1.2. Shear box

Shear box consists of two halves, namely, upper-half and lower-half. Samples are placed inside the shear box and adjusted, depending on the sample dimensions, in such a way that the interface between two materials aligns with the plane between both halves of the shear box.

During the consolidation, both halves of the shear box are aligned properly and connected tightly with two bolts. Vertical stress was applied to the test specimen while no horizontal movement was allowed. Upon the completion of the consolidation stage, both bolts were removed and the shearing started. During shearing, the lower-half was driven at a constant rate while the upper-half was fixed.

5.1.3. Load plate

The load plate converts the applied vertical load to a force which is uniformly distributed over the whole surface of the sample. The weight of the load plates of the large and small shear boxes are 13.792 kg and 0.382 kg, respectively.

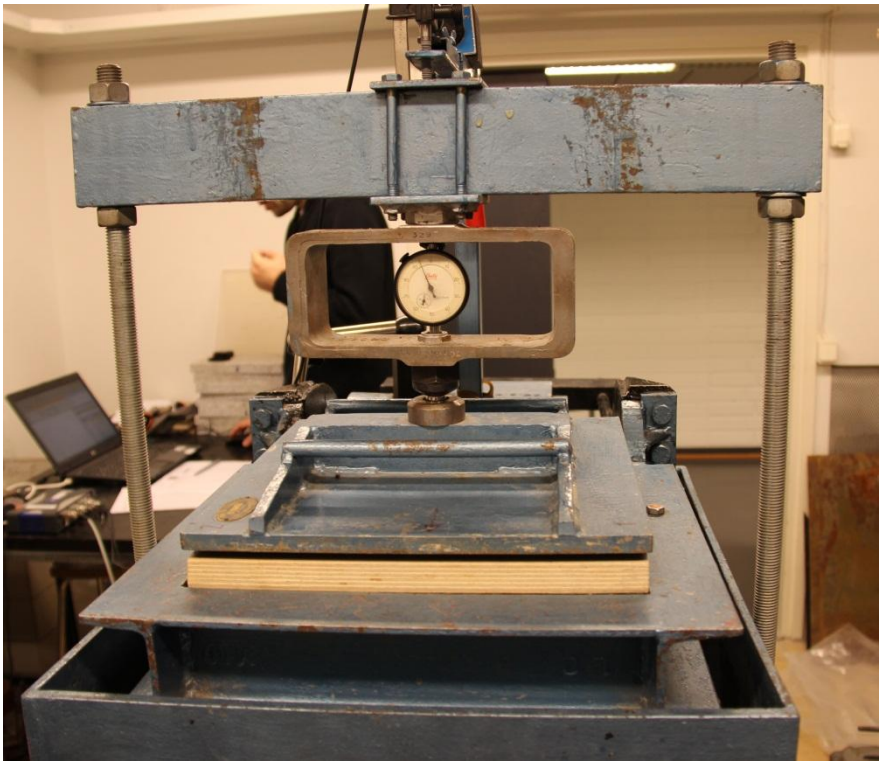

Figure 5-5. Load plate and load hanger (large shear box)

In case of the large shear box, a smooth wooden plate with an average thickness of 20.65 mm was placed between the load plate and the top of the sample to provide an even surface and thus the normal force would be evenly distributed on the sample.

5.1.4. Load hanger

The load hanger transfers the entire normal load to the load plate. In the case of the small shear box, the load was applied directly to the load hanger as it is shown in Figure 5-3. The weight of the load hanger in the small shear box apparatus was 5.465 kg. In the large shear box apparatus, the load hanger was connected to a load beam which weighed 32.703 kg. A dial gauge was placed between the load plate and the load hanger to measure the compressive force that was transmitted to the sample (Figure 5-5).

5.1.5. Transducers

Transducers were used to measure the displacement and the shear force in each test. In total three transducers were used; two of them were used to measure the vertical and horizontal displacements while the third transducer was used to measure the horizontal shear force. The transducer that was measuring the vertical displacement was placed above the load hanger and the horizontal displacement transducer was placed in such a way to make contact with the lower-half which was the moving part of the shear box.

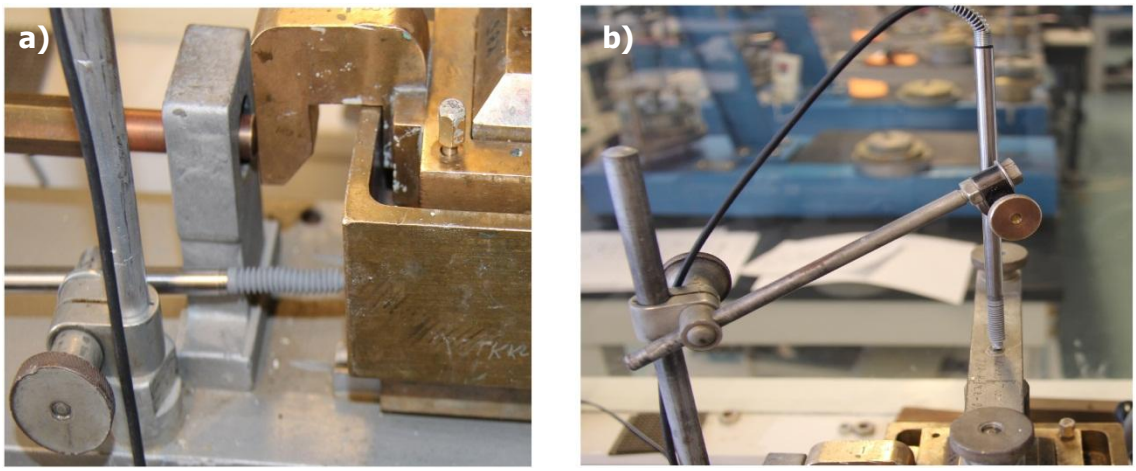

Figure 5-7. Alignment of (a) Horizontal and (b) vertical transducers

In the large shear box, the transducer that was measuring the shear force was connected to the piston applying the shear force. In the small shear box transducer was connected to the piston that received the reaction force that was in contact with the upper-half. In the large shear box apparatus, transducer with a measuring capability of 200 kN was used while in the small shear box, transducer with a measuring capability of 20 kN was used.

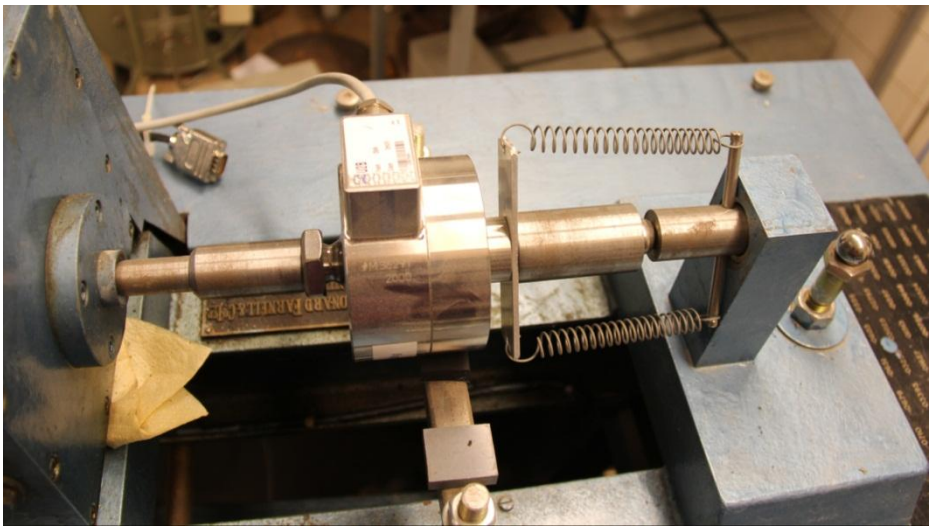

Figure 5-8. Shear force transducer (large shear box)

5.1.6. Computer and software

All transducers were linked to a hub which collected the data. This hub was then connected to a computer in which CatmanAP v3.3.1, a software programme was installed to process the data.

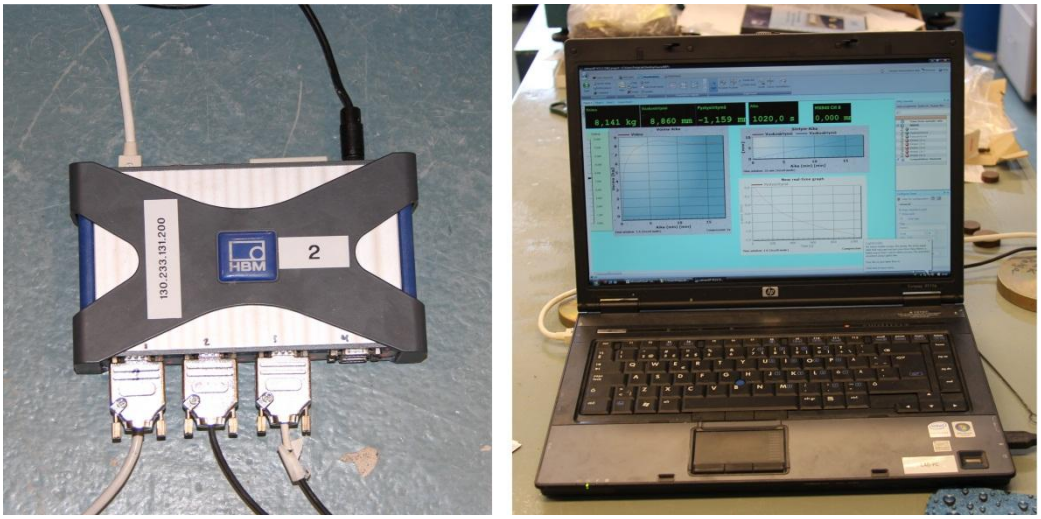

Figure 5-9. Hub and CatmanAP v3.3.1 software

5.2. Methodology

All the direct shear box tests were carried out according to the technical specifications given in the European standard CEN ISO/TS 17892-10:2004. Following steps were carried out according to the above standard:

1) Preparation of specimen:
    a) The specimen was prepared and placed in such a way without affecting its original properties or with minimum disturbance
    b) The specimen was placed inside the shear box and the upper and lower halves of the shear box were clamped together.
    c) Due to practical difficulties, the specimens were weighed after each test even though the above standard suggests a pre-test measurement.

2) Testing procedure:
    a) Consolidation stage:
        - Pre-determined normal stress was applied allowing the specimen to drain excess pore water.
        - Vertical deformation was recorded until the consolidation was complete.
    b) Shearing:
        - The clamp was removed and the lower half was allowed to move horizontally.
        - The specimen was sheared at a constant rate of 0.5 mm/s.
        - Displacements (vertical and horizontal) and the shear force were measured. Shearing load was applied very slowly, in order to allow the pore pressure to dissipate.
        - Once the test was completed, the sample was removed from the box and weighed in order to determine the final water content.

5.3. Testing program

A total of 112 direct shear box tests, including both interface and internal were carried out as summarized in Table 5-1 to Table 5-4. Table 5-1 show the testing program for internal shear strength while varying the water content of the granular material. Then, Table 5-2 and Table 5-3 are referred to those tests performed to study the temperature and salinity effect to the block/block interface shear strength. Finally, Table 5-4 is related to the changes in water content of the granular material as well as the water content of the interface while studying the shear strength of block/granular material interface.

Table 5-1. Internal shear strength testing program (Small shear box)

TEST	Date	Material
Pellet 1-9	November 2012	Cebogel QSE Pellets (natural water content)
Pellet 10-17	November 2012	Cebogel QSE Pellets (20 % water content)
Pellet 18-25	November 2012	Cebogel QSE Pellets (30 % water content)
Pellet 26-29	December 2012	Cebogel QSE Pellets (40 % water content)
Pellet 30-35	December 2012	Cebogel QSE Pellets (50 % water content)
Gran.bent 1-5	December 2012	Granulated bentonite (natural water content)
Gran.bent 6-9	December 2012	Granulated bentonite (40% water content)
Gran.bent 10-13	December 2012	Granulated bentonite (60% water content)

Table 5-2. Interface shear strength - Temperature dependent tests (Large shear box)

Test	Date	Material 1 (lower-half)	Material 2 (upper-half)	Temperature
Block 38-40	October 2012	Friedland-clay block	Friedland-clay block	+40 ^{0}C
Block 41-43	January 2013	Friedland-clay block	Friedland-clay block	+3 ^{0}C
Block 44-46	January 2013	Friedland-clay block	Friedland-clay block	+10 ^{0}C

Table 5-3. Interface shear strength – Salinity dependent tests (Small shear box)

Test	Date	Material 1 (lower-half)	Material 2 (upper-half)	Salinity
Salt 1-4	February 2013	Friedland-clay block	Friedland-clay block	1% NaCl
Salt 5-8	February 2013	Friedland-clay block	Friedland-clay block	3% NaCl
Salt 9-12	February 2013	Friedland-clay block	Friedland-clay block	7% NaCl
Salt 13-16	February 2013	Friedland-clay block	Friedland-clay block	0% NaCl (distilled water)

Table 5-4. Interface shear strength - Water content tests

Test	Date	Material 1 (lower-half)	Material 2 (upper-half)	Shear box
Test 38-40	December 2012	Friedland-clay block (natural)	Cebogel QSE pellets (20%)	Big shear box
Test 41-43	December 2012	Friedland-clay block (natural)	Cebogel QSE pellets (40%)	Big shear box
Test 44-46	December 2012	Friedland-clay block (natural)	Cebogel QSE pellets (60%)	Big shear box
Test 47-50	February 2013	Friedland-clay block (2g water)	Cebogel QSE pellets (60%)	Small shear box
Test 51-54	February 2013	Friedland-clay block (3g water)	Cebogel QSE pellets (60%)	Small shear box
Test 55-58	February 2013	Friedland-clay block (4g water)	Cebogel QSE pellets (60%)	Small shear box
Gran.bent 19-21	February 2013	Friedland-clay block (natural)	Granulated bentonite (40%)	Big shear box
Gran.bent 22-24	February 2013	Friedland-clay block (natural)	Granulated bentonite (60%)	Big shear box
Gran.bent 15-18	February 2013	Friedland-clay block (2g water)	Granulated bentonite (60%)	Small shear box
Gran.bent 25-28	February 2013	Friedland-clay block (3g water)	Granulated bentonite (60%)	Small shear box
Gran.bent 29-32	February 2013	Friedland-clay block (4g water)	Granulated bentonite (60%)	Small shear box

Whenever clay blocks were used in a test, they were placed in the lower half of the shear box. Assuming that the clay blocks are incompressible, only the height of the upper half of the shear box (i.e., only the granular material consolidated under vertical loading) was considered for effective height calculations.

It should be noted that in all the tests where clay blocks were used, the longest side aligned parallel to the direction of shearing (i.e., the joint is in the direction of the movement of the shear box) in order to minimize the influence of the joint on the end result.

Extra thin wooden and steel pieces were placed on three of the four sides around the clay blocks to bridge the gap between the shear box and the solid material as the dimensions of the combination of two clay blocks were smaller than the dimensions of the shear box (Figure 5-10). Also, a wooden plate was placed at the base of the lower half of the shear box to lay an even surface to place the blocks.

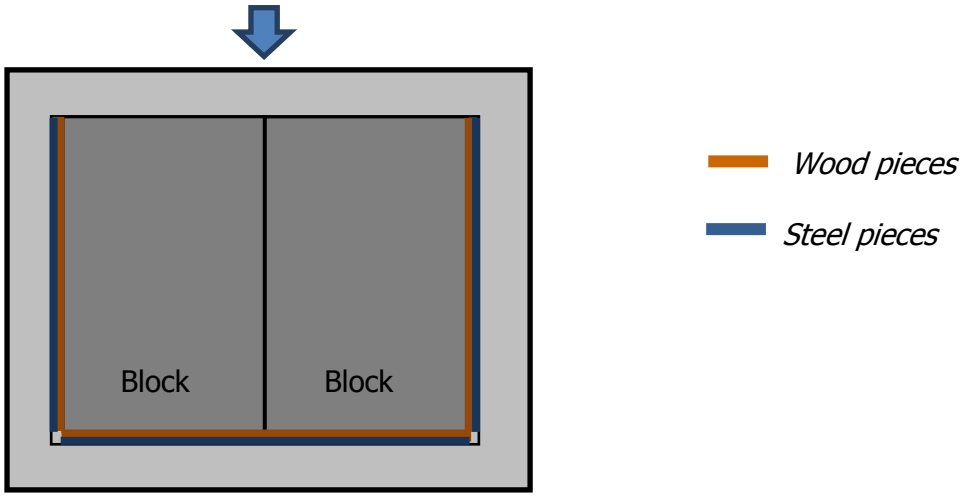

Figure 5-10. Alignment of blocks and extra wooden and steel pieces (Gallardo, 2012)

5.3.1. Internal shear strength

Granular materials (Cebogel QSE pellets and granulated bentonite) were tested for internal shear strength with varying water contents. Small shear box was used for this purpose. The main reason for performing the internal shear strength tests was to understand the material behaviour and the workability during the test. This helped to plan the interface shear strength testing programme with possible water contents. Due to the difficulties in the workability of these clay based granular materials at high water contents, tests were limited to a maximum targeted water content of 60%. For

pellets tests were carried out at natural water content (13%), 20%, 30%, 40% and 60% while for granulated bentonite at natural water content (20%), 40% and 60%.

The desired water content was achieved by adding water to the specimen and keeping it inside a sealed air-tight plastic bag for at least 24 hours. The specimens were weighed after the completion of each test to determine its properties (Table 5-6 and Table 5-7). Water density (ρ_w) of 997.8 kg/m^3 was used in the calculations and grain densities (ρ_s) of 2780 kg/m^3 and 2750 kg/m^3 were used for pellets and granulated bentonite, respectively (Gallardo, 2012).

Table 5-5. Dimensions of small shear box - internal shear tests

Height (mm)	Area (mm^2)	Volume (mm^3)
44	3565	156860

Table 5-6. Data from pellets - internal shear strength tests.

TEST	m (g)	ρ (kg/m^3)	ρ_d (kg/m^3)	w (%)	$e_o = \frac{\rho_s}{\rho_d} - 1$	$S_R = \frac{w_o \cdot \rho_s}{e_o \cdot \rho_w}$
					e_o	S_R (%)
Pellet 7	180.63	1150	1010	13.92	1.75	22.08
Pellet 8	181.44	1160	1020	13.94	1.72	22.46
Pellet 9	185.76	1180	1040	14.03	1.67	23.31
Pellet13	158.80	1010	840	20.53	2.31	24.71
Pellet 14	167.10	1070	890	19.70	2.12	25.79
Pellet 15	158.90	1010	850	19.65	2.27	24.06
Pellet 16	168.10	1070	900	19.42	2.09	25.85
Pellet 17	169.80	1080	910	19.10	2.06	25.84
Pellet 22	138.40	880	680	28.94	3.09	26.05
Pellet 23	140.60	900	700	28.93	2.97	27.07
Pellet 24	142.00	910	700	30.00	2.97	28.07
Pellet 25	154.70	990	760	29.36	2.66	30.71
Pellet 26	121.70	780	570	25.23	3.88	18.09
Pellet 27	122.70	780	560	39.22	3.96	27.50
Pellet 28	124.90	800	580	36.93	3.79	27.07
Pellet 29	126.50	810	590	37.45	3.71	28.05
Pellet 30	138.30	880	580	52.22	3.79	38.27
Pellet 31	140.00	890	600	47.96	3.63	36.70
Pellet 32	136.40	870	590	46.46	3.71	34.80
Pellet 33	114.90	730	500	46.52	4.56	28.36
Pellet 35	144.90	920	610	52.56	3.56	41.07

Table 5-7. Data from granulated bentonite - internal shear strength tests.

TEST	m (g)	ρ (kg/m³)	ρ_d (kg/m³)	w(%)	$e_o = \frac{\rho_s}{\rho_d} - 1$	$S_R = \frac{w_o \cdot \rho_s}{e_o \cdot \rho_w}$
					e_o	S_R (%)
Gran.bent 1-5	196.08	1250	1050	20.61	1.62	35.01
Gran.bent 6	147.20	940	670	39.91	3.10	35.35
Gran.bent 7	153.00	980	720	34.75	2.82	33.89
Gran.bent 8	149.30	950	690	37.24	2.99	34.30
Gran.bent 9	140.60	900	630	42.13	3.37	34.43
Gran.bent 10	147.50	940	600	57.96	3.58	44.48
Gran.bent 11	156.60	1000	580	72.97	3.74	53.64
Gran.bent 12	123.90	790	480	64.97	4.73	37.78
Gran.bent 13	137.40	880	540	62.63	4.09	42.08

5.3.2. Interface shear strength - temperature dependent tests

These tests were performed only on block/block interface and they were done with the large shear box. Four blocks were used in each test; two of them in the lower-half and the other two in the upper-half. The grain density (ρ_s) was taken as 2790 kg/m^3 (Gallardo, 2012). The initial data that is presented in Table 5-8 for the block/block temperature dependent tests were the same for all the tests (Block 38– 46).

Table 5-8. Dimensions and initial data - Temperature dependent block/block tests

DIMENSIONS UPPER HALF			INITIAL DATA					
Height (mm)	**Area (mm²)**	**Volume (mm³)**	**m(g)**	**ρ (kg/m³)**	**ρ_d (kg/m³)**	**w(%)**	$e_o = \frac{\rho_s}{\rho_d} - 1$	$S_R = \frac{w_o \cdot \rho_s}{e_o \cdot \rho_w}$
							e_o	S_R (%)
75	90000	6750000	13500	2000	1880	6.24	0.48	37

The whole room was heated to the desired temperature. Tests were carried out at +3ºC, +10ºC and +40ºC.

5.3.3. Interface shear strength - salinity dependent tests

The block/block interface was tested for salinity in the small shear box. Small pieces of 60 x 60 x 19.5 mm blocks were cut from the original Friedland-clay blocks with the help of two radial engines. A large radial engine was used for cutting a volume of 300

x 150 x 20 mm (Figure 5-11 (a)) and subsequently a smaller one was used to make pieces of 60 x 60 x 20 mm (Figure 5-11 (b)). Then, the cut pieces were sanded until the pieces fitted perfectly in the shear box. It should be noted that the tested surfaces were kept untouched during sanding in order to represent the natural block surface.

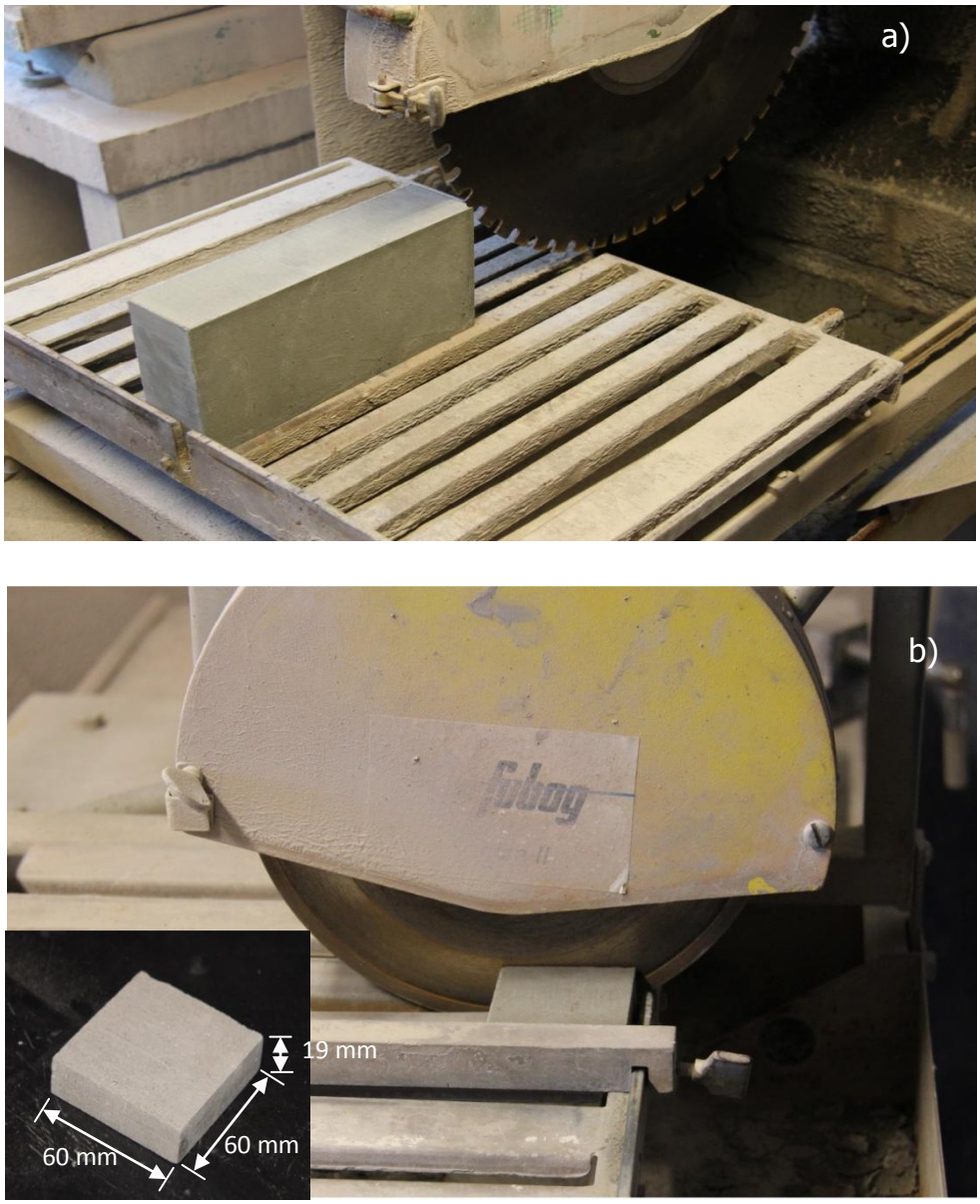

Figure 5-12. Process of cutting blocks (a & b)

The objective of these salinity tests was to have a thin film of salty water in the block/block interface and then test for shear. The salty water was added to the surface of the lower block with the aid of a pipette and the upper block was placed

immediately on top of the lower block. The blocks were left unattended for about 10 minutes to absorb the water in both surfaces before starting the consolidation. 3 g of distilled water was added to the surface which corresponds to a surface water content of approximately 833 g/m^2.

Different quantities of marine salt (non-iodized) were added to distilled water to form saline water of 1% (1g/100ml), 3% (3g/100ml) and 7% (7g/100ml). Pure distilled water (0%) was also used as a control test. The mixture was put together inside a mixer for 10 minutes until it became a homogeneous mixture. Table 5-9 summarizes the dimensions of the blocks. It was not possible to determine the density, bulk density, water content, void ratio and degree of saturation of the block as the water was added only to the block surface.

Table 5-9. Dimensions of the upper half of the small shear box (block) - salinity dependent tests.

Height (mm)	Area (mm^2)	Volume (mm^3)
19.5	3600	70200

5.3.4. Interface shear strength – water content tests

As the saturation of the deposition tunnel progresses, the amount of water that is present in the backfill material interface would increase. For this purpose, interface shear strength tests with varying amount of interface water content were carried out to simulate possible real world scenarios. When the ground water reaches the tunnel backfilling through the fractures in the host rock, it is expected to wet the pellet filling first (at this stage a dry block backfill can be assumed as the blocks covered by pellet filling, and the pellet filling absorbs the entire ground water until it becomes saturated) and subsequently the block backfilling through interfaces. To simulate these two stages of saturation in the laboratory, two types of tests have been proposed; in one, the water content of the granular material (pellets and granulated bentonite) was changed while the block was kept at its natural water content. In the other, the water content of the granular material was kept constant at 60% while the amount of water on the block surface was changed.

- **Block (natural w/c ~ 6%) – Granular material**

These tests were performed in the large shear box. Two blocks were placed in the lower half and the upper half was filled with the granular material with different water contents of 20%, 40% and 60%. Since the natural water content of the granulated bentonite is approximately 20%, this material was tested only for 40% and 60%.

Upon the completion of each test, two specimens were taken, one from the upper part and the other from the lower part of the granular material in order to determine the average dry density and the water content of the specimen (Table 5-11 and 5-12).

Table 5-10. Dimensions of upper half (where pellets and granulated bentonite were used).

Height (mm)	Area (mm^2)	Volume (mm^3)
87	90000	7830000

Table 5-10. Test data - Block (natural w/c ~ 6%) – Pellet.

TEST	m (g)	ρ (kg/m^3)	ρ_d (kg/m^3)	w(%)	$e_o = \frac{\rho_s}{\rho_d} - 1$	$S_R = \frac{w_o \cdot \rho_s}{e_o \cdot \rho_w}$
					e_o	S_R (%)
Test 38	8394	1072	897	19.51	2.10	25.84
Test 39	8518	1088	906	20.07	2.07	26.97
Test 40	8392	1072	894	19.84	2.11	26.14
Test 41[1]	7207	920	714	28.88	2.89	27.74
Test 42[1]	7283	930	692	34.47	3.02	31.76
Test 43[1]	7535	962	722	33.36	2.85	32.50
Test 44	6858	876	645	35.94	3.31	30.15
Test 45	8211	1158	673	56.00	3.13	49.67
Test 46	9067	1049	727	59.66	2.83	58.68

[1] Although the desired water content for Test 41, 42 and 43 was 40%, it was only achieved an average of 32.2%. This is because the waiting time was not enough. Nevertheless, the main point is to find out a trend line, hence they can be accepted.

Table 5-11. Test data - Block (natural w/c ~ 6%) – Granulated bentonite.

TEST	m (g)	ρ (kg/m^3)	ρ_d (kg/m^3)	w(%)	$e_o = \frac{\rho_s}{\rho_d} - 1$	$S_R = \frac{w_o \cdot \rho_s}{e_o \cdot \rho_w}$
					e_o	S_R (%)
Gran.bent 19	6731	860	600	43.33	3.58	33.33
Gran.bent 20	6956	888	620	43.40	3.44	34.78
Gran.bent 21	7226	923	644	43.39	3.27	36.53
Gran.bent 22	6990	893	579	54.39	3.75	39.94
Gran.bent 23	6928	885	562	57.57	3.90	40.71
Gran.bent 24	7074	903	566	59.59	3.86	42.56

- **Block (varying surface w/c) – Granular material (w/c ~60%)**

This series of testing was done with the small shear box by using small specimens of clay blocks (see 5.3.3). Three different quantities of distilled water on the block surface were considered; 2g, 3g and 4g which corresponding to surface water contents of 500g/m^2, 750g/m^2 and 1000g/m^2, respectively. Granular material with a water content of 60% was placed on top of one block. A water content of 60% was chosen due the practical issues with the workability of the material. Furthermore, for water contents above 60% the structure of the material starts to change so that its dissipation time will increase remarkably.

Table 5-12. Dimensions of upper half (granular materials ~ 60% w/c)

Height (mm)	Area (mm^2)	Volume (mm^3)
25.3	3565	90194.5

Table 5-13. Test data, Block– Pellet (water content ~ 60%)

TEST	m (g)	ρ (kg/m^3)	ρ_d (kg/m^3)	w(%)	$e_o = \frac{\rho_s}{\rho_d} - 1$	$S_R = \frac{w_o \cdot \rho_s}{e_o \cdot \rho_w}$
					e_o	S_R (%)
Test 47[1]	74.90	830	532	56.21	4.23	37.06
Test 48[1]	71.10	788	519	51.93	4.36	33.21
Test 49[1]	74.50	826	523	57.82	4.32	37.33
Test 50[1]	76.80	851	527	61.46	4.28	40.05
Test 51[2]	71.50	793	496	59.68	4.61	36.11
Test 52[2]	82.00	909	582	56.20	3.78	41.46
Test 53[2]	55.30	613	402	52.35	5.92	24.66
Test 54[2]	85.20	945	622	51.88	3.47	41.66
Test 55[3]	76.80	851	561	51.66	3.96	36.39
Test 56[3]	80.00	887	567	56.34	3.90	40.22
Test 57[3]	80.00	887	582	52.35	3.78	38.62
Test 58[3]	88.40	980	645	52.00	3.31	43.77

[1]2g of water on the block surface / [2]3g of water on the block surface./ [3]4g of water on the block surface.

Table 5-14. Initial data - Block – Granulated bentonite (water content ~ 60%)

TEST	m (g)	ρ (kg/m³)	ρ_d (kg/m³)	w(%)	$e_o = \frac{\rho_s}{\rho_d} - 1$	$S_R = \frac{w_o \cdot \rho_s}{e_o \cdot \rho_w}$
					e_o	S_R (%)
Gran.bent 15[1]	72.40	803	539	48.95	4.10	32.89
Gran.bent 16[1]	78.50	870	576	51.02	3.77	37.26
Gran.bent 17[1]	50.90	564	374	51.09	6.35	22.16
Gran.bent 18[1]	79.00	876	584	50.10	3.71	37.23
Gran.bent 25[2]	83.20	922	515	79.26	4.34	50.34
Gran.bent 26[2]	83.00	920	579	58.82	3.75	43.23
Gran.bent 27[2]	86.20	956	592	61.40	3.65	46.42
Gran.bent 28[2]	85.70	950	604	57.41	3.55	44.53
Gran.bent 29[3]	83.50	926	595	55.51	3.62	42.24
Gran.bent 30[3]	85.40	947	623	52.08	3.41	42.04
Gran.bent 31[3]	99.30	1010	731	50.61	2.76	50.50
Gran.bent 32[3]	91.30	1012	674	50.25	3.08	44.96

[1]2g of water on the block surface / [2]3g of water on the block surface./ [3]4g of water on the block surface.

6. Results

This chapter presents all the test results from the direct shear box tests that were carried out. Internal shear strength of backfill materials are presented at the beginning in section 6.1 followed by the interface shear strength test results in section 6.2.

6.1. Internal shear strength

Internal shear strength results of pellets at different water contents are shown in Figures 6.1 to 6.5. The water contents showed are the achieved average water contents, not the aforementioned targeted water contents.

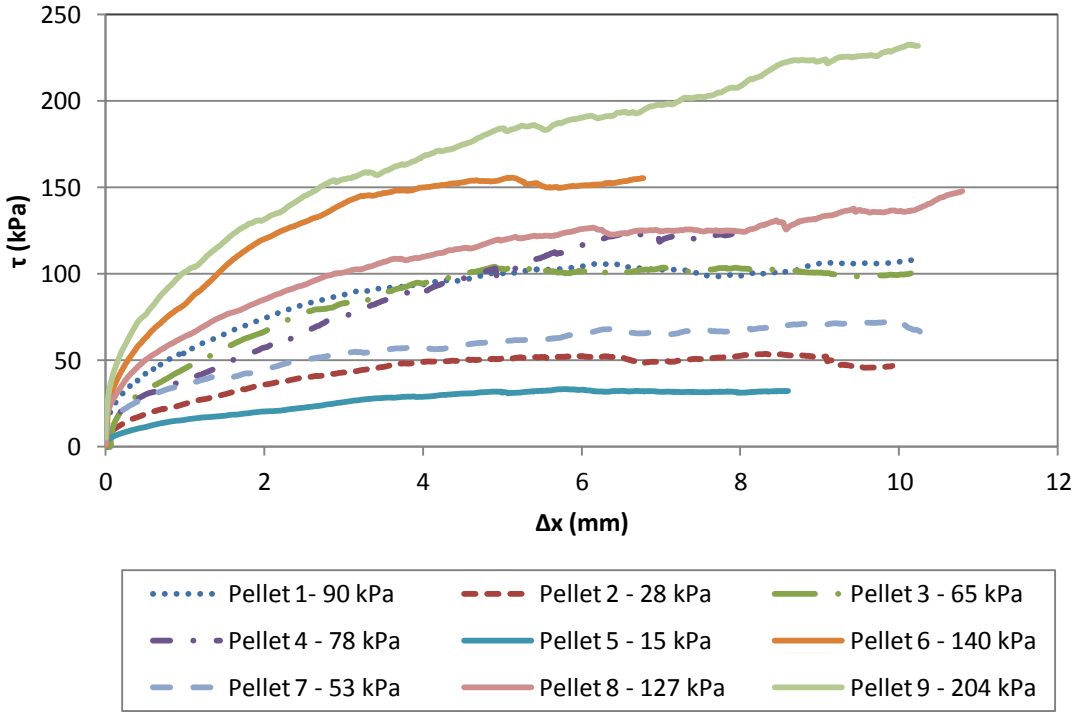

Figure 6-1. Shear strength against horizontal displacement – Pellet (w/c 14 %)

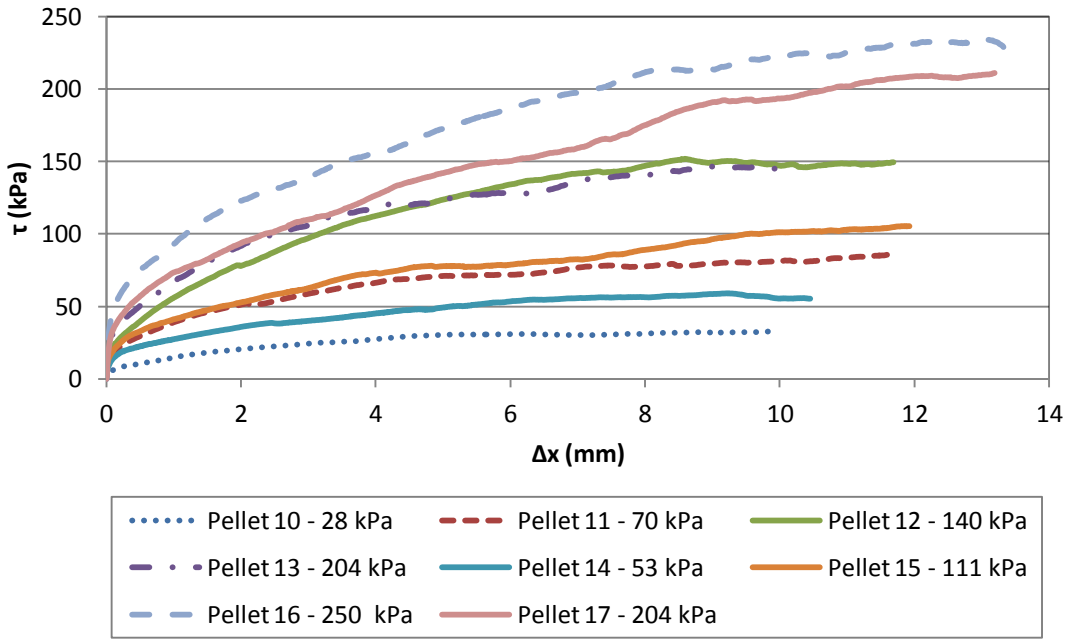

Figure 6-2. Shear strength against horizontal displacement – Pellet (w/c 19.7%)

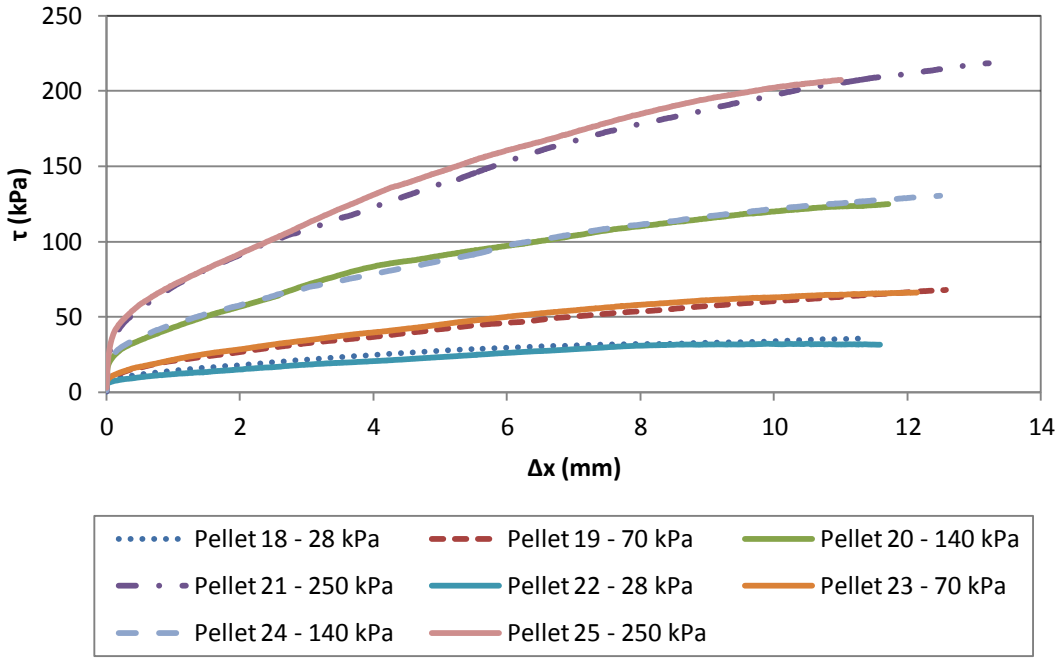

Figure 6-3. Shear strength against horizontal displacement – Pellet (w/c 29.3%)

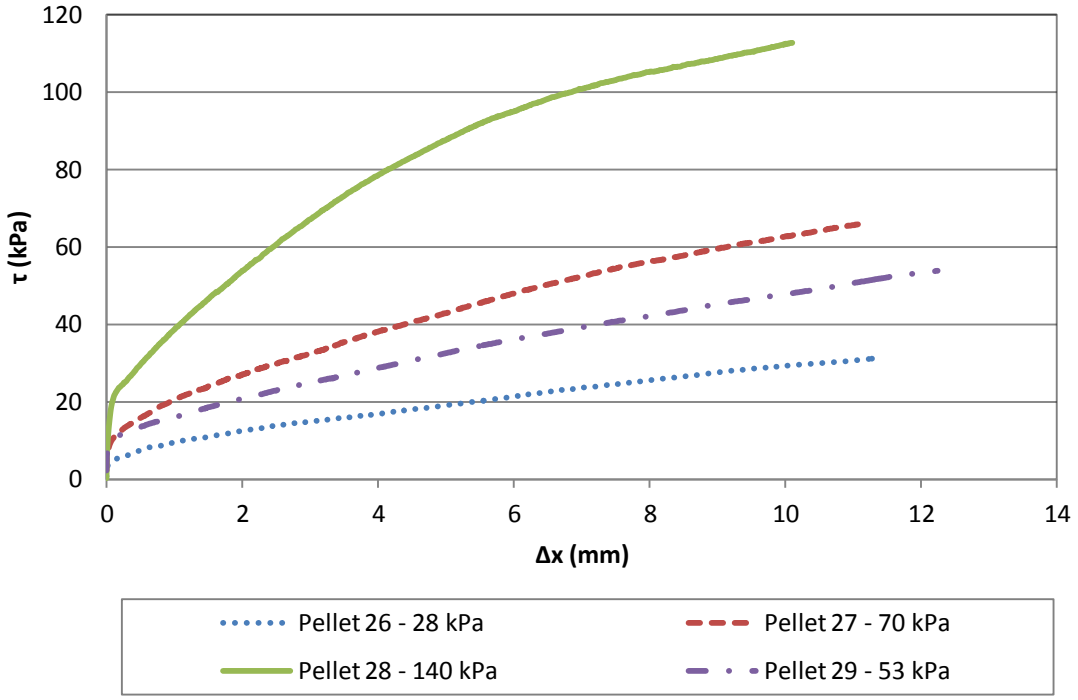

Figure 6-4. Shear strength against horizontal displacement – Pellet (w/c 37.9%)

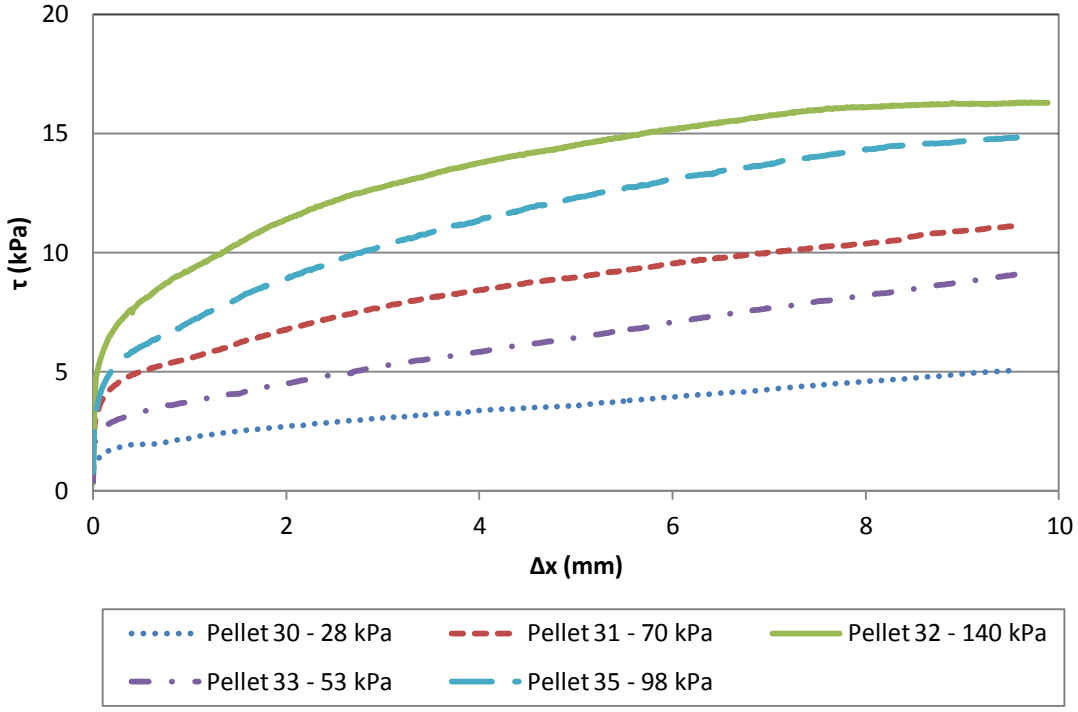

Figure 6-5. Shear strength against horizontal displacement – Pellet (w/c 50%)

Figures 6-6 to 6-8 show the internal shear strength of granulated bentonite at three different water contents of 20.6%, 38.5% and 64.6%.

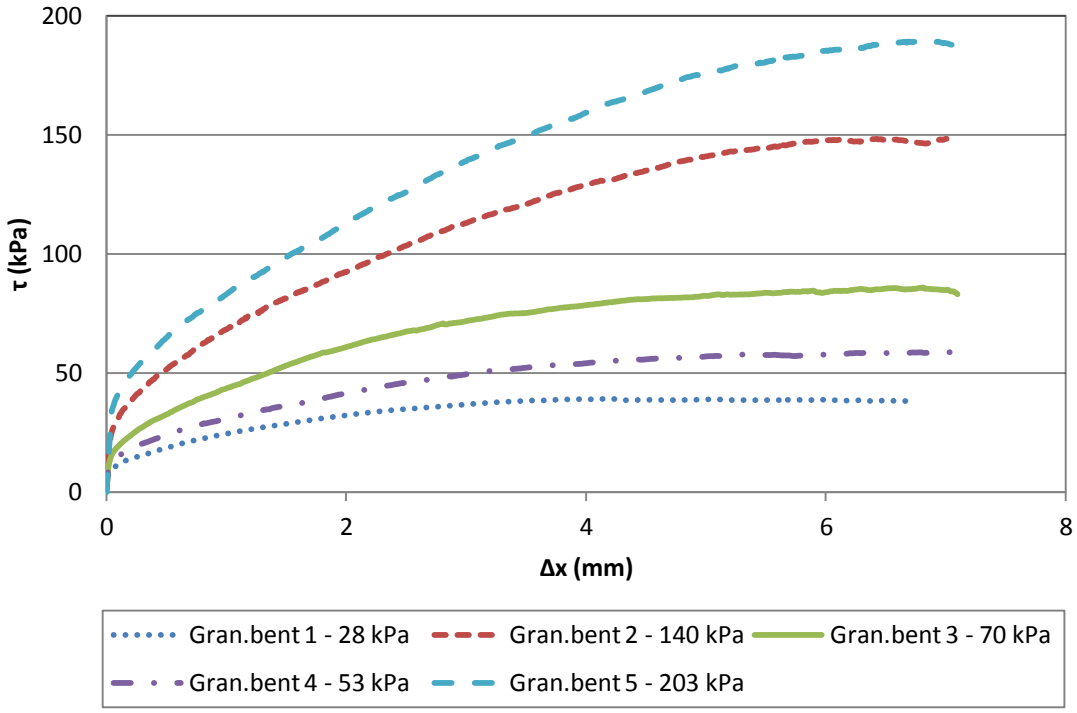

Figure 6-6. Shear strength against horizontal displacement – Granulated bentonite (w/c 20.6%)

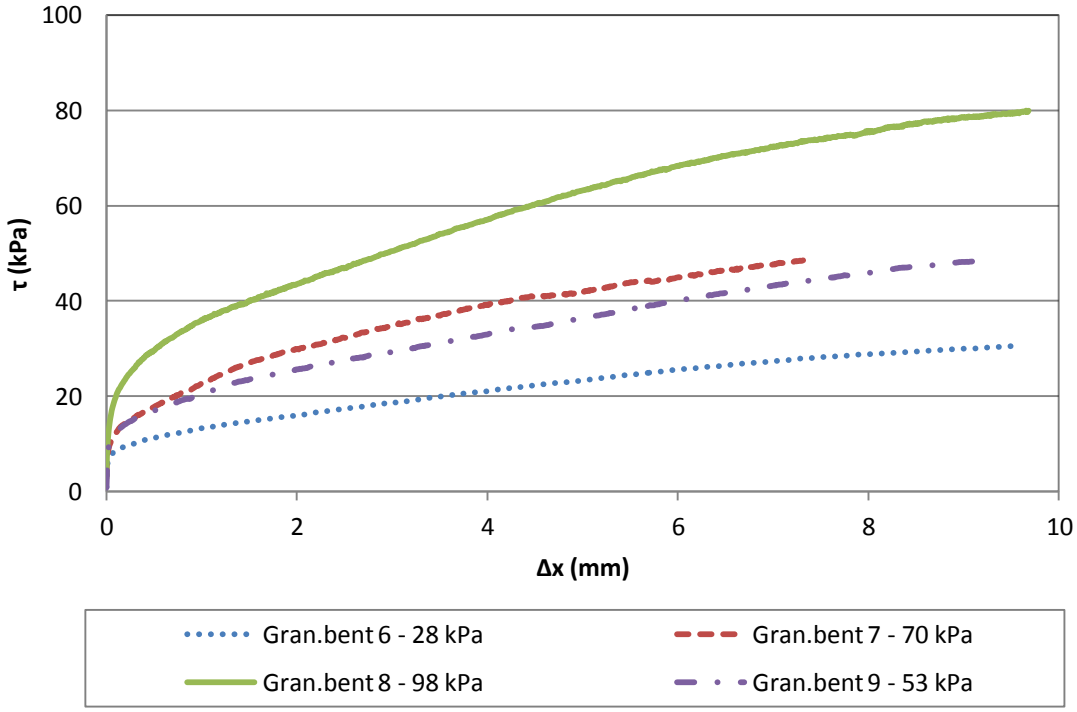

Figure 6-7. Shear strength against horizontal displacement – Granulated bentonite (w/c 38.5%)

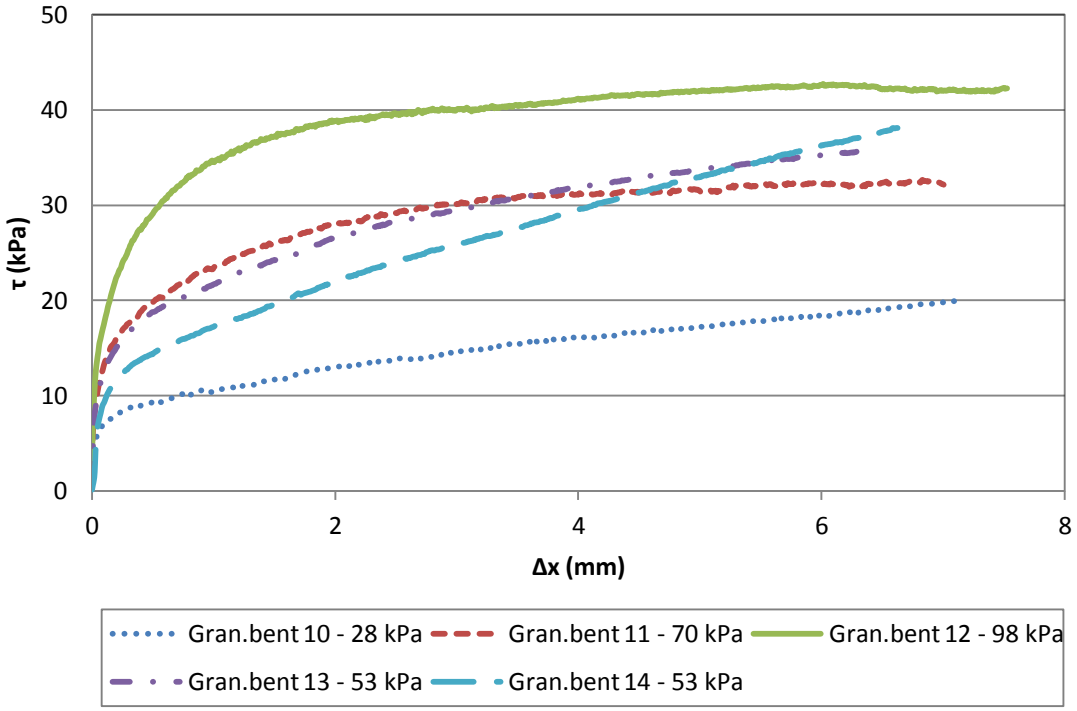

Figure 6-8. Shear strength against horizontal displacement – Granulated bentonite (w/c 64.6 %)

Figure 6-8 shows that Gran.bent 13 and Gran.bent 14 are not good tests because their behaviour differs from the other tests, and they are not going to be taken into account in the forward calculations.

6.2. Interface shear strength test results

This section presents the results from interface shear strength tests that were carried out under varying temperature, salinity and water content.

Figure 6-8 shows three different curves obtained for the temperature at +3°C. Figures 6-9 and 6-10 show similar temperature dependent curves at +10°C and +40°C, respectively.

For salinity, 4 tests were performed for each salt content that was considered (1%, 3%, 7% and 0%) and the results can be seen in Figures 6-11 to 6-14.

Finally, Figures 6-15 to 6-24 correspond to the tests that were carried out at different water contents of the granular material, as well as on the interface between the Friedland clay blocks and the granular materials.

Temperature dependent tests.

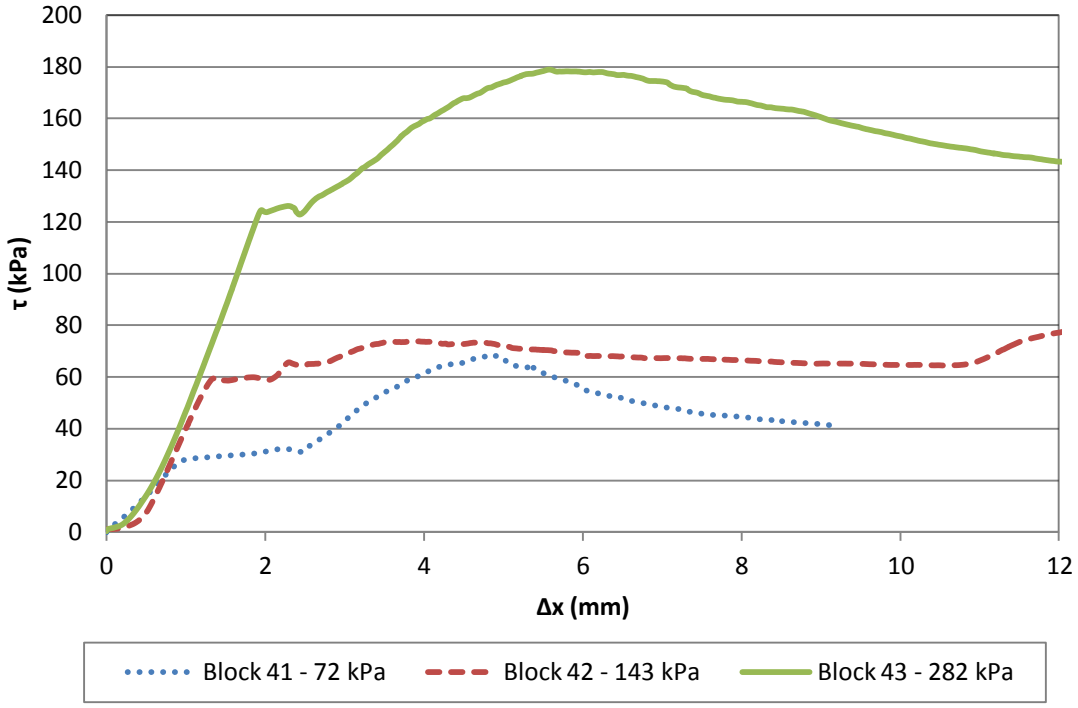

Figure 6-8. Block/Block interface shear strength (interface at +3°C) against horizontal displacement

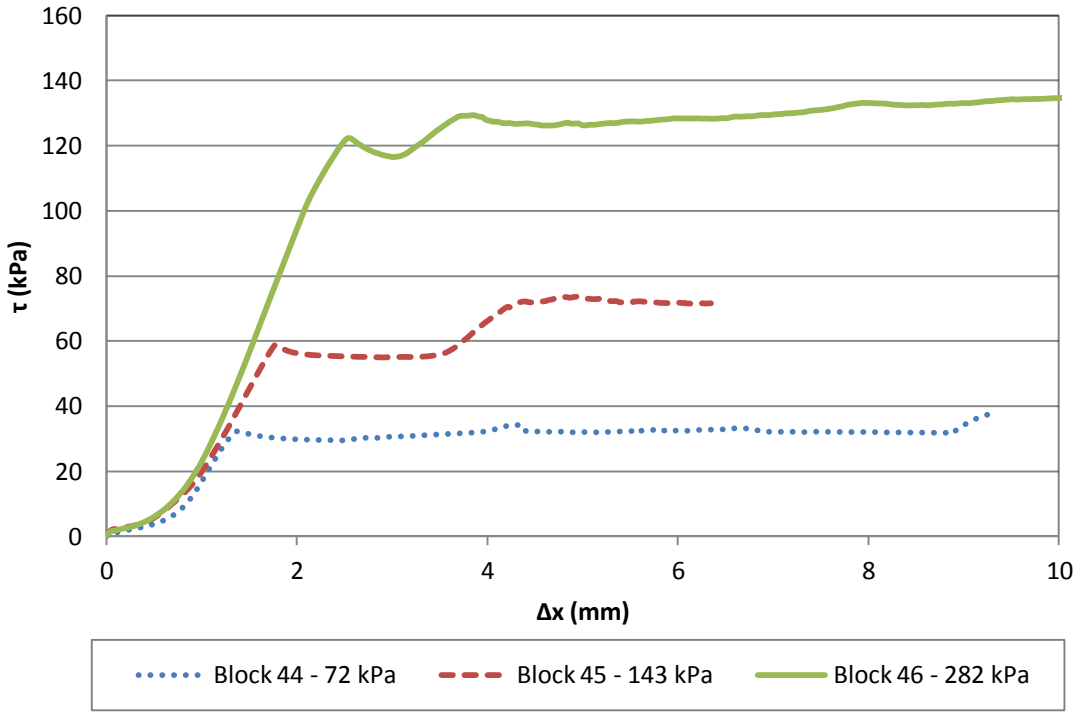

Figure 6-9. Block/Block interface shear strength (interface at +10°C) against horizontal displacement

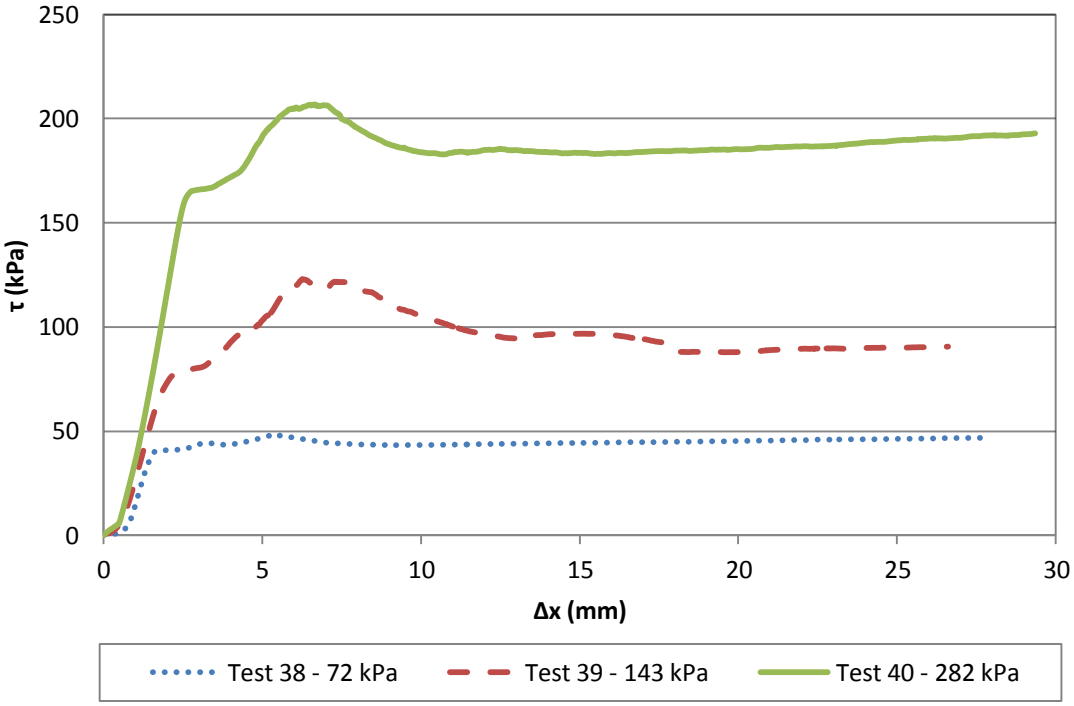

Figure 6-10. Block/Block interface shear strength (interface at +40°C) against horizontal displacement

Salinity dependent tests.

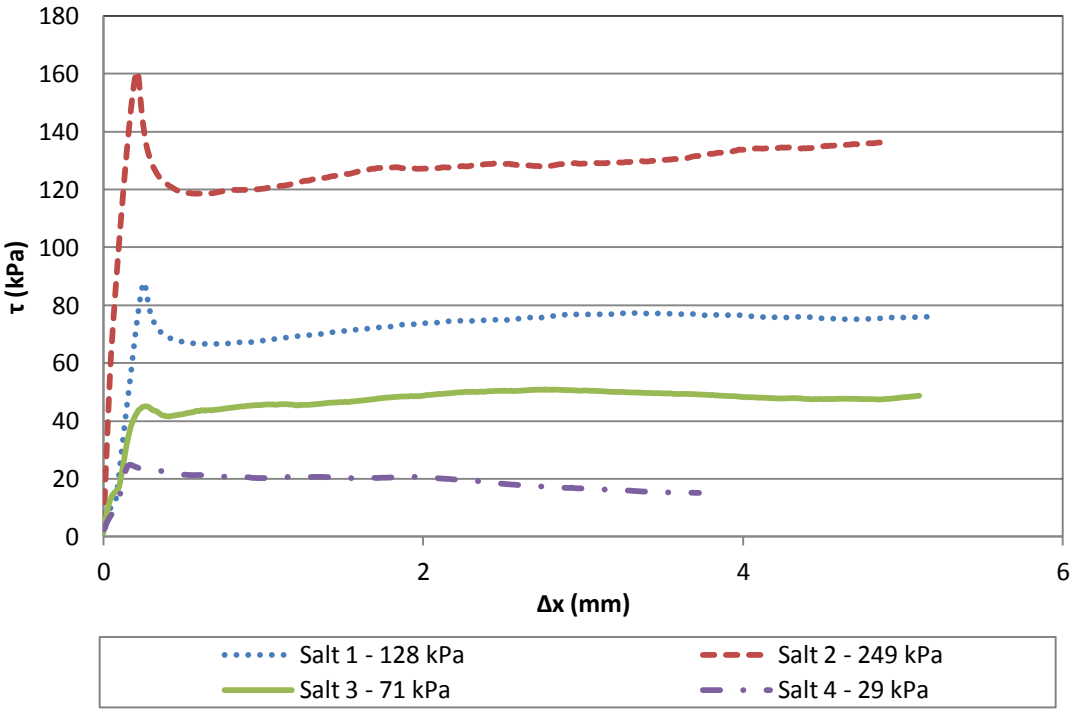

Figure 6-11. Block/Block interface shear strength (1% NaCl) against horizontal displacement (3g water on surface)

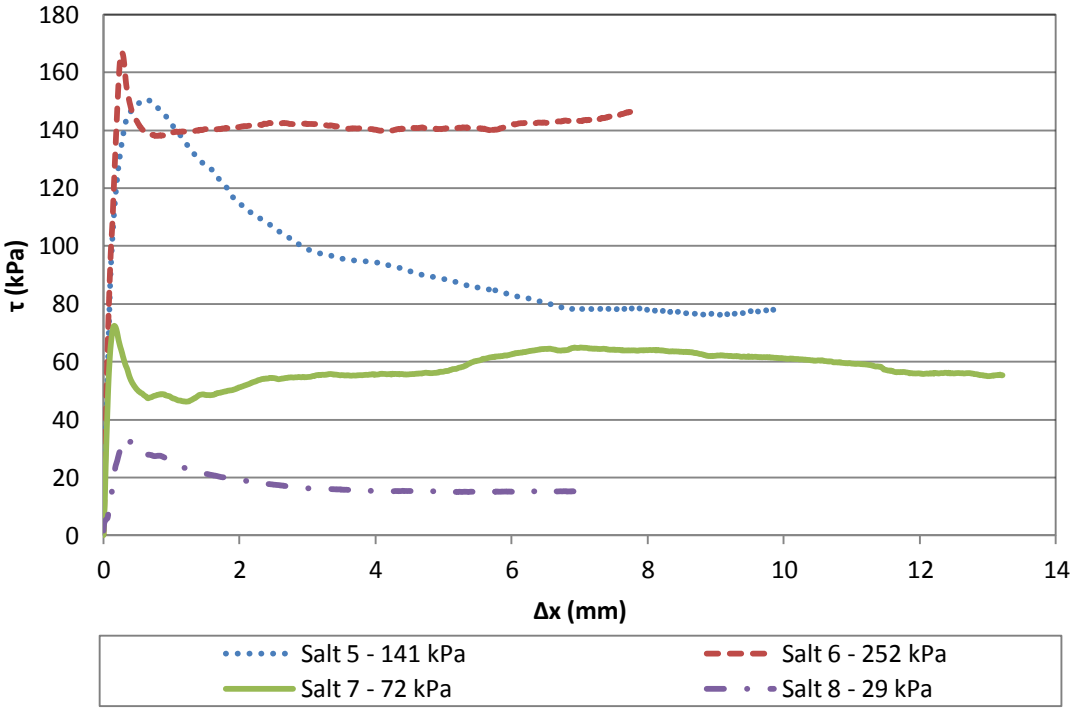

Figure 6-12. Block/Block interface shear strength (3% NaCl) against horizontal displacement (3g water on surface)

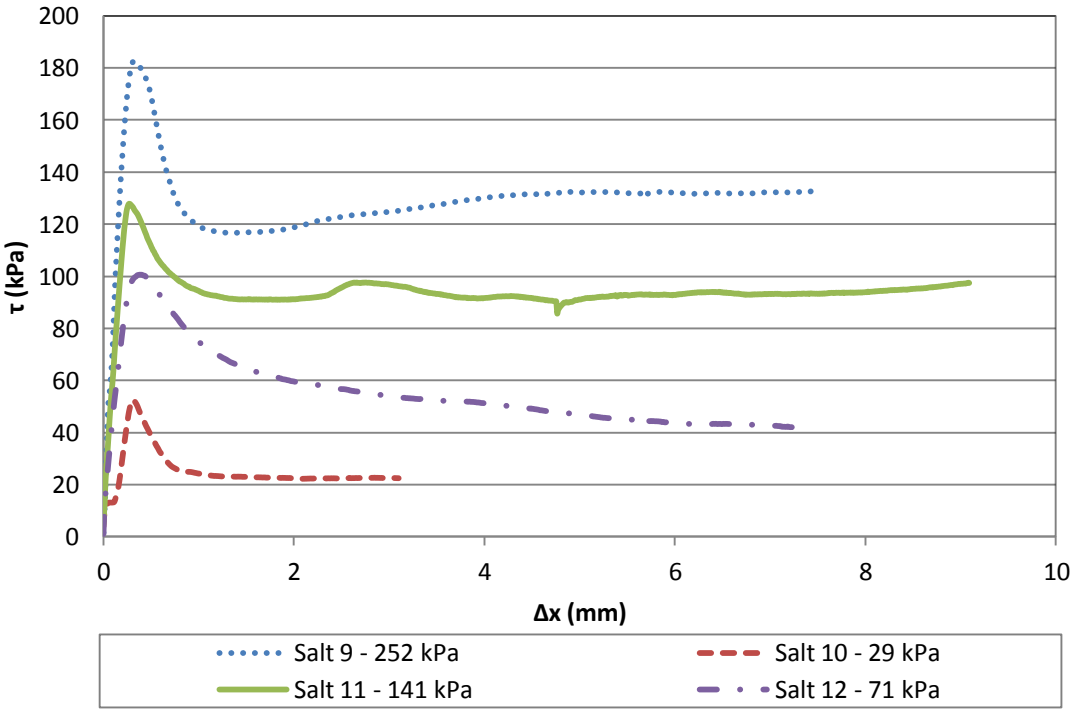

Figure 6-13. Block/Block interface shear strength (7% NaCl) against horizontal displacement (3g water on surface)

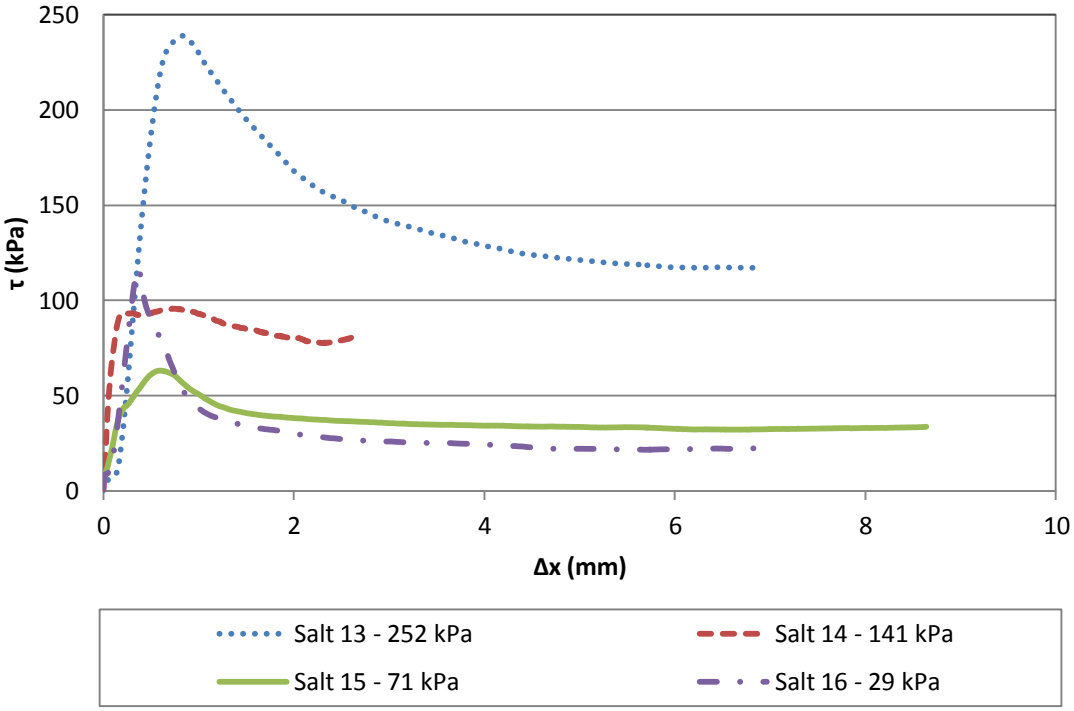

Figure 6-14. Block/Block interface shear strength (0% NaCl) against horizontal displacement (3g water on surface)

Water content dependent tests

A. Block (w/c 6 %) – Granular material (varying w/c)

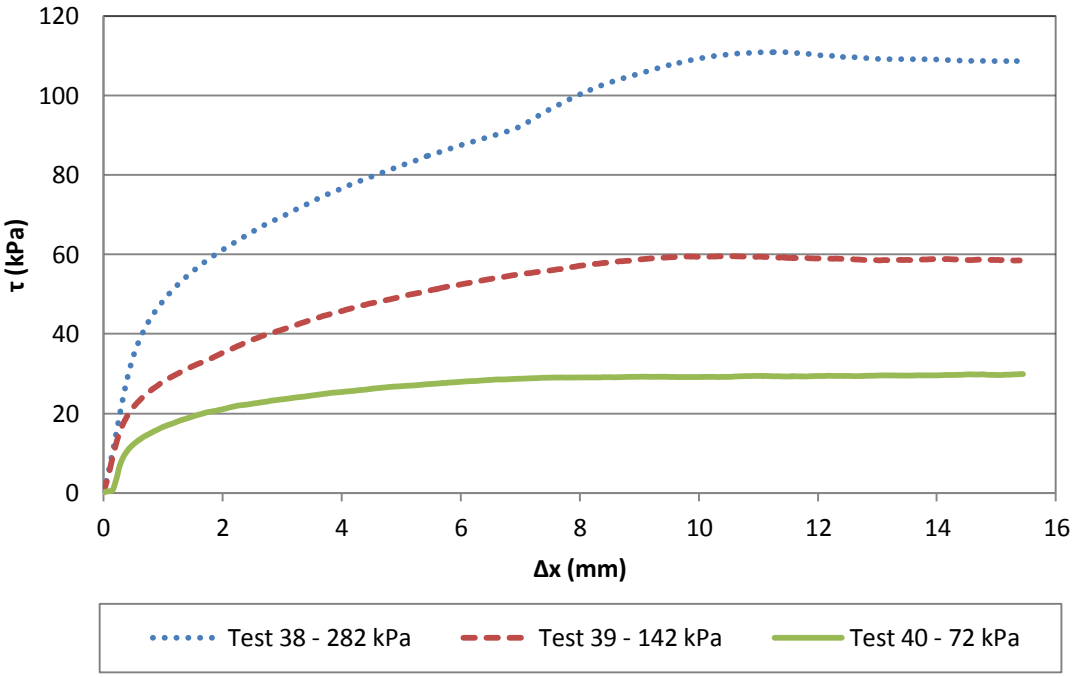

Figure 6-15. Block (natural w/c 6%)/Pellet (w/c 19.8 %) interface against horizontal displacement

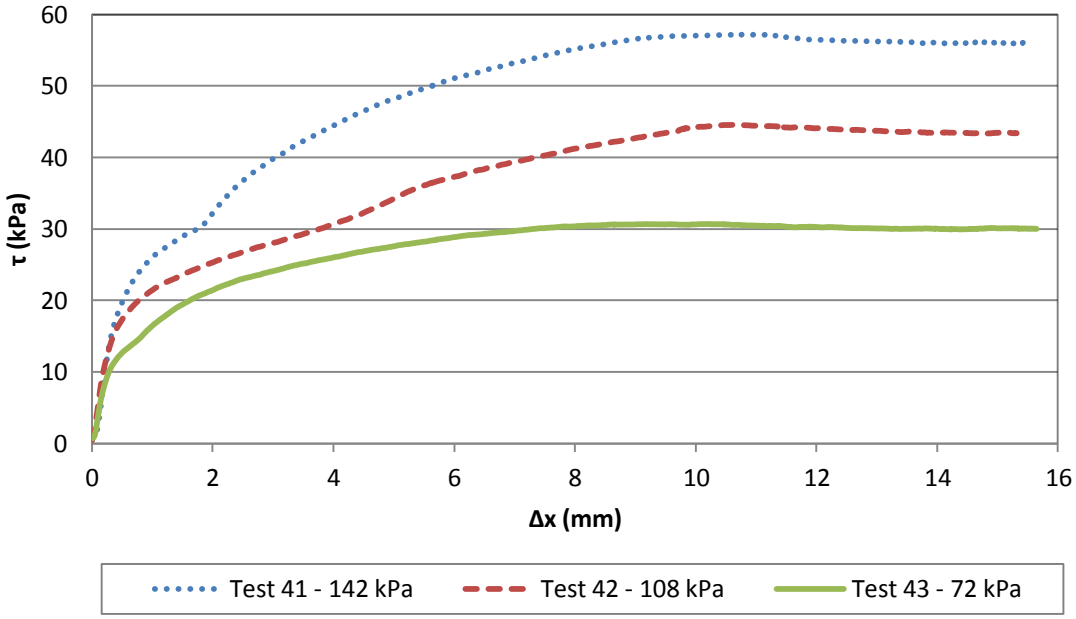

Figure 6-15. Block (natural w/c 6%)/Pellet (32.2 % w/c) interface against horizontal displacement

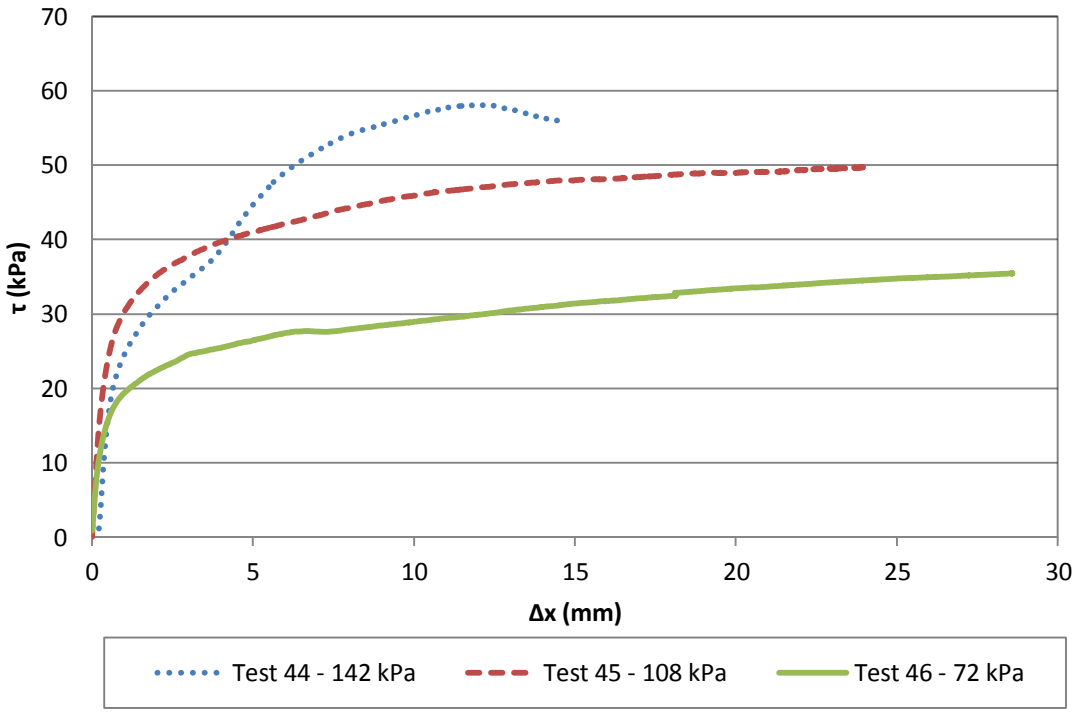

Figure 6-16. Block (natural w/c 6%)/Pellet (50.5 % w/c)

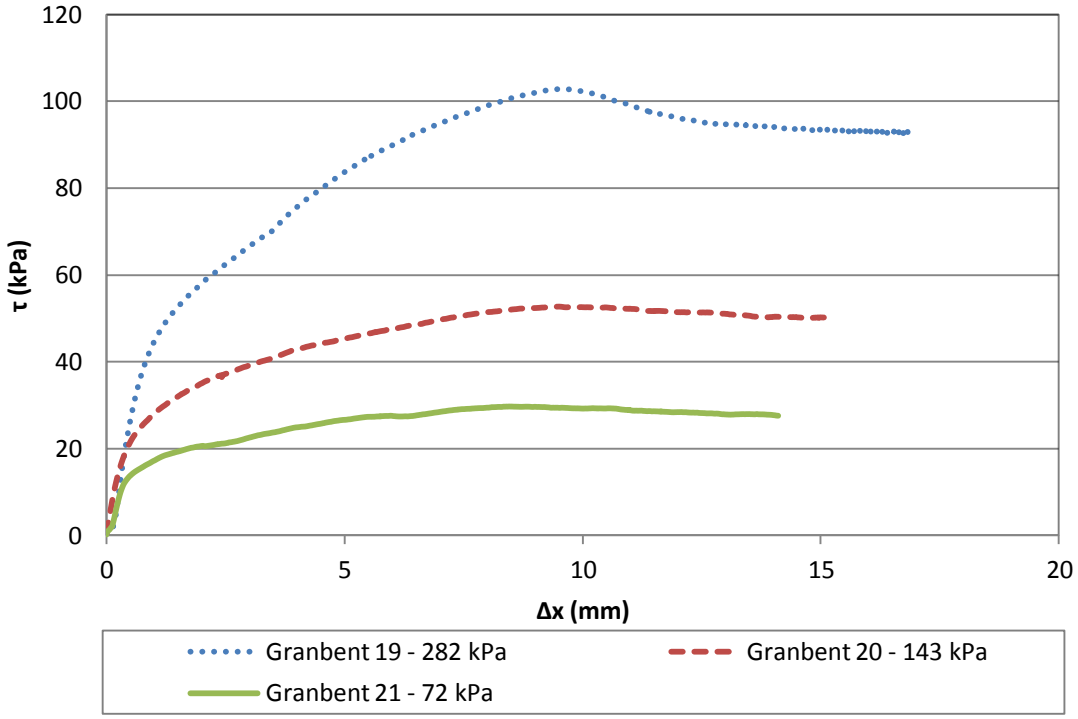

Figure 6-17. Block (natural w/c 6%)/Granulated bentonite (w/c 43.4 %) interface against horizontal displacement

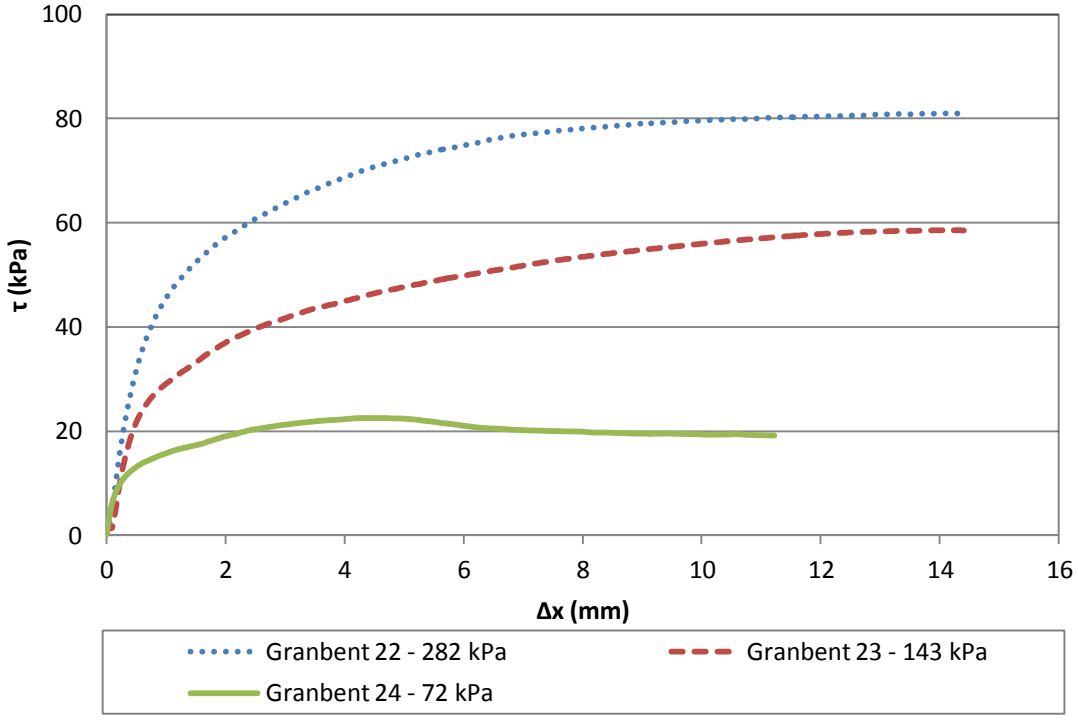

Figure 6-18. Block (natural w/c 6%)/Granulated bentonite (w/c 57.2 %) interface against horizontal displacement

B. Block (varying interface w/c) – Granular material (w/c 60%)

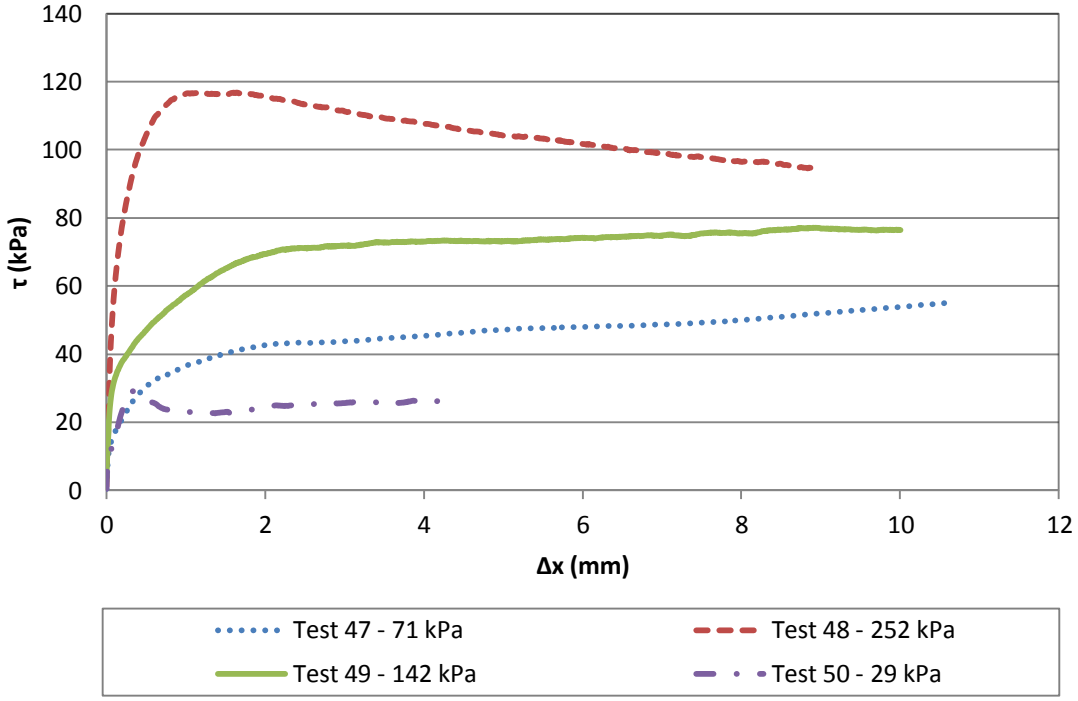

Figure 6-19. Block (2g surface water)/Pellet (w/c 56.9 %) interface against horizontal displacement

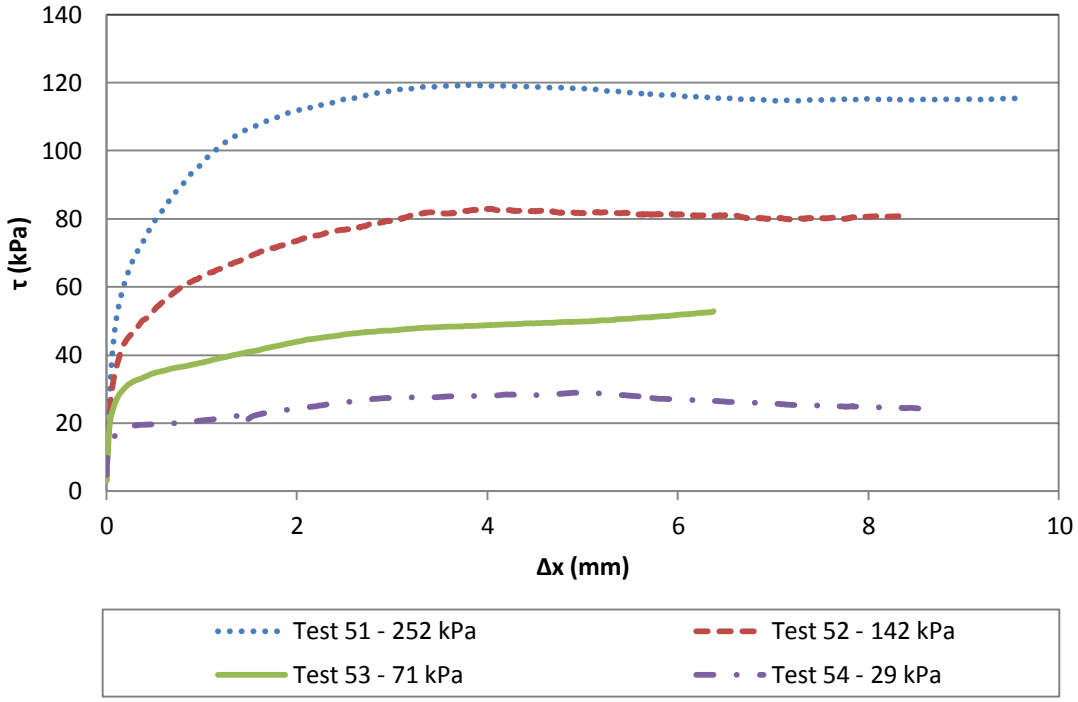

Figure 6-20. Block (3g surface water)/Pellet (w/c 55 %) interface against horizontal displacement

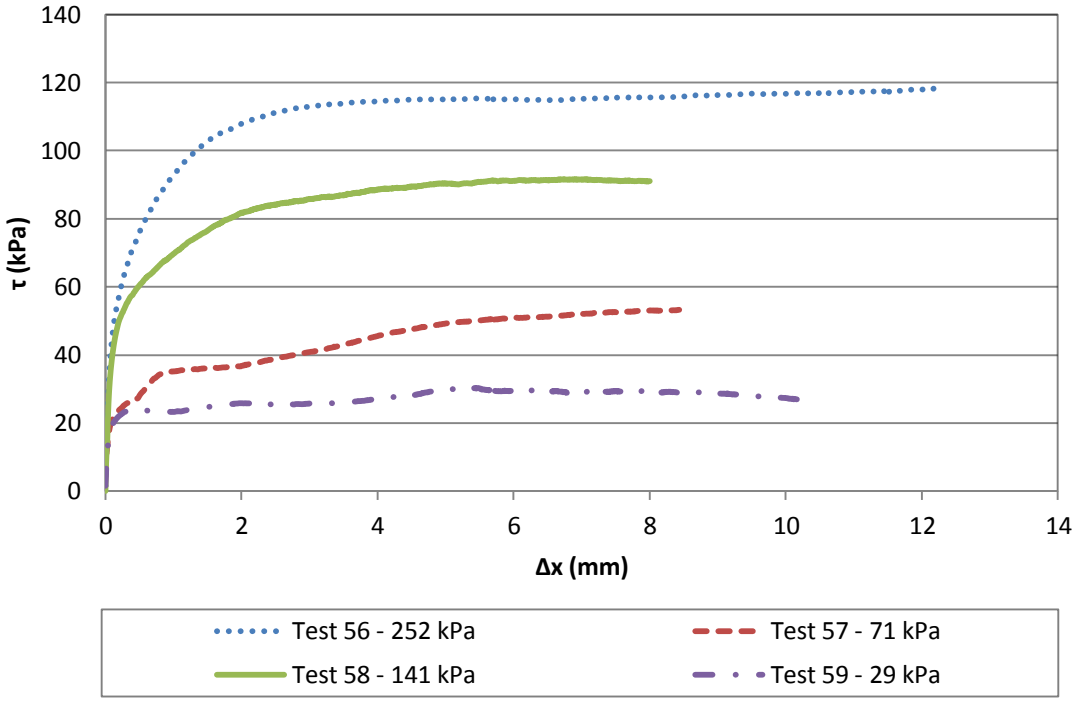

Figure 6-21. Block (4g surface water)/Pellet (w/c 53 %) interface against horizontal displacement.

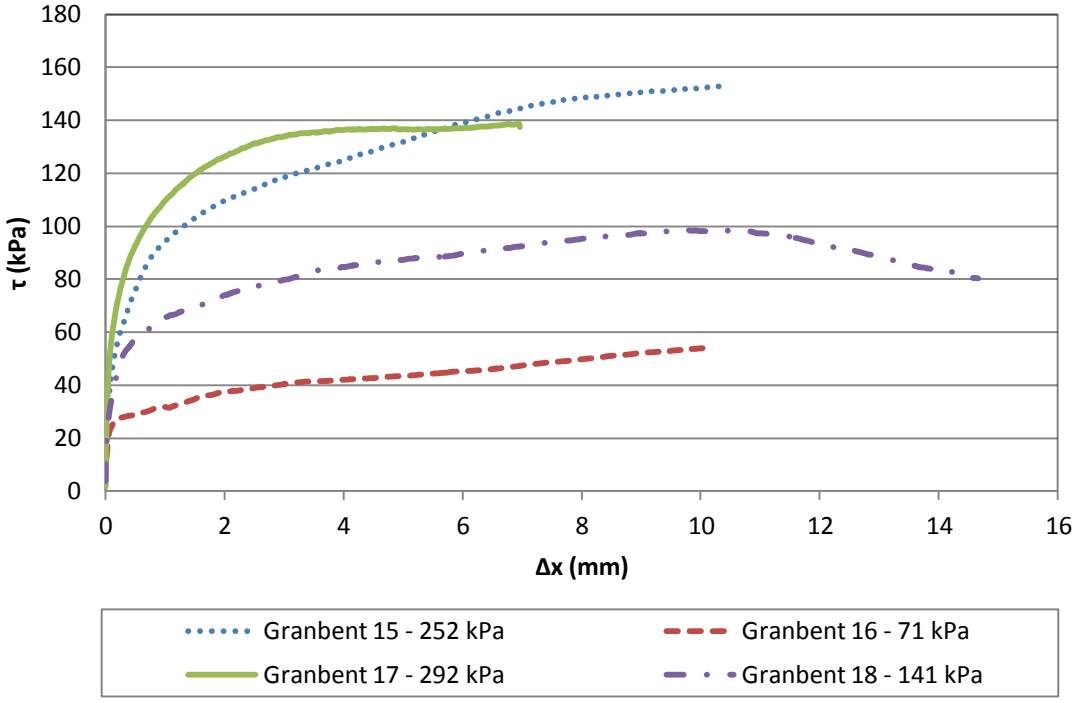

Figure 6-22. Block (2g surface water)/Granulated bentonite (w/c 50.3 %) interface against horizontal displacement.

The results obtained from Gran.bent 17 (Figure 6-22) are not taken into account for the further calculations as its curve represent an anomalous behaviour.

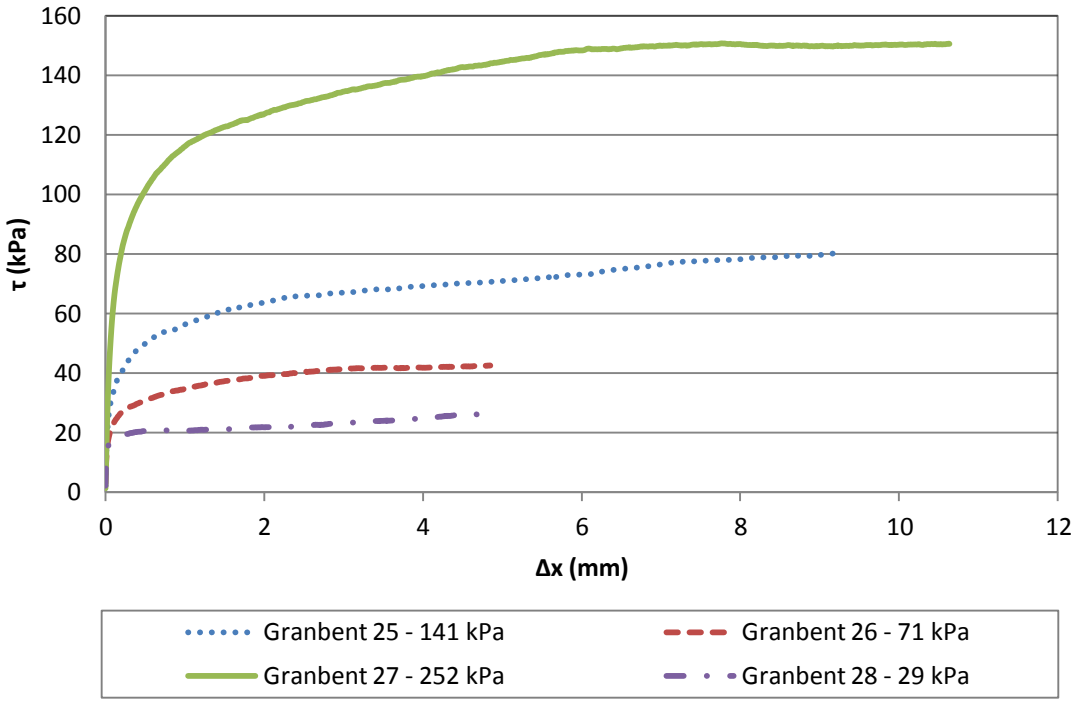

Figure 6-23. Block (3g surface water)/Granulated bentonite (w/c 64.2 %) interface against horizontal displacement

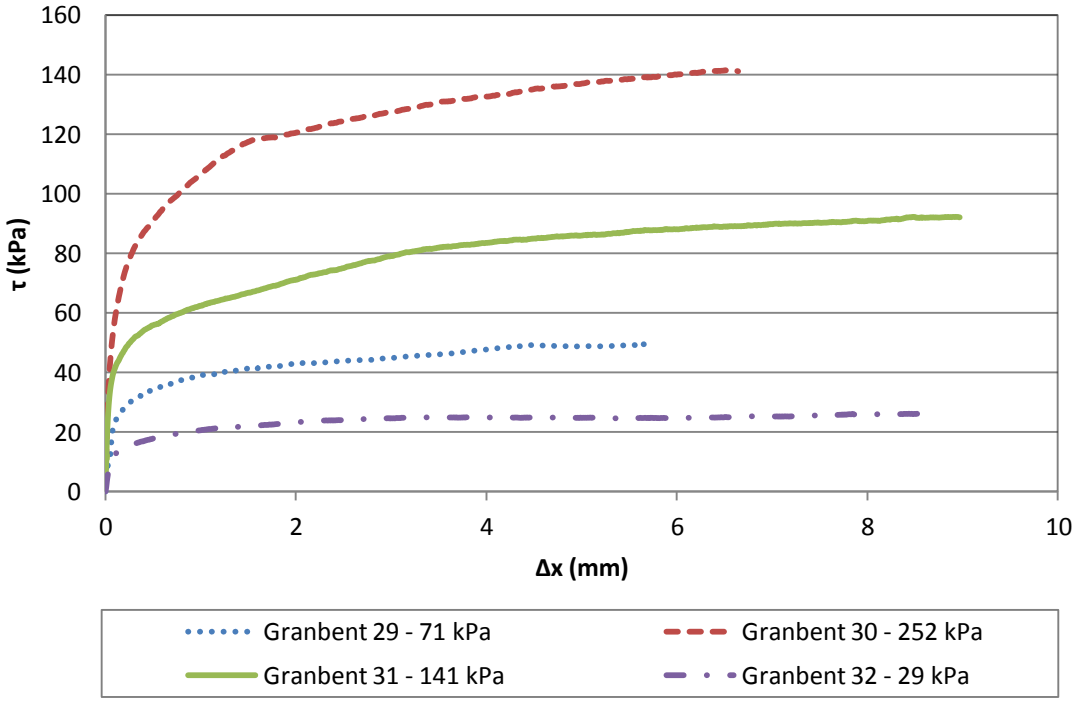

Figure 6-24. Block (4g surface water)/Granulated bentonite (w/c 52.1 %) interface against horizontal displacement

7. Analysis of the results

7.1. Applied theory

Mohr-Coulomb failure criterion has been chosen to analyse the interface shear strength in this study. This theory describes the response of a material to an applied external stress. In general, the theory is applied to materials where the compressive strength exceeds the tensile strength (Labuz & Zang, 2012).

The Mohr- Coulomb failure criterion is a linear equation in principal stress space which describes the conditions where the material would fail (Labuz & Zang, 2012). This linear equation represents the envelope that is obtained from a plot of the shear strength of a material against the normal stress (Equation 1).

$$\tau = c + \sigma \cdot \tan(\varphi) \qquad \text{(Eq. 1)}$$

where c is the inherent shear strength, also known as cohesion and φ is the angle of internal friction with the coefficient of internal friction tanφ (Labuz & Zang, 2012).

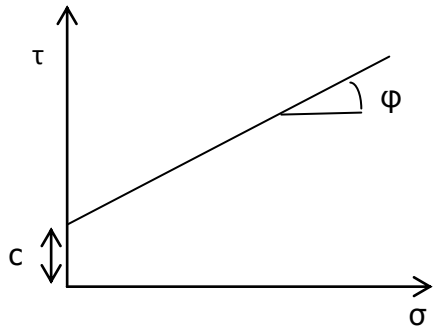

Figure 7-1. Mohr-Coulomb failure criterion (Coulomb, 1773)

The results of different tests give a pair of normal stress (σ) and shear stress (τ) which are then plotted in an X-Y coordinate, in order to fit a linear relationship between σ and τ from which the shear strength parameters c and φ are obtained (Figure 7-1).

Notice that in this study the shear plane is between two different surfaces, so slightly different parameters have to be used. Thus, the equation to calculate the shear strength has been modified (Zhang et al., 2001):

$$\tau = c_a + \sigma_n \cdot \tan(\delta) \qquad \text{(Eq. 2)}$$

where c_a is the adhesion between the surfaces, σ_n the normal stress applied, δ the boundary surface angle of friction. c_a and δ play the same roles on an interface as do cohesion and angle of internal friction do in Eq. (1). Although the author understands the differences between the internal and interface shear strength parameters of the tested materials, as a traditional way of expressing the shear strength parameters, cohesion (c) and friction angle (ϕ) has been used throughout this thesis.

Figures 7-2 to 7-9 show the Mohr-Coulomb failure lines of all the tests performed. Tables 7-1 to 7-8 show the calculated shear strength parameters (c and ϕ) and the relevant regression correlation coefficients (R^2). In order to obtain reliable results, these coefficients should be higher than 0.98 (EN 1997 Eurocode 7: Geotechnical design. Part 2: Ground investigation and testing).

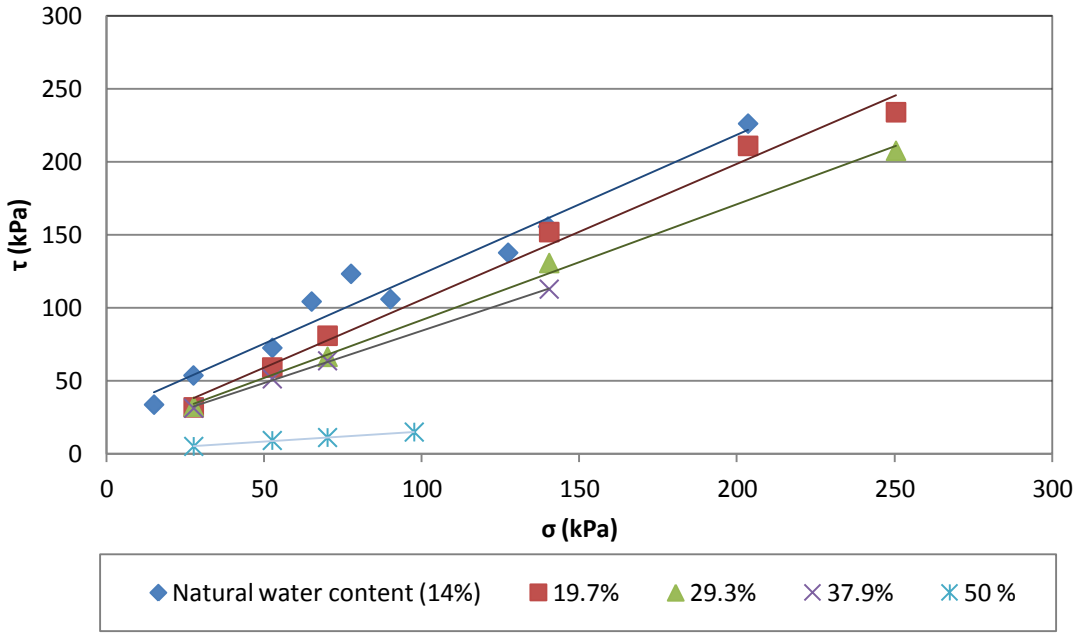

Figure 7-2. Internal shear strength with different water contents in pellet

Table 7-1. Internal shear strength parameters of pellet

w(%)	c (kPa)	φ (°)	tan φ	R^2
natural 14	20,22	44,45	0,980983	0,9944
19.7	12,56	42,94	0,930559	0,99
29.3	12,55	38,36	0,791454	0,9963
37.9	12,68	35,62	0,716458	0,999
50	1,45	7,88	0,138406	0,9959

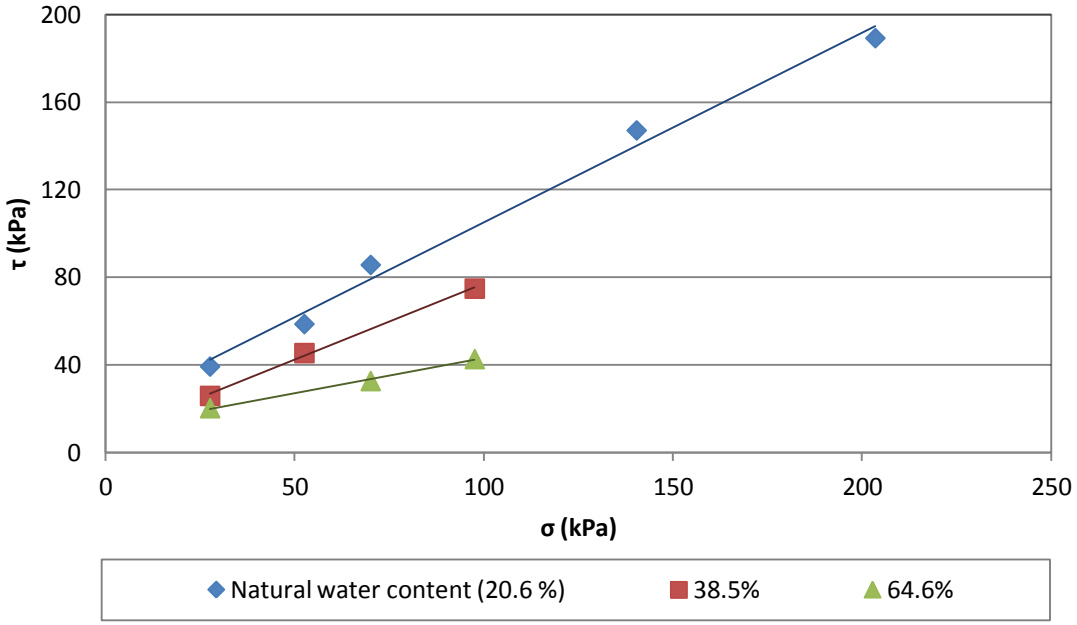

Figure 7-3. Internal shear strength with different water contents in granulated bentonite.

Table 7-2. Internal shear strength parameters of granulated bentonite

w(%)	c (kPa)	φ (°)	tan φ	R^2
natural 20.6	18,47	40,89	0,865922	0,9898
38.5	7,62	34,78	0,694501	0,9977
64.6	11,2	17,65	0,318179	0,9961

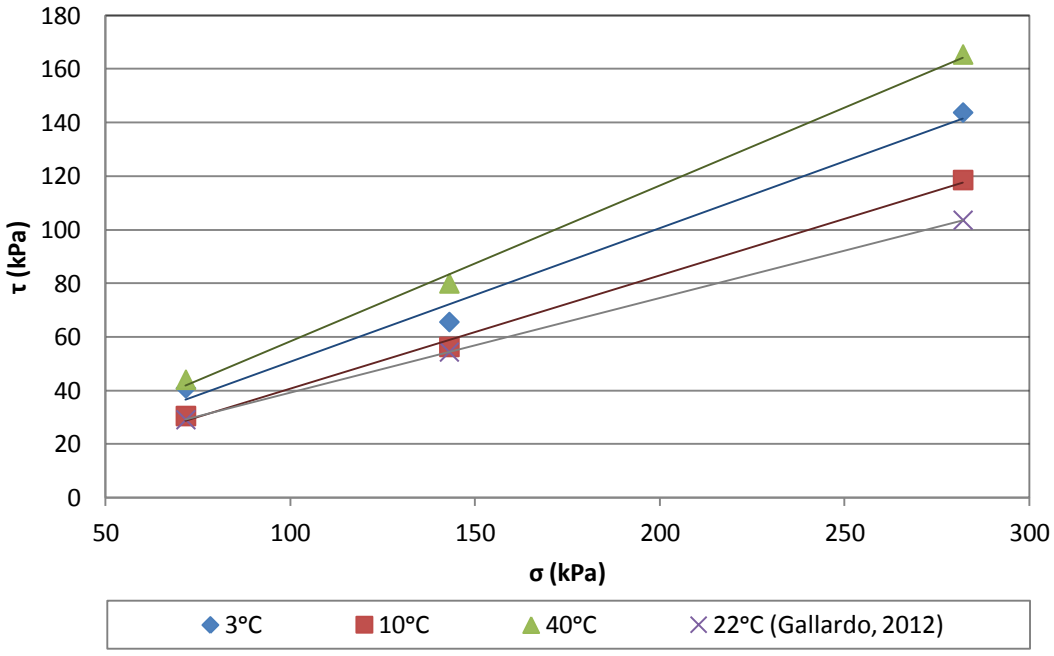

Figure 7-4. Interface shear strength of with different temperatures - block/block

Table 7-3. Interface shear strength parameters - Block/block (temperature dependent tests)

Temperature (°C)	c (kPa)	φ (°)	tan φ	R^2
+3	0,69	26,54	0,499	0,9885
+10	0	22,56	0,415	0,997
+40	0	30,22	0,582	0,9978
+22 (Gallardo, 2012)	3,70	19,50	0,345	0,9999

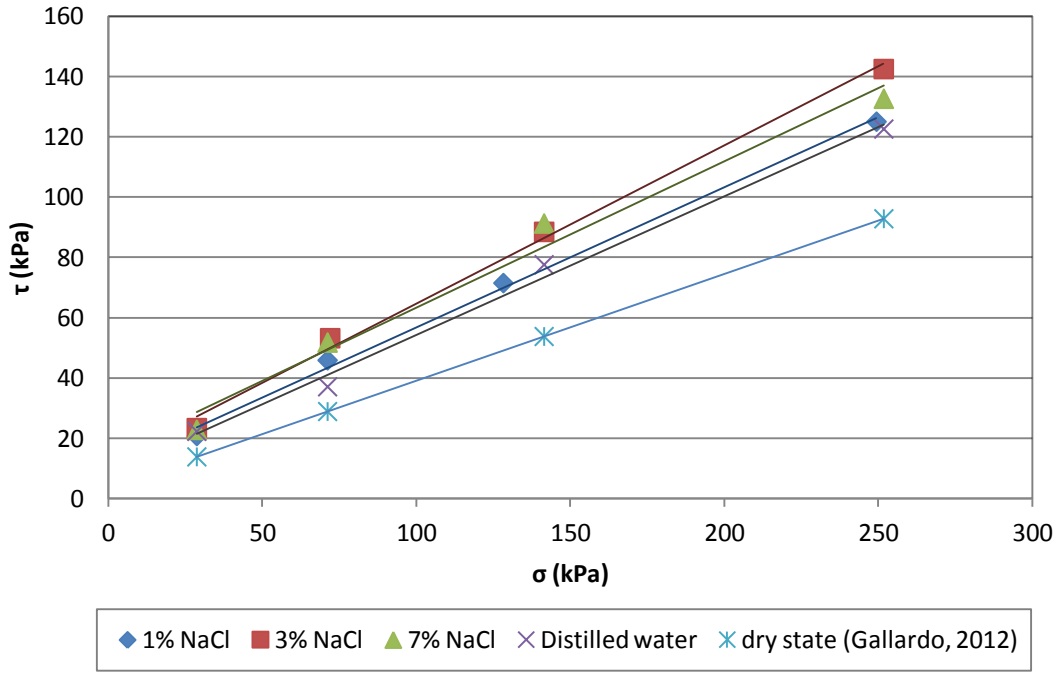

Figure 7-5. Interface shear strength with different salt contents – block/block

Table 7-4. Interface shear strength parameters - Block/block (Salinity dependent tests)

Salt content (%)	c (kPa)	φ (°)	tan φ	R^2
distilled water 0	8,28	24,72	0,460	0,9969
1	10,35	24,93	0,464	0,9965
3	12,1	27,7	0,525	0,9824
7	14,75	25,92	0,486	0,994
dry (Gallardo, 2012)	3,70	19,50	0,354	0,999

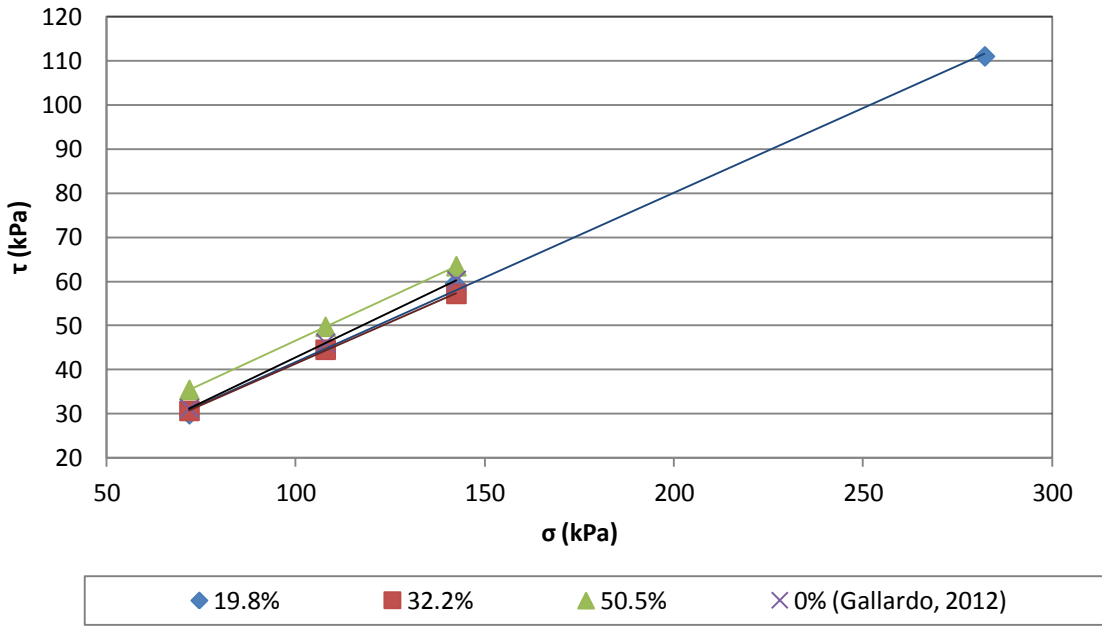

Figure 7-6. Interface shear strength - Block (natural w/c)/Pellet

Table 7-5. Interface shear strength parameters - Block (natural w/c)/pellet

w(%)	c (kPa)	φ (°)	tan φ	R^2
19.8	3,48	20,95	0,3828	0,9988
32.2	3,81	20,59	0,3756	0,9998
50.5	6,93	21,65	0,3969	1,0000
14 % (Gallardo, 2012)	1,69	22,36	0,4114	0,9834

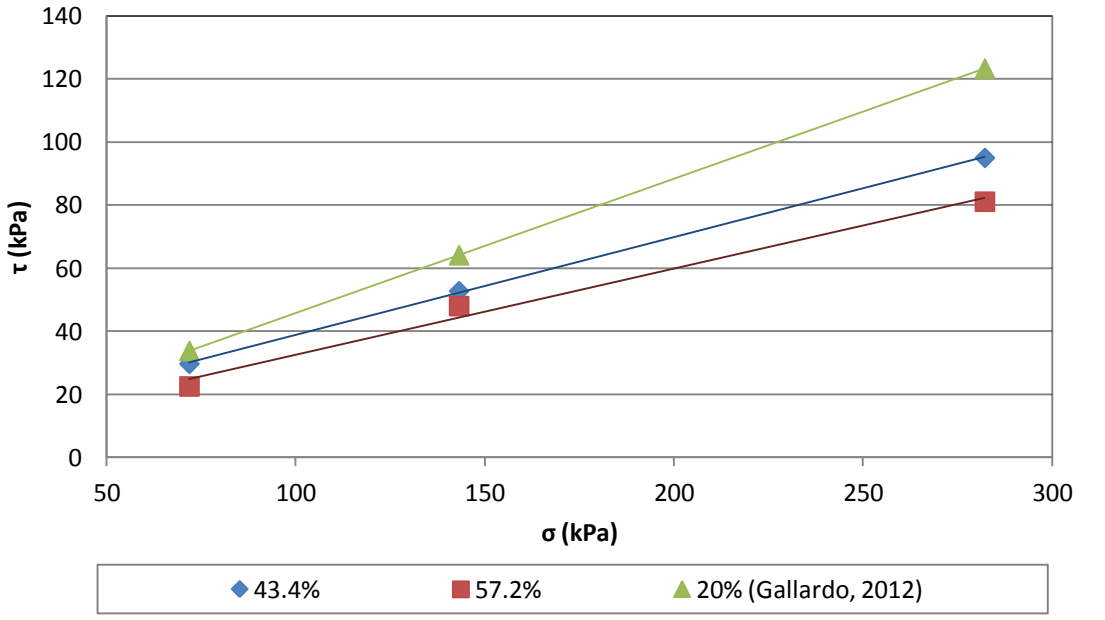

Figure 7-7. Interface shear strength - Block (natural w/c)/Granulated Bentonite

Table 7-6. Interface shear strength parameters - Block (natural w/c)/granulated bentonite.

w(%)	c (kPa)	φ (°)	tan φ	R^2
43.4	7,82	17,21	0,3097	0,9998
57.2	5,30	15,27	0,2730	0,9882
20 (Gallardo, 2012)	3,17	23,06	0,4257	0,9994

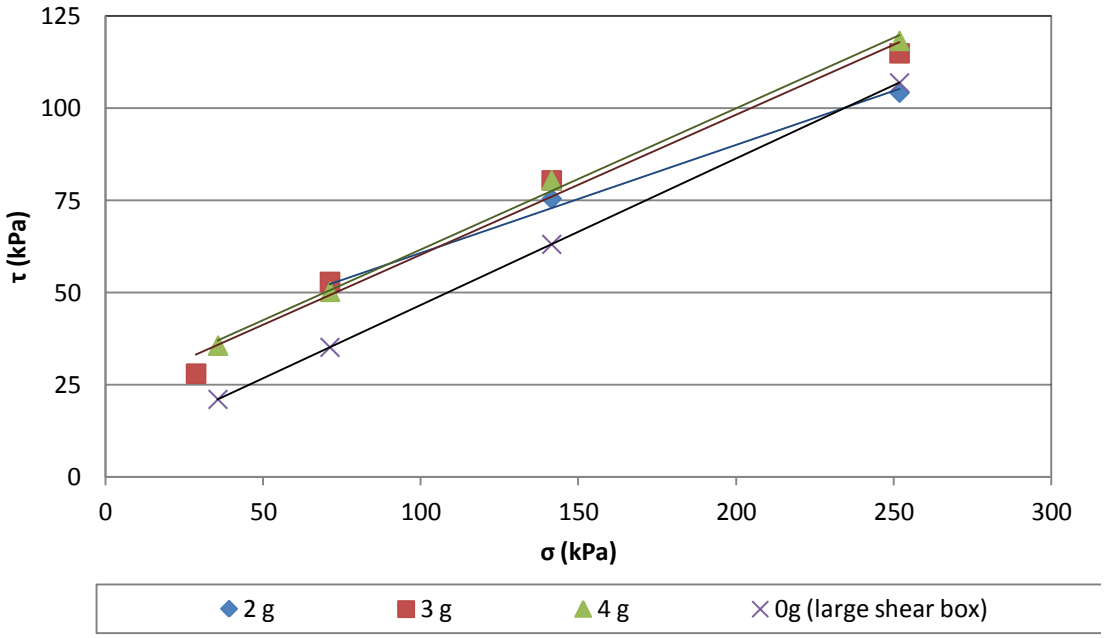

Figure 7-8. Interface shear strength - Pellet (w/c 55%)/Block (varying surface w/c)

Table 7-7. Interface shear strength parameters - Block (varying surface water)/Pellet (w/c 55%)

Surface water (g)	c (kPa)	φ (°)	tan φ	R^2
2	31,36	16,35	0,2933	0,993
3	30,04	18,8	0,3404	0,9961
4	21,03	21,52	0,3943	0,9941
0 (Large shear box)	6,93	21,65	0,3969	1,000

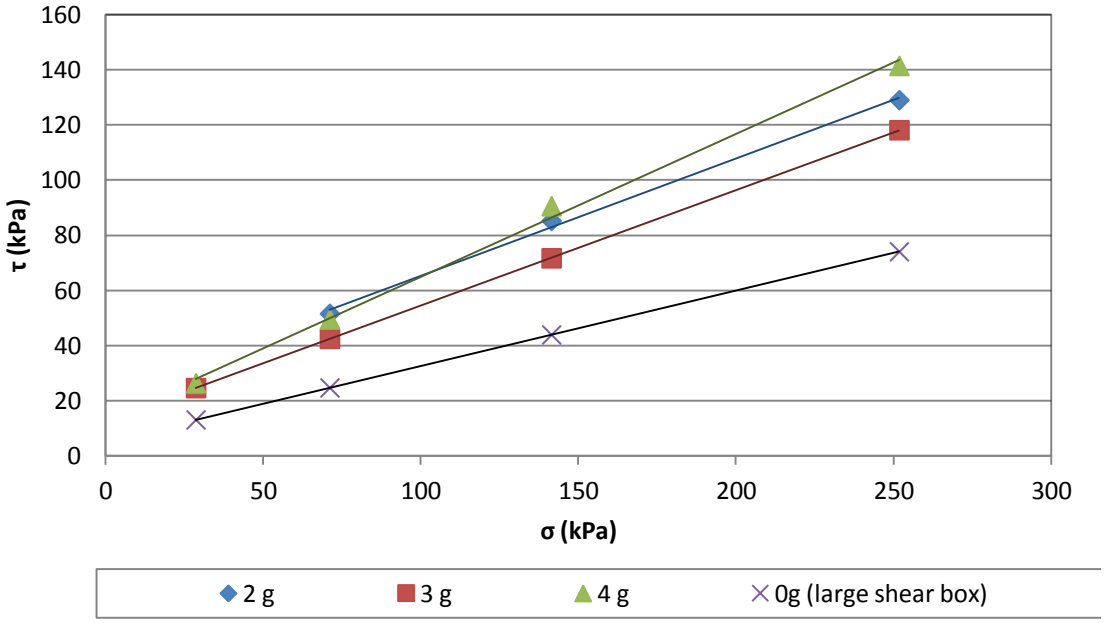

Figure 7-9. Interface shear strength - Granulated bentonite (w/c 55%)/Block (varying surface w/c)

Table 7-8. Interface shear strength parameters - Block (varying surface w/c)/granulated bentonite (w/c 55%)

Surface water (g)	c (kPa)	φ (°)	tan φ	R^2
2	22,71	23,05	0,4255	0,9973
3	12,65	22,71	0,4185	1
4	12,40	27,53	0,5212	0,9968
0 (large shear box)	5,30	23,06	0,4257	0,9994

7.2. Discussion of the results

This chapter analyses and discusses the results that are reported in chapter 6. Several aspects are discussed in relation to some previous experimental and numerical modelling studies of tunnel backfilling of Finnish KBS-3V type repository.

Several failure lines have been drawn based on Mohr-Coulomb principle and the relevant regression correlation coefficients (R^2) are reported in Tables 6-1 to 6-8. According to the additional informative annex for triaxial tests in "Eurocode 7: Geotechnical design. Part 2: Ground investigation and testing", R^2 must be higher than 0.98 in order to ensure the reliability of the test results and hence no further testing is needed. This statement has been taken into account during the present direct shear testing programme, even though the above statement is specifically mentioned for triaxial tests. It was found that the R^2 was higher than 0.98 in all tests and therefore no additional tests were needed.

Firstly, the results for the temperature dependent tests are discussed. No cohesion was found in the block/block interface tests. It is understandable that the solid interface would not yield any cohesion, however, if they do result in small cohesion that can be concluded as "apparent cohesion" and it can be neglected. Apparent cohesion can be caused either by the testing arrangements itself or by the tendency of soil to expand when sheared due to the capillarity attractive forces exist between unsaturated soils (Moayed & Alizadeh 2011).

Figure 7-10 illustrates that the friction angle decreases as the temperature increases until +22°C and then increases again with temperature. However, as the test data at higher temperatures (above +50°C) are not available, the behaviour of the friction angle at elevated temperatures is not conclusive. Up to the room temperature (+22 °C), the results can be explained due to an increased pore water pressure at raised temperature (Jefferson, 1994). On the contrary the higher friction angle in +40°C was not anticipated. When the temperature is increased, many material properties tend to be affected leading to a complex process. Therefore, the higher friction angle at +40°C may partly be caused by drying processes, which leads to increase the stiffness as the temperature increases (Åkesson, 2012). Unfortunately the water content was not controlled during these tests. There might also have been some problems with test arrangements and this value cannot be considered valid.

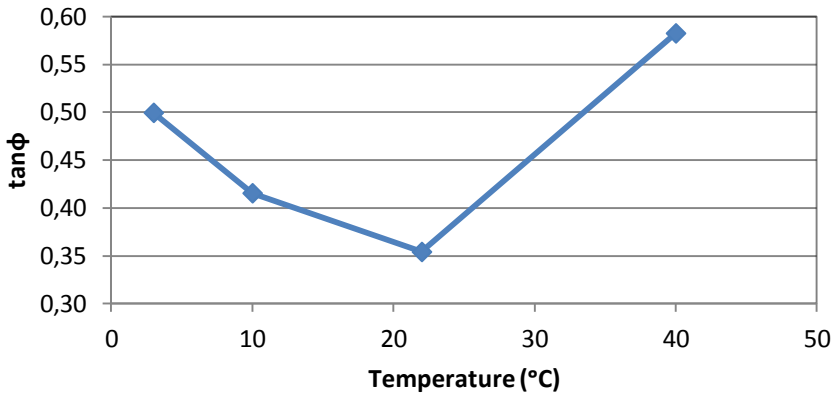

Figure 7-10. Interface friction against temperature (Value for +22°C obtained from Gallardo (2012))

Secondly, salinity dependent tests are analysed. The cohesion and friction angle were increased with salinity (Figure 7-11) if the value of the friction angle for 3%NaCl is not taken into account. Karland et al. (2005) stated that as salt concentrate increases, the swelling pressure decreases and consequently, the shear strength also decreases. In spite of this fact, the obtained results show higher shear strength when the salt content is higher. This can be explained because during the shearing the expansion was prohibited to some extent, and the swelling pressure can locally rise (Karland, 1997). In addition, double layers between the surfaces are reduced as the salt content is higher, which, in last instance, will increase shear strength (Moore & Lockner, 2007). This can explain the decrease of shear strength with higher salt content. It is important to note that the amount of salty water used was very small affecting only on the interfaces.

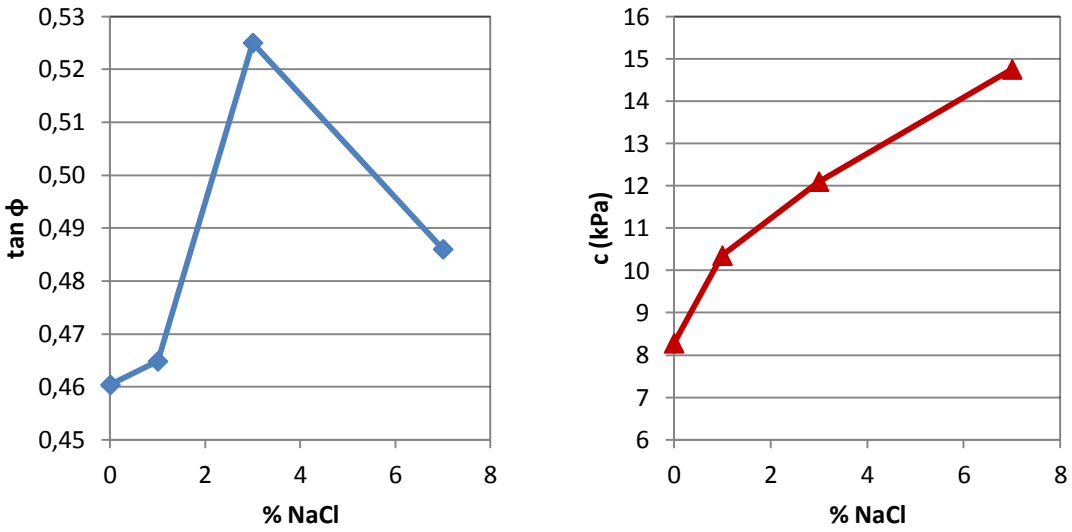

Figure 7-11. Interface friction parameters against salt content

Results from block (natural water content) – granular material (varying water content) interface did not show major differences. The cohesion varied between 3 to 8 kPa which are very small cohesion values and can mainly be considered as apparent cohesion (Figure 7-4).

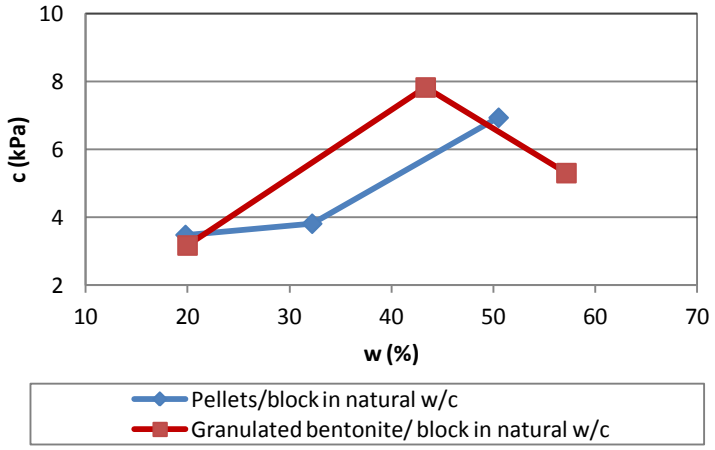

Figure 7-4. Interface cohesion of block (natural water content)/granular material against water content of granular material

Figure 7-5 shows the change in friction angle of the granular material/block interface with the change in water content of the granular material. In the case of pellets, the friction angle slightly increases with water content, which can probably be caused by the swelling nature of the materials and the capillarity attractive forces in unsaturated soils that join the wetted particles and form a weak cohesion (Moayed & Alizadeh,

2011). Nevertheless, a decrease of shear strength was expected with increasing water content, the same way as in the case of granulated bentonite and internal friction of the granular material (Figure 7-6). When water is added to a material, it becomes lubricant between adjacent particles, which allow the particles to move freely against each other with less friction. This would eventually decrease the frictional resistance of the entire mass (Tonnizam et al., 2001). Therefore, the interface shear strength for higher water contents of pellets is expected to decrease.

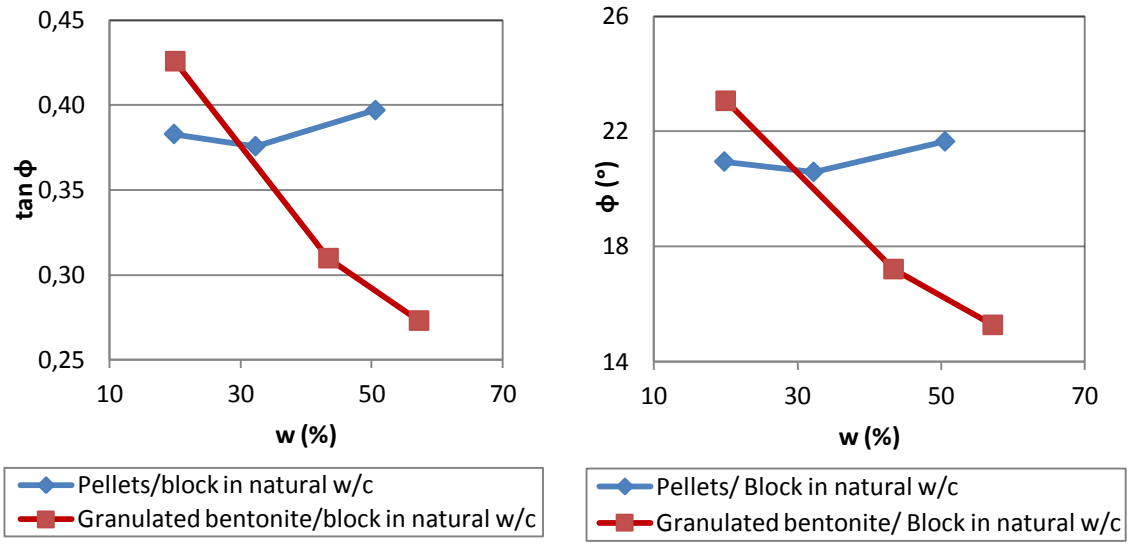

Figure 7-5. Interface friction of block (natural water content)/granular material against water content of granular material

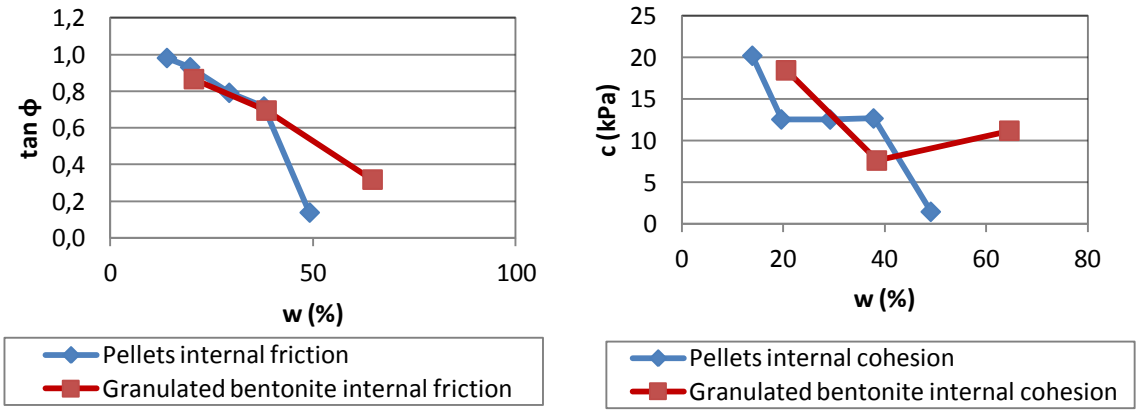

Figure 7-6. Internal shear parameter of the granular materials (pellets and granulated bentonite)

Figure 7-7 shows that the cohesion between the surfaces decreases as the amount of water was added to the block surface. This can be attributable to the attractive forces between both surfaces which depend on electrical properties of the elements involved and the distance between them. These forces are inversely related to the square of the distance between the particles; hence the higher the distance between the surfaces the lower the attractive forces that leads to less cohesion (Fowkes, 1964). Figure 7-7 also shows that the higher the amount of water on the block surface, the higher the friction angle of the corresponding interfaces. This tendency is expected to change with higher amount of water leading to a decrease of the shear strength.

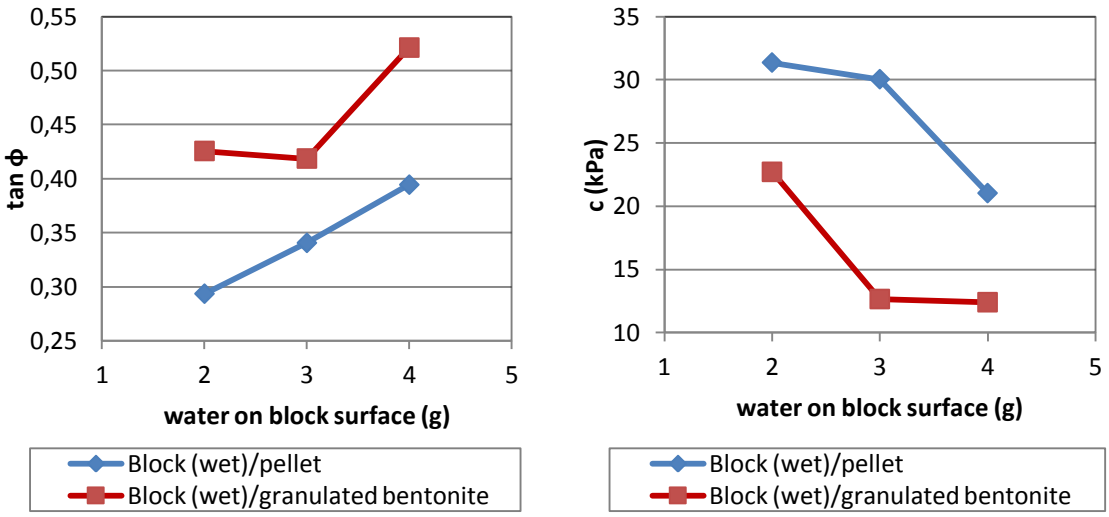

Figure 7-7. Interface shear strength parameters of block (wet)/granular material against water on block surface

The interface cohesion when the block was wetted and the water content of the granular material was kept approximately constant at 60%, was considerably higher compared to the block (natural water content) interface (Figure 7-7). Nevertheless, the scale effect of the shear boxes should be taken into account since the tests with and without adding water on the block surface were done in shear boxes with different dimensions. According to Moayed & Alizadeh (2011), the friction angle is affected by the dimensions of the shear box and so does also the cohesion. Both parameters are supposed to be inversely proportional to the dimension of the shear box. The quantity of internal errors, such as apparent cohesion is less when larger shear boxes are used. Although the difference between the tests results with wetted and not wetted blocks are still remarkable, it might not be as high as it is showed in the tests results caused by these scaling factors.

Table 7-1. Summary of test results

TEST		Material	Temp.	w (%)	water on surface	Salt content	c (kPa)	ϕ (°)
INTERNAL SHEAR STRENTH		Pellet	+22°C	14,0	-	-	20,22	44,45
		Pellet	+22°C	19,7	-	-	12,56	42,94
		Pellet	+22°C	29,3	-	-	12,55	38,36
		Pellet	+22°C	37,9	-	-	12,68	35,62
		Pellet	+22°C	49,1	-	-	1,45	7,88
		Granulated bentonite	+22°C	20,6	-	-	18,47	40,89
		Granulated bentonite	+22°C	38,5	-	-	7,62	34,78
		Granulated bentonite	+22°C	64,6	-	-	11,2	17,65
INTERFACE SHEAR STRENGTH	Temperature	Block/Block	+3°C	-	-	-	0,69	26,54
		Block/Block	+10°C	-	-	-	0	22,56
		Block/Block	+40°C	-	-	-	0	30,22
	Salinity	Block/Block	+22°C	-	3g	0% NaCl	8,28	24,72
		Block/Block	+22°C	-	3g	1% NaCl	10,35	24,93
		Block/Block	+22°C	-	3g	3% NaCl	12,1	27,7
		Block/Block	+22°C	-	3g	7% NaCl	14,75	25,92
	Water content	Block/pellet	+22°C	19,8	-	-	3,48	20,95
		Block/pellet	+22°C	32,2	-	-	3,81	20,59
		Block/pellet	+22°C	50,5	-	-	6,93	21,65
		Block/ granulated bentonite	+22°C	43,4	-	-	7,82	17,21
		Block/ granulated bentonite	+22°C	57,2	-	-	5,3	15,27
		Block/pellet	+22°C	56,9	2g	-	31,36	16,35
		Block/pellet	+22°C	55,0	3g	-	30,04	18,8
		Block/pellet	+22°C	53,0	4g	-	21,03	21,52
		Block/ granulated bentonite	+22°C	50,3	2g	-	22,71	23,05
		Block/ granulated bentonite	+22°C	64,2	3g	-	12,65	22,71
		Block/ granulated bentonite	+22°C	52,1	4g	-	12,4	27,53

Some differences can be observed between the results from the present study and a similar study that was conducted in Tampere University of Technology (TUT), Finland (Kuula-Väisänen et al., 2007). They reported a friction angle of 18.4° in Friedland-clay blocks with 250 g/m^2 of tap water on the surface and 18.5° in block-block interface with 500 g/m^2 of salty water (3.5% NaCl) on the interface. The present study was done for 750 g/m^2 and the resulted friction angle was 24.7° for distilled water and 27.7° for salty water (3%NaCl). The reason could be due to the difference in the amount of water on the surface which has been proved that in this range of amount of water on surface, the higher water leads to an increase of the friction angle. Also, the difference in the equipment and the testing method might affect.

Kuula-Väisänen et al. (2007) also studied the internal shear strength of MX-80 pellet which its saturation degree was 15%, approximately and reported friction angles of 21.9º and 26.9º from triaxial test and direct shear test, respectively. The friction angle of Cebogel QSE pellets from the present study is 44.45º which means that Cebogel QSE pellets are more suitable as backfill material around the block backfill.

Börgesson & Hernelind (2009) concluded that the interface friction angle should be higher than 8° in order to keep the vertical movement of the buffer in a safety value and consequently, satisfy the lower bond of the density criteria (1950 kg/m^3). This value of the interface friction angle was obtained considering a swelling pressure of 0 MPa which is a very conservative assumption. The heave reduces with higher swelling pressure, so the lower bond for the friction angle will be even smaller than 8°. However, Table 7-1 shows that all the values of interface friction angle are high enough to satisfy this requirement. In addition, Leoni (2012) considered a fully saturated buffer and a completely dry tunnel backfill as the worst scenario and concluded that for a block/block interface friction angle of 24°, among other interfaces considered, the maximum heave was less than 100 mm which was less than the maximum heave permitted to satisfy the density criteria (141 mm). The minimum block/block interface friction angle of 19.5º was reported by Gallardo (2012) and corresponds to a temperature of +22°C. Except this value and the friction angle for +10ºC (22.56º), all the other cases studied report a friction angle higher than 24° and will lead to a vertical movement of less than 100 mm under the assumptions made by Leoni (2012).

7.3. Measurement uncertainty and accuracy

Several measuring and evaluation errors could have affected the results and some of them are listed below:

1. There were multiple mechanical components of the equipment responsible of transmitting the normal stress to the sample that can modify the real stress applied.

2. Although the measuring system was capable of standing different temperatures, there could be different behaviour of these components that may affect to the reliability of the measurements.

3. Testing interface shear strength in the shear box is a hard job which can lead to some errors. The perfect alignment of both halves is not easy, and also when the shear phase is been carried out, the samples tends to tilt varying the initial position of the materials. Therefore, in some cases the interface might not be tested perfectly.

4. Due to the basis of Mohr-Coulomb theory, it is needed to adjust a straight failure line which it depends in some extent to the person who is adjusting this line.

5. The normal statistical variation of the experimental studies is of course present causing some scatter to the test results.

8. Conclusions and recommendations

The aim of this study was to investigate the effect of temperature, salinity and water content on the mechanical behaviour of the tunnel backfilling interfaces in KBS-3V type repository. The above parameters were tested independently in several backfilling interfaces.

Block-block interface was tested under different temperatures, resulting in increased interface shear strength on either side of the room temperature. The lowest shear strength parameters were observed at the room temperature (+ 22°C). Further tests have to be carried, both in sub-zero temperatures and elevated temperatures (above +50 °C) for better understanding of the effect of temperature on shear strength.

In addition, block-block interface was also tested for the effect of salt content in the surface water. The results showed that the interface shear strength increased with salt content in the surface water.

Two types of testing were performed to study the effect of water content on the shear strength:

1. Block (natural water content) – Granular material (varying water content)
2. Block (varying water on surface) – Granular material (~60% water content)

In type 1 tests where the water content of the block was fixed (natural) and the water content of granular materials (both granulated bentonite and pellet) varied, the shear strength decreased with increasing water content. However, an opposite trend was observed in the type 2 tests where the water content of the block was varied while the water content of the granular material was fixed at 60%.

It is recommended that the effect of changing the temperature and salinity should be tested also for other interfaces such as block-granular material (pellets and granulated bentonite). It is also important to test the interface shear strength between the surrounding bedrock and the granular material.

In order to study different stages during the operational phase until the backfill behaves as a single mass, further numeric models should be done using the laboratory results and not only consider the backfill in dry state as it has been done by Leoni (2012).

REFERENCES

Åkesson, M., Jacinto, A. C., Gatabin, C., Sánchez, M. & Ledesma, A. (2009). Bentonite THM behavior at high temperatures: experimental and numerical analysis. *Géotechnique,* 59 (4), 307-318.

Åkesson, M. (2012). Temperature buffer test. Final report. *SKB Report TR-12-04.* ISSN 1404-0344.

Börgesson, L., Chijimatsu, M., Fujita, T., Nguyen, T.S., Rutqvist, J., Jing, L. (2001) Thermo-hydro-mechanical characterization of a bentonite-based buffer material by laboratory tests and numerical back analyses. *International Journal of Rock Mechanics & Mining Sciences,* 38, 95-104.

Börgesson, L., Hernelind, J. (2009). Mechanical interaction buffer/backfill. Finite element calculations of the upward swelling of the buffer against both dry and saturated backfill. *SKB Report R-09-42.* ISSN 1402-3091

Dixon, D., Sandén, T., Jonsson, E., Hansen, J. (2011). Backfilling of deposition tunnels. Use of bentonite pellets. SKB Report P-11-44. ISSN 1651-4416.

Féron, D., Crusset, D. & Gras, J-M. (2008). Corrosion issues in nuclear waste disposal. *Journal of Nuclear Materials,* 379, 16-23.

Fowkes, F.M. (1964). Attractive forces at interfaces. *Industrial & Engineering Chemistry,* 56 (12), 40-52.

Gallardo, J. (2012). Shear resistance of backfill components' interfaces in nuclear waste deposition tunnels. Master thesis. Aalto University, school of engineering. Department of Civil and Environmental Engineering.

Graham, J., Tanaka, N., Crilly, T. & Alfaro, M. (2001). Modified Cam-Clay modelling of temperature effects in clays. *Canadian Geotechnical Journal*, 38 (3), 608-621.

Grim R.E. & Güven N.(1978). Bentonites. Geology, Mineralogy, Properties and Uses. Elsevier, Amsterdam.

Hansen, J., Korkiala-Tanttu, L., Keski-Kuha, E., Keto, P. (2010). *Deposition Tunnel Backfill Design for a KBS-3V Repository.* Posiva Working Report 2009-129.

Horseman, S.T., Harrington, J.F. & Sellin, P., (1999). Gas migration in clay barriers. *Engineering Geology,* 54, 139-149.

Jefferson, I. (1994). *Temperature effects on clay soils.* PhD thesis. Loughborough University of Technology.

Johannesson L.-E., Sandén T., Dueck A. & Ohlsson L. (2010). Characterization of a backfill candidate material, IBECO-RWC-BF. Baclo Projekt – Phase 3. Laboratory tests, Report SKB R-10-44.

Juvankoski, M., Marcos N. (2010). Design basis for buffer components. Working Report 2009-132. Posiva Oy.

Karland, O. (1997). Bentonite swelling pressure in strong NaCl solutions. Correlation between model calculations and experimentally determined data. *SKB technical report.* TR-97-31.

Karnland, O., Muurinen, A. & Karlsson, F. (2005).Bentonite swelling pressure in NaCl solutions – Experimentally determined data and model calculations. Advances in understanding Engineered Clay Barriers, Alonso & Ledesma (eds), 2005 Taylor & Francis Group, London,ISBN 04 156544 9.

Karnland, O & Birgesson, M (2006). Montmorillonite stability with special respect to KBS-3 conditions. SKB report. TR-06-11

Keto, P. (2004). *Natural Clays as Backfilling Materials in Different Backfilling Concepts.* Posiva Working Report 2004-79.

Keto, P., Gunnarsson, D., Johannesson, L.-E., Hansen, J. (2008). Assessment of backfilling materials and methods for Deposition Tunnels. *Science & Technology Series,* 334.

Keto, P., Dixon, D., Jonsson, E., Gunnarsson, D., Börgesson, L., Hansen, J. (2009). Assessment of backfill design for KBS-3V repository. *SKB Report R-09-52. ISSN 1402-3091*

Korkiala-Tanttu, L. (2009). Finite element modeling of deformation of unsaturated backfill due to swelling of the buffer. *Posiva Working Report 2008-88.*

Kuula-Väisänen, P., Leppänen, M., Kolisoja, P. (2007)Processes during saturation of the block backfill. MECHANICAL PROPERTIES AND SATURATION OF THE BLOCK BACKFILL. *Backfilling and closure of the deep repository.*

Labuz, J. & Zang, A. (2012). Mohr-Coulomb Failure Criterion. *Rock Mechanics and Rock Engineering,* 45,6, 975-979.

Leoni, M. (2012). 2D and 3D finite element analysis of buffer-backfill interaction. *Wesi Geotecnica Srl.* Working report.

Moore, D.E. & Lockner, D.A. (2007). Friction of the smectite clay montmorillonite. In: Dixon, T. & Moore, C. (eds.) *The seismogenic zone of subduction thrust faults.* Columbia University Press, pp. 317-345.

Murray, H.H. (1999). Applied clay mineralogy today and tomorrow. *Clay minerals,* 34, 39-49.

Pastina, B. & Hellä, P. (2006). Expected evolution of a spent fuel repository at Olkiluoto. Posiva 2006-05. Posiva Oy, Olkiluoto, Finland.

Pedersen, K. (1999) Subterranean microorganisms and radioactive waste disposal in Sweden. *Engineering Geology,* 52, 163-176.

Phillips, D. H., Sinnathamby, G., Russell, M. I., Anderson, C. & Pasky, A. (2011). Mineralogy of selected geological deposits from the United Kingdom and the Republic of Ireland as possible capping materials for low-level radioactive waste disposal facilities. Applied Clay Science, Vol. 53, p. 395-401.

Posiva (1999). *The final disposal facility for spent nuclear fuel.* Environmental impact assessment report

Posiva (2003). Baseline Conditions at Olkiluoto. Posiva Report 2003-02.

Pusch, R. (1998). Backfilling with mixtures of bentonite/ballast material or natural smectitic clay?. SKB report TR-98-16

Raiko, H. (2005). Disposal Canister for Spent Nuclear Fuel – Design Report. *Posiva 2005-02.*

Rautioaho, E. & Korkiala-Tanttu L. (2009). Bentomap:Survey of bentonite and tunnel backfill knowledge. State-of-the-art. *VTT Working papers,* 133, ISSN 1459-7683.

Sandén, T., Börgesson, L., Dueck, A., Goudarzi, R., Lönnqvist, M. (2008). Deep repository-Engineered barrier system. Erosion and sealing processes in tunnel backfill materials investigated in laboratory. SKB report R-08-135. ISSN 1402-3091.

Sivakumar, V., Kodikara, J., O'Hagan, R., Hughes, D., Cairns, P. & McKinley, J.D. (2013). Effects of confining pressure and water content on performance of unsaturated compacted clay under repeated loading. *Géotechnique*, 63 (8), p.628-640

Tonnizam, E., Abdulqawi, B., Anuar, K. & Saad, R., (2011). Shear Strength Behaviour for Older Alluvium Under Different Moisture content. *Electronic Journal of Geotechnical Engineering,* 16, 605-617.

Warkentin, B.P. & Yong, R.N. (1960). Shear strength of montmorillonite and kaolinite related to interparticle forces. *Clay and Clay Minerals,* 9 (1), 210-218.

Zhang, B., Zhao, Q.G., Horn, R. & Baumgartl, T. (2001). Shear strength of surface soil as affected by soil bulk density and soil water content. *Soil & Tillage Research,* 59, 97-106